Extinction, Fixation, and Invasion in an Ecological Niche

by

MattheW Badali

A thesis submitted in conformity with the requirements
for the degree of Doctor of Philosophy
Graduate Department of Physics
University of Toronto

Abstract

Extinction, Fixation, and Invasion in an Ecological Niche

MattheW Badali
Doctor of Philosophy
Graduate Department of Physics
University of Toronto
2019

Remarkable biodiversity exists in biomes such as the human microbiome, the ocean surface, and every speck of soil. Despite their importance in human health and conservation biology, the long term dynamics, diversity and stability of communities of multiple interacting species are still incompletely understood. The competitive exclusion principle postulates that due to abiotic constraints, resource usage, inter-species interactions, and other factors, ecosystems can be divided into ecological niches, with each niche supporting only one species in steady state. However, maintenance of biodiversity of species that occupy similar niches is still not fully understood. Biodiversity decreases as species go extinct, which is often caused by interactions with other species. Stochastic fluctuations allow for an otherwise stable population to exhibit extinction. Mathematical biologists employ stochastic models like the Moran or Lotka-Volterra models to emulate extinction or species competition.

The Moran model is the cleanest example of two competing species in an ecosystem in which eventually one goes extinct and the other fixates. The extinction occurs on a short timescale with a characteristic dependence on system size. Recently, some authors have observed that the Lotka-Volterra model, which typically has a long extinction timescale, exhibits dynamics similar to those of the Moran model in one parameter limit. Given the widespread use of these models in mathematical biology, this correspondence of models is significant, but no one has investigated how the system transitions between its slow and fast extinction limits. To contribute to the problem of biodiversity I look at how the Lotka-Volterra model's transition depends on its parameters. I show that competing species can coexist unless their ecological niches entirely overlap. I identify the nature of the transition by calculating the mean extinction time with an arbitrarily accurate technique. This technique also allows me to appraise the stability of the Lotka-Volterra and Moran models with regards to immigrant invasion attempts. My research predicts at what parameter values two species will effectively coexist, or whether one will be susceptible to the invasion of the other. This allows me to make some general comments on why ecosystems should display such biodiversity.

Contents

List of Figures

Chapter 0

Introduction

0.1 Motivation and background

Mathematical ecology is the oldest discipline of mathematical biology, with its relevance dating back at least since Malthus used a model of exponential growth to argue that overpopulation would lead to widespread famine and disease, and that was more than two hundred years ago [121]. It is certainly older than modern biology, with the structure of DNA only being reconstructed sixty years ago [102, 183]. About a century ago, Lotka [**?**] and Volterra [180] extended the logistic equation of Verhulst [179] and applied it to biological systems, arriving at the famous predator-prey equations. Midway through the last century, Wright [187], Fisher [61], and Moran [133] proposed urn models that demonstrate fixation and extinction in a way that is easily intuited and also treatable mathematically. Around the same time, Kimura was revolutionizing genetics by proposing models that could account for the evolution and eventual fixation or extinction of mutant alleles [49, 93]. Ecology benefited from the island biodiversity theory of MacArthur and Wilson [119**?**]. In the last couple decades there has been debate as to the extent of neutral versus niche effects in ecological dynamics, sparked by Hubbell's unified neutral theory of biodiversity and biogeography [76]. The history of mathematical and theoretical biology, especially as applied to ecology, is punctuated by significant models like these inspiring deeper investigations of both the quantitative details and qualitative trends that the biological world might contain.

The application of mathematics to ecology opens up the possibility of addressing a variety of problems central to the field. It allows us to be quantitative and predictive. One of the simplest problems, and one treated in this thesis, is this: what is the probability of and timescale over which a species will go extinct in an ecosystem [17, 18]? There is the related question: given two competing species in a system, what is the probability of extinction of either species before the other, and the timescale over which this occurs? In an ecosystem with competing species, when all but one species has gone extinct, that final species is said to have fixated in the system.

The lifetime and extinction of species is both of theoretical interest and a pressing concern for humanity, as we exist in an epoch of unprecedented rates of extinction [166]. Conservation biology is concerned with managing and maintaining the biodiversity on Earth, to avoid these massive extinctions and potential system collapse. Biodiversity, simply put, refers to the number of species or genetic strains in an ecosystem. I would like to highlight the issue of biodiversity, one of the stubbornly unsolved problems in modern ecology [37, 125, 150**?**]. In 1961 Hutchinson published "The paradox of the

plankton" [80], in which he speculated about an apparent contradiction: for plankton living in the upper layer of the ocean far from shore there are few different resources on which to live, yet there is an immense diversity of different species of plankton that appear to coexist. Surely those species that reproduce the quickest or use the resources most efficiently would outcompete all others such that only the fittest would survive. For my purposes, a species is a collection of organisms with the same mean birth and death rates, that are distinguishable from members of other species. This principle of competitive exclusion, sometimes called Gause's Law [**?**] states that "two species cannot coexist if they share a single [ecological] niche." In systems with few resources and therefore few niches, one expects that only few species will persist at any given time. The expectation is that in this homogeneous ecosystem with extreme nutrient deficiency the competition should be severe, and only a few species should persist, many fewer than the number observed.

A variety of solutions have been proposed to resolve the paradox of the plankton but there is as yet no consensus [165]. These include: the system is approaching a steady state of fewer species but very slowly; there exist other limiting factors like resources or toxins overlooked by scientists that help define more niches; environmental fluctuations or oscillations stabilize the system; spatial heterogeneity allows for local extinction but supports the great biodiversity on larger length scales; the system is stabilized by life-history traits of the plankton; the system is stabilized by the presence of predators to the plankton; there is symbiosis or commensalism between the various plankton species. This lack of consensus is a gap in the literature. In this thesis I address a small part of the problem by calculating the mean lifetime of a species, either surviving independently or undergoing competition with another species of varying similarity.

The theories dealt with in this thesis have many applications. Most obvious, and arguably most pressing to society, is the realm of conservation biology. Biodiversity is often used as an indicator of the health of an ecosystem [129, 151, 155, 166**?** **?**]. A clearer understanding of the forces that maintain biodiversity could provide new and easier metrics for evaluating the health of an ecosystem, and hence the efficacy of various conservation efforts. The mechanisms of species maintenance are related to those of speciation, and an ecosystem losing stability can refer to both its collapse or invasion of a foreign species. Invasion of a new mutant or immigrant strain or species into the system is a problem deeply intertwined with that of biodiversity maintenance [76].

Invasion is also relevant in the domain of health care. We are only recently learning, for example, about the composition of the microbiome in humans and its relation to health [43, 98, 104, 122, 174]. Imbalance of the microbiome composition, or invasion of a new species, can greatly impact a person's wellbeing, and a theory of whether an invasion will be successful and how long it might persist would go a long way toward diagnostics and prognostication. The other end of the process, namely the extinction of a species, also has a number of applications. Other than the obvious modern ecological ones, extinction times are useful in paleontology. The fossil record shows a number of species in different epochs, and these data make more sense in the light of a consistent theory of species survival and eventual decline. Similarly, extinction and fixation times are already used in the construction of phylogenetic trees [26, 159, 162]. The more accurate a theory of extinction timescales developed, the more precisely we can perform phylogenetic analyses. Mapping existent species to their common ancestors falls under the purview of coalescent theory [97]. This is part of the impact of the results presented in this thesis, in that I calculate extinction times to arbitrary accuracy, using a controlled approximation largely ignored in the literature.

0.2 Niche theories

The competitive exclusion principle states that in any given niche one species will eventually dominate. It is inextricably linked to the concept of an ecological niche, which Grinnell popularized more than a century ago [**?**]. Since then there has been debate as to its meaning and utility as a concept. Following Leibold [111], I refer to the definition of a niche according its two major uses: as the habitat or requirement niche and the functional or impact niche.

The requirement niche: Grinnell [**?**] defines a niche as those ecological conditions that a species can live within. These ecological conditions include environmental levels and those organisms on different trophic levels than the species, like their predators and prey, but not those on the same trophic level that might compete with them. Hutchinson [**?**] agrees with Grinnell, and has provided one of the most enduring conceptualizations of a niche, that of an "n-dimensional hypervolume" in the space of factors that could affect the growth or death of a species. For each factor there is some range at which the species can reproduce faster than it dies out. This is true both for abiotic factors such as temperature, and biotic factors like the concentration of predators. Sometimes these ranges are bounded by zero (eg. cannot survive with no carbon source), sometimes they are unbounded (eg. no amount of prey is too much), and sometimes they depend on the values of the other factors involved (eg. salt is fine for sea creatures so long as there is an appropriate amount of water along with it). But in the space of all these factors, Hutchinson calls the fundamental niche that volume in which the species would have a greater birth rate than death rate. He defines the realized niche as the point or subspace in this high dimensional space that the species effectively experiences, given that it is existing and potentially coexisting in an ecosystem. This also lends a natural definition of niche overlap, as the (normalized) overlap of the fundamental niches of two species [119]. The requirement niche tells us whether the coexistence point of two species is physical, according to simple model of two species [75]. It is inherently linked to the argument of limiting factors as the delimiters of niches as outlined earlier [9, 10, 127].

The other usage of the term niche, that of a functional or impact niche, was popularized by Elton [**?**] and MacArthur & Levins [119]. Whereas the requirement niche focuses on what factors a species needs to live, the impact niche looks at how the species affects these factors. Their conception of a niche describes how a species influences its environment, or how that species fits in a food web; essentially, what role it plays in an ecosystem. This idea is especially attractive to those who study keystone species (those species that play a disproportionate or critical role in maintaining an ecosystem) [37, 110, 125] but is easily understood from an elementary understanding of what an ecosystem is. By way of example, in every ecosystem with flowers there is something that pollinates them. Whether the pollinator is a bird or an insect species is irrelevant; this role exists in the ecosystem, and so a species evolves to occupy this niche, to take advantage of the nectar the flower offers. The niche, in this view point, is the role the species plays in the ecosystem with regards to the other species and the environment; how it impacts the system. As per one simple model of two species, the impact niche tells us whether a coexistence point of two species is stable [**?**].

Both of these categories of semantics for the word niche have their use. The literature shows attempts to resolve the discrepancies that arise when the two definitions are at odds [110, 111]. In chapter 2 I show an example derivation of the Lotka-Volterra system based on an argument of limiting factors that aligns better with the requirement niche definition. However, so long as niches exist in some sense and a niche overlap parameter can be defined, the results I arrive at in this thesis are sound.

The original Lotva-Volterra model was introduced around a century ago to describe the dynamics

of a population of a predator and its prey. It can be seen as an extension of the Verhulst, or logistic, equation, from one to two dimensions. In its modern incarnation the generalized Lotka-Volterra model is typically written as

$$\begin{aligned} \dot{x}_1 &= r_1 x_1 \left(1 - x_1/K_1 - a_{12} x_2/K_1\right) \\ \dot{x}_2 &= r_2 x_2 \left(1 - a_{21} x_1/K_2 - x_2/K_2\right). \end{aligned} \tag{1}$$

The generalized Lotka-Volterra model is the accepted terminology for a dynamical system that depends linearly and quadratically on the populations modelled, with no explicit time dependence. The Verhulst model is one of these equations with its $a = 0$. The classic Lotka-Volterra model is attained by taking the K's to infinity, keeping the a/K ratios positive and finite, choosing r to be negative for the predator and positive for the prey. This predator prey model has oscillating dynamics about a center fixed point. To restrict our investigation to viable species in the same trophic level (treating predators and prey of the species of interest as being some of the limiting factors) we assume K is finite and r is positive. More details of the Lotka-Volterra model will be provided as they become relevant, particularly in chapter 2. Chapter 1 is inspired by the single logistic equation, while chapter 3 further explores the 2D generalized Lotka-Volterra model then considers a Moran model with immigration. Some authors [40, 44, 114, 190] have observed that for certain parameter values the stochastic 2D generalized Lotka-Volterra model exhibits dynamics similar to those of the Moran model. They did not examine how the effect on the dynamics as the Moran limit is approached; the transition to this limit is one of the main investigations of this thesis.

The parameters in the Lotka-Volterra equation are easy to understand, albeit hard to measure, being phenomenological rather than physical. The turnover rate r gives the maximum growth rate a species can achieve, specifically when first colonizing an empty system, such that the intraspecific $(1/K)$ and interspecific (a/K) competition terms are small. The parameter K is called the carrying capacity of the ecosystem, the maximum population the system can sustain in the absence of competitor species, given the resources available and other limiting factors present in the system. Together these two parameters, which are the only two that show up in a single logistic equation $\dot{x} = rx(1 - x/K)$, motivate r/K selection theory, coined by MacArthur and Wilson [117]. The theory of r/K selection posits that there is a trade-off between the quantity and the quality of offspring, based on the effects of increased r or K. The other parameters in the Lotka-Volterra equations are the a's. These parameters represent the niche overlap between the two species, or the ratio of interspecific to intraspecific competition. They can be derived from limiting factors (see [119] for one example and [118] or chapter 2 of this thesis for a different argument). There is an unresolved debate in the field as to how niche overlap should be measured or defined [1, 2, 36, 38, 79, 101, 111, 152, 153, 167**?**].

The parameter space of the deterministic Lotka-Volterra model presented above shows a variety of regimes of the relationship between the two species [137**?**]. It is also summarized in chapter 2. The Lotka-Volterra model is of further interest because recent research has shown that inclusion of noise to the model recovers dynamics similar to the Moran model in a certain parameter limit [**?**]. The Moran model is a neutral model that shows qualitatively different dynamics. The Moran model also underpins the Hubbell model, which is the simplest model that successfully describes abundance distributions in ecosystems with high biodiversity. In niche models like the Lotka-Volterra model each species exists at its carrying capacity, and abundance distributions have to be predicted by more complicated models

called niche partitioning or apportionment [**?**].

0.3 Neutral theories

Neutral models like that of Hubbell are favoured for their parsimony, the simplicity with which they can be understood simultaneous with the accuracy of their predictions [76, 110, 163]. Hubbell's neutral theory of biodiversity is a minimal working model for calculating species abundance curves. Similarly, the models of Wright, Fisher, Moran, and Kimura are minimal models that show extinction and fixation. These models allow not just for fixation probabilities but also the distribution of times such a random occurrence might take. In fact these models can describe any system where individuals of different species or strains undergo strong but unselective competition in some closed or finite ecosystem, for instance those constrained by space. Such ecosystems could include microbiomes, of humans [43, 98] or others [28, 141, 161, 174, 178, 186]. These microbiomes have limited space and resources and so any death of an organism is quickly replaced by the birth of another. Immigration is relatively rare due to the closed nature of the system. Neutral models also underlie the simplest version of coalescent theory and phylogenetic tree reconstruction [97, 159], showing their use not only as minimal models but in whole fields of ecology.

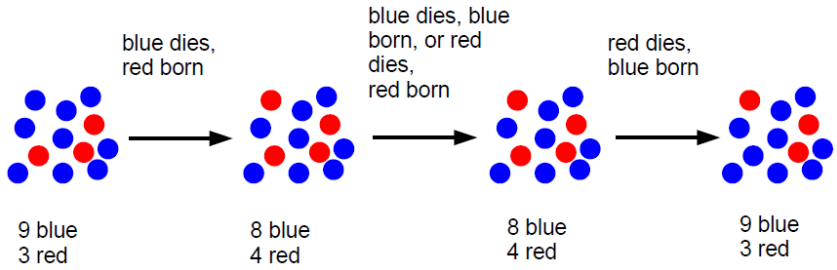

Figure 1: *Example Time Steps of the Moran Model* Here is a sample Moran model with $K = 12$ individuals, initially $n = 3$ of which are red. In the first time step, a red individual is chosen to reproduce (which would happen with probability 3/12) and a blue one dies (probability 9/12). This increases the number of red individuals in the system. Other possibilities each time step are that the number of reds remains the same or decreases. There is a non-zero chance that in as few as three steps a colour will have fixated in the system. Over time the probability of fixation increases such that it is almost certain the system will fixate eventually. Once only one colour remains in the system the chance that a different colour reproduces (and is thus introduced into the system) is zero, since there are none of that different colour around to reproduce.

Figure 1 gives a sketch of a few time steps of evolution of the Moran model. Moran's is a classic urn model used in population dynamics in a variety of ways. It is easy to arrive at, requiring only a few simplifying assumptions. The first is that no individual is better than any other in terms of reproducing faster or living longer; that is, whether an individual reproduces or dies is independent of its species and the state of the system [133]. This makes the Moran model a neutral theory, and any evolution of the system comes from chance rather than from selection [25, 26, 42**?**]. The next assumption is that the population size is fixed, owing to the (assumed) strict competition for resources or space in the system. That is, every time there is a birth the system becomes too crowded and a death follows immediately. Alternately, upon death there is a vacancy in the system that is filled by a subsequent birth. In the classic Moran model each pair of birth and death event occurs at a discrete time step. (The

similar Wright-Fisher model, where each step is longer and involves N of these events, has the same limiting dynamics [26].) This assumption of discrete time can be relaxed without a qualitative change in results, as will be reviewed in chapter 3. The Moran model is most appropriate for modelling a system of asexually reproducing organisms, like bacteria in an enclosed space.

In the Moran model, each time step involves a birth and a death event. For each event the participating species is chosen with a chance proportional to its abundance in the system. Since a species is equally likely to increase or decrease each time step, the model is akin to an unbiased random walk. And since each event has an equal probability of happening for a given species, the frequency of that species tends to stay constant on average [92, 133]. However, due to the randomness inherent in the model the species' frequency in fact fluctuates. This fluctuation is not indefinite; there are two states from which the system cannot exit and thus only accumulate in probability of occurrence. These static states are extinction and fixation: the species has no chance of reproducing when at zero population (extinction) and does not change abundance when it is the only species in the system (fixation) as it constantly is both reproducing and dying with unit probability each time step. Both of these cases are absorbing states, so called since once the system reaches either it will stay in that state indefinitely. In this system we can define the first passage time as the time the system takes to reach either fixation *or* extinction. The first passage time can also be calculated, and its mean gives an estimate of the time two species will coexist in a system (or the inverse fixation rate of the system).

The unbiased random walk underlying the Moran model is a consequence of its neutral nature. Briefly, a neutral theory is one for which intraspecies interactions are the same as interspecies interactions. That is, an organism competes equally strongly with members of its own species as with those of other species. No species is distinguished or exceptional in a neutral theory. Thus, unless the whole system's net population is increasing or decreasing, a given organism (and hence its species) is equally likely to reproduce or die, and on average its species abundance is constant. Whether and why different species should regard each other the same as themselves is a matter of debate [76, 110, 163**?**]. It is important to clarify the difference between neutral theories and those that are simply symmetric. In a symmetric theory an exchange of labels between two species has the same effect as an exchange of population sizes. Calling the red species of figure 1 blue and the blue species red does not change how the system will evolve. Neutral theories are a subset of symmetric theories, since a neutral theory in which each species does not distinguish between self and others automatically allows for an exchange of species labels with no noticeable effect beyond exchanging abundances.

The Moran model, under the approximation of continuous population fraction, effectively becomes that of Kimura [92, 96]. Kimura was inspired by alleles rather than species, but the rationale is similar. Alleles are the different variants/species of a gene, the segment of DNA that serves a single function. Most non-lethal mutations to an existing allele tend to leave its function entirely unchanged, which clearly makes for a neutral theory. The seminal work of Hubbell [76] is also similar to that of Moran. Whereas Kimura regarded allele mutations which were often synonymous and therefore neutral, Hubbell argues that different species also follow neutral behaviour and calculates the steady state abundance distribution that follows from such an assumption plus a constant influx of immigrants. The Hubbell model assumes that each organism from any species competes equally with all others, and therefore as with Moran the species' probability of reproducing or dying is proportional to its fraction of the population. Hubbell predicts the distribution of species abundances, a binned plot of the number of species that belong in bins of exponentially increasing population size. Following the arguments of Hubbell, one can get an

estimate of the expected biodiversity of a community, the number of species that should exist in the trophic level (those species which generally consume upon the same set of prey and are preyed upon by the same set of predators). The abundance distribution he predicts matches well with Fisher's log series distribution [**?** **?**] and with experimental observations in a variety of biological contexts, from trees to birds to microbiomes [76]. The Moran model with immigration analyzed in chapter 3 can be thought of as a variant of Hubbell's theory with recurring immigrants from the same species. While I do discuss abundance distributions I also calculate the (temporary) extinction probability and timescale, something Hubbell's work does not address (but see [91, 130, 154**?** **?**] for approximate solutions or models with speciation rather than immigration).

Hubbell's assumption of complete neutrality whereby each species competes with all others to the same degree as intraspecies competition strains credibility. However, slight perturbations from Hubbell's theory do not significantly alter its results [163]. Furthermore, supporters claim that in some sense the different species are equivalent and behave neutrally, which is why Hubbell's theory seems to work so well in such disparate ecologies [77, 110, 163**?**].

0.4 Stochastic analysis

The confusion and debate that surrounds niche overlap and other such parameters originates because they are phenomenological parameters rather than strictly physical ones. A phenomenological parameter is one that is consistent with reality without being directly based on physical interactions. In principle these parameters can be derived from physical, measureable quantities. The common problem is that there are too many factors, and so many are unknown, that it is easier simply to subsume them all into one phenomenological parameter like carrying capacity and use that in our modelling and analyses. Including noise in our modelling accounts for the many unknown and variable factors contributing to each phenomenological parameter.

Stochasticity is the technical term for randomness or noise in a system. Whereas over time the solution to, for example, a logistic differential equation simply increases continuously (and differentiably) toward its asymptote at the carrying capacity, a stochastic version allows for deviations from this trajectory, sometimes decreasing rather than steadily increasing toward the steady state, and thereafter fluctuating about the carrying capacity. See figure 0.4 for a visualization. Depending on the system of interest, stochasticity may or may not be relevant: it is usually most important for systems with highly variable environments or small typical population sizes. In the biological context Wright and Fisher were pioneers in applying randomness and statistical reasoning. There have since been renaissances in the stochastic treatment of genetics due to Kimura and ecology due to Hubbell, and with new mathematical and computational developments it is popular today.

Fluctuations caused by stochasticity empower us to find new features in our models. Most importantly, in rare cases the fluctuations can bring a system to an absorbing state of zero population, in which case it does not recover. This arrival at zero population is known as extinction, and is the main phenomenon of study in this thesis. Each stochastic model has a deterministic analogue that is arrived at as fluctuations go to zero; extinction is not typically seen in the deterministic analogue and is a uniquely stochastic processes. The time before extinction is a random variable and hence follows a probability distribution with a defined mean. More generally in the field of stochastic analysis this is known as a mean first passage time, the mean time before a system first reaches some predefined state or collection

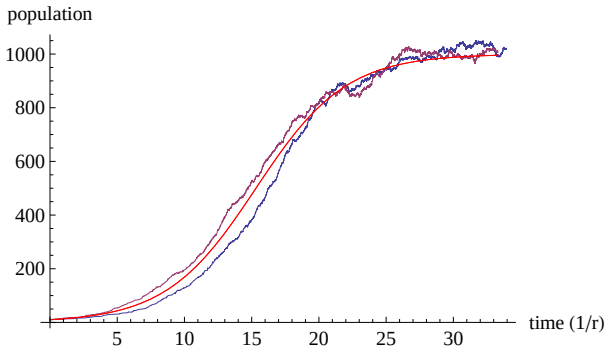

Figure 2: *A single logistic system with deterministic and stochastic solutions.* The smooth red line shows the deterministic solution to a one dimensional logistic differential equation (x from equation 0.2 with $a = 0$) with carrying capacity $K = 1000$, which the system asymptotically approaches. The jagged blue and purple lines are each an instantiation of a 'noisy', or stochastic, version of the logistic equation, as simulated using the Gillespie algorithm. Notice that the stochastic versions tend to follow their deterministic analogue but with some fluctuations, sometimes being greater than the deterministic result, sometimes being lesser.

of states. The first passage time is random because the state itself is a random variable, described by its own probability distribution. The probability distribution of being at a given state (in a biological context, a population size) evolves in time according to its master equation. The master equation for a birth-death process, one that only allows transitions of increasing (birth b) or decreasing (death d) one individual at a time, is a continuity equation for the probability P_n of being at state n at time t [65, 139]:

$$\frac{dP_n}{dt} = b_{n-1}P_{n-1}(t) + d_{n+1}P_{n+1}(t) - (b_n + d_n)P_n(t). \tag{2}$$

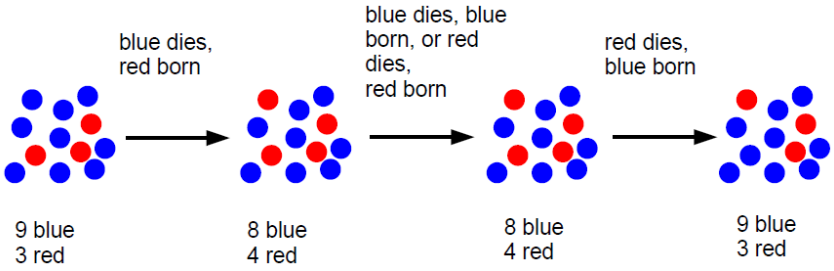

Figure 3: *1D lattice figure.* This is just a placeholder. Make sure to reference this in the text as well!

Stochasticity originates from two main causes. It can arise from the extrinsic fluctuations of the environment [86**?**], in that limiting factors like resource availability or temperature fluctuate over time. It is also intrinsic to any system with a finite countable size. A deterministic system like the logistic one shown in figure **??** has a continuous solution, but the number of bacteria cannot vary continuously between 999 and 1000 but is discretized. Constraining the system to integer values, and the inherent randomness in the birth and death times of the individuals, leads to demographic noise [13, 40, 44, 54, 58, 62, 68, 114, 190]. Demographic stochasticity is the focus of my thesis. Chapter 1 deals with the inclusion of demographic fluctuations in a deterministic equation.

It is accepted in the literature that demographic noise in a system whose deterministic analogue has a stable fixed point leads to extinction times scaling exponentially in the system size [48, 54, 85, 108, 191**?**

]. That is, if K is the constant or mean system size, then demographic fluctuations lead to:

$$\tau \propto e^{cK}$$

for some constant c. This scaling is most readily observed in the logistic system [7, 13–15, 55, 140**?**], which is also covered in chapter 1. Environmental noise in the logistic system has polynomial scaling of the mean extinction time [142**?**]:

$$\tau \propto K^d$$

for some constant d. Importantly for this thesis, polynomial dependence on system size is also found when there is no fixed point in the deterministic analogue, or one of neutral stability, like the Moran model [47, 54]. When the deterministic fixed point is unstable extinction happens even in the deterministic limit, and is logarithmic when starting from the fixed point [54, 108, 145]:

$$\tau \propto \ln(K).$$

In all these cases K is the system size, typically taken to be some measure of the magnitude of the fixed point when relevant. Often this fixed point is the carrying capacity. For those systems where the fixed point is stable, the extinction time also does not tend to depend on the initial conditions [40], as the deterministic draw to the fixed point is greater than the destabilizing effects of noise, and it is only a rare fluctuation that leads to extinction. A mean time to extinction that is exponential in the population size is commonly considered to imply stable long term existence for typical biological examples, which have large numbers of individuals [81, 142]. A sub-exponential extinction time implies exclusion of a species, and a reduction of the biodiversity of the ecosystem.

Stochastic equations are generally hard to solve, with a solution only reliably being found for one dimensional systems of birth-death processes [65, 139**?**]. The dimensionality, in an ecological context, is given by the number of distinct species or strains being modelled. Particular realizations of solutions to the master equation are found via the Gillespie algorithm, also knows as the stochastic simulation algorithm [29, 66]. For most of my research I calculate the mean time to extinction exactly, or at least to arbitrary accuracy, following a textbook formulation that involves inverting the transition matrix [139, 140, 146, 147]. There also exist many approximation techniques to deal with stochastic problems, which I discuss in the next chapter.

0.5 Structure of Thesis

The major questions of this thesis are: What are the probability and timescale of a single species extinction in an ecosystem? How should the probability and mean time to extinction be calculated? Inspired by problems of biodiversity, what is the mean time to fixation of two competing species? Conversely, what is the probability and timescale of invasion of a second species into an ecosystem occupied by a first? The structure of the thesis is as follows.

First, I use the exact techniques mentioned above and introduced more completely in sections 1.3 and 1.4 to investigate a one dimensional logistic system, comparing the influence of the linear and quadratic terms to the quasi-steady state distribution and the mean time to extinction. Chapter 1 is largely technical in nature, though I do show that intraspecies interactions are most prone to lead to

extinction when they increase death rates rather than reduce birth rates. The simple system considered in this chapter also affords a thorough comparison of the common approximation techniques to stochastic problems. I demonstrate the Fokker-Planck approximation works well close to the deterministic fixed point, but incorrectly estimates the scaling of the extinction time with system size, as is known by.... The WKB approximation performs better, but misidentifies the prefactor to the exponential scaling. The failure of Fokker-Planck exists in the literature [55, 70, 142, 191], but to my knowledge the WKB method is trusted to be exact, and no one has done a careful investigation of these approximation techniques (but see [7, 191]). The exact techniques and the approximations together make up chapter 1, regarding a one dimensional system. This chapter is being prepared as a paper for publication [**?**].

The natural extension from a one dimensional logistic is to couple two such systems together. This two dimensional generalized Lotka-Volterra system, the subject of chapter 2, allows me to study biodiversity maintenance. I probe how long two species will coexist by calculating the mean time to fixation in the system. It was already known that the overlap of their ecological niches is the parameter that controls the transition between effective coexistence and rapid fixation. I determine that two species will effectively coexist unless they have complete niche overlap, even if they have only a slight niche mismatch. Along with the MTE, my analysis uncovers a typical route to fixation, or rather a lack of a typical route, the discussion of which wraps up this chapter.

The next chapter, chapter 3, extends the scope of this thesis to invasion of a new species into an already occupied niche. I calculate the probability of a successful invasion as a function of system size and niche overlap. Then the MTE conditioned on the success of the invasion is analyzed. I discover that the closer the invader is to having complete niche overlap with the established species, the less likely it is to successfully invade, and the longer an invasion attempt will take before it is resolved. Once these timescales are developed, I regard the Moran/Hubbell model modified to account for repeated invasions of the same species. I identify the critical value of the immigration rate above which a species will have a moderate population size and below which the population is either large or largely absent in its contribution to the abundance distribution. Chapter 2 and half of chapter 3 together form another paper being reviewed for publication [16].

In the final chapter I address some of the big questions I have raised. Based on chapter 2 I infer when two species will coexist, and discover that even a small departure from Hubbell's assumption of neutrality drastically complicates its predictions. So long as there are slight differences in their niches the many species of plankton can coexist. Chapter 3 does not show a qualitative difference in invasion probabilities as niche overlap approaches unity. But between its analysis of invasion into the Lotka-Volterra model and its steady state solution of the Moran model with immigration... The final chapter is also where I explore experimental tests, applications and extensions of the results arrived at in this thesis, and suggest next steps for this research, both continuations and implementations to novel situations.

Chapter 1

Going from One Species to Zero

This chapter is based on a paper written by myself, Jeremy Rothschild, and our supervisor Anton Zilman, which is currently be prepared for submission [**?**].

1.1 Introduction

As deterministic dynamics have a longer history of being applied in a biological context than their stochastic analogues, and as deterministic mathematics are easier to solve, many researchers start with a deterministic approach to their problem of choice. This is not a bad thing; it allows them to get a sense of the problem if noise is minimal or negligible, which is often the case. One problem with going from deterministic to stochastic dynamics is that the mapping is not unique; many stochastic problems give the same deterministic limit as noise becomes small. For this reason I argue that the stochastic description should be explicitly chosen and motivated, for any analysis which involves stochasticity even in part. In this chapter I will justify my argument in two ways, both of which use the ubiquitous example of the Verhulst, or logistic, model. Using the metrics of the quasi-stationary probability distribution function (QPDF) and the mean time to extinction (MTE) I will show that the allocation of linear and nonlinear contributors between the birth and death rate has a drastic effect, and I will evaluate the validity of various commonly employed approximation techniques.

The deterministic equation I consider is the logistic equation, one of the most common models to describe a biological system [5, 6, 15, 72, 136, 138, 140, 142**?**]. It shows up in epidemiology [12**?**], biodiversity [**?** **?**], and generally as a default for modelling a population that grows to a constant value [**?** **?**]. For a population of n individuals, I will be dealing with stochastic equations that give the deterministic limit

$$\frac{dn}{dt} = r\,n\left(1 - \frac{n}{K}\right), \tag{1.1}$$

where r is a rate constant and K is a carrying capacity, a phenomenological measure of the system size. The deterministic equation arises as a large population limit of a stochastic system [64, 139, 164]; namely it is the difference of the stochastic birth and death rates. Therefore when starting from only a deterministic equation there is some freedom to choose the stochastic rates for birth (b_n) and death (d_n). As the choice of birth and death rates contains ambiguity, researchers have leeway in making their decision, resulting in a variety of similar but distinct models [5, 6, 15, 72, 136, 138, 140, 142**?**]. These models, despite showing the same limit when fluctuations are small, are not equivalent for

the stochastic measures chosen in this chapter. The logistic equation includes interactions between organisms by introducing a nonlinearity into the birth or death rates [5, 6, 15, 72, 136, 138, 140, 142**?**]. Biologically this means the per capita birth rate is reduced by the presence of competitors, for instance if the competitors reduce the resource abundance and growth is slowed [135, 181]. Alternatively, the per capita death rate can be increased by neighbours, perhaps due to secreted factors like toxins or waste products introduced by those neighbours [72, 158, 177]. The biological reality determines how this shows up in a mathematical model that captures the growth and decay of the population. I include the parameter δ to account for the stochastic relevance of the absolute values of the per capita birth and death rates, but in the deterministic limit only their difference r affects the dynamics of the system. Parameter q describes where the intraspecies inhibition acts: a high q near unity implies competition for resources and a decreased effective birth rate, whereas a low q near zero reflects more direct conflict, with intraspecies interactions resulting in greater death rates of organisms. Only the difference of the stochastic birth and death rates is observed in the deterministic dynamics, so anything that acts to commensurately change both the birth and death rates is undetected [136, 140]. A systematic exploration of the effect of these "hidden parameters has not been undertaken.

There is a choice to be made when modelling a particular biological system as to how much intraspecies interactions should affect a species birth rate, death rate, or both. The objective of this work is to investigate the impact of this choice on one measurable quantity, the mean time to extinction (MTE). Generally a community is made up of many species; mathematically the dimensionality of the problem is constrained to the number of species [10]. This will be elaborated upon in the next chapter. In most cases, only the one dimensional MTE can be solved exactly [140]. In more complicated situations an approximation is necessary, and there exist many such techniques [64, 139]. These techniques tend to rely on a system size expansion and assume that the population is typically large, a reasonable assumption in most biological systems.

First, I will introduce the model in more detail, motivating it and presenting the parameters associated with the ambiguity of the deterministic equation. Then both the steady state population distribution and the MTE will be calculated under different biological assumptions. Various common approximation techniques will be investigated and compared to the exact results. Finally, a discussion of the results will conclude that increasing the birth and death rates commensurately leads to greater population variance and lesser MTEs, and that the choice of model is of critical importance when establishing a system from which to draw conclusions.

1.2 1D logistic model

The simplest model of an isolated population has linear birth and death terms (that is, the per capita birth and death rates are constant: $b_n/n = \beta$, $d_n/n = \mu$). The difference between per capita birth and death gives some rate constant r, the Malthusian or exponential growth rate, such that the deterministic per capita growth would be $\frac{1}{n}\frac{dn}{dt} = r$. This model is a classic but gives the outcome of population explosion. Even in the stochastic case, there is a finite probability of population explosion, and the mean diverges [139]. To mathematically curb this infinite growth, and to biologically allow for intraspecies interactions, a non-linear term is required. A quadratic is the easiest non-linearity to handle, such that $\frac{1}{n}\frac{dn}{dt} = r\left(1 - \frac{n}{K}\right)$. The rate constant is inhibited by the density of the population, hence a decrease by n/K, giving the desired quadratic term. This is exactly the logistic equation 1.1.

Extinction occurs at $n = 0$, with flux from small populations. In this thesis I consider only birth-death processes, so in fact extinction would only occur from the last individual organism dying before reproducing. This adds additional motivation to the choice of a quadratic equation. For any per capita dynamics $r\, f(n/\tilde{K})$ with some large system parameter $\tilde{K}$ that gives exponential growth at small population we can write an expansion $f(n/\tilde{K}) \approx f(0) + f'(0)n/\tilde{K}$. Defining $K \equiv -\tilde{K}/f'(0)$ we recover the logistic equation for small populations. For example, if exponential growth is inhibited by Michaelis-Menten kinetics such that $\frac{1}{n}\frac{dn}{dt} = r\left(1 - \frac{n}{n+\tilde{K}}\right)$, at small population the dynamics are the same as the logistic equation, with $K = \tilde{K}$. Since I concern myself with extinction, it is exactly the dynamics of small populations that interests me; the population can have different behaviour at large n, but my MTE results should still hold validity. Note that the QPDF will in general be different, and that most approximation techniques considered in this chapter work best near the mean of the QPDF rather than near the small population sizes relevant to extinction.

Extinction occurs at $n = 0$, an unstable fixed point of the logistic equation, whereas there is a stable fixed point at $n = K$. Common practice in dynamical systems analysis is to rescale variables to remove parameters and simplify the system. Since we are dealing with continuous time we can remove the rate constant from our equation; I do so by rescaling the time by r. Similarly, in the deterministic equation 1.1 we could rescale n by K and have no remaining parameters. However, in the stochastic version we cannot apply this latter rescaling, because of the implicit population scale of ± 1 organism for each birth/death event. The integer number of organisms in systems with demographic noise has an implicit population scale of 1.

The system being constrained to integer populations gives a clear example of why the deterministic analysis is insufficient. Instead of the continuous, fractional populations of equation 1.1, I must define birth and death rates. I assume that each birth event is independent and distributed exponentially with a probability $b_n\, dt$ of occurring in each infinitesimal time interval dt, and this is similarly assumed for death events. In this chapter/to this end I use the birth rate

$$b_n = (1+\delta)\, r\, n - \frac{r\, q}{K} n^2 = r\, n \left(1 + \delta - q\frac{n}{K}\right) \tag{1.2}$$

and death rate

$$d_n = \delta\, r\, n + \frac{r(1-q)}{K} n^2 = r\, n \left(\delta + (1-q)\frac{n}{K}\right). \tag{1.3}$$

Note that I introduce two new parameters in the equations 1.2 and 1.3: $q \in [0, 1]$ shifts the nonlinearity between the death term and the birth term, whereas the parameter $\delta \in [0, \infty)$ establishes a scale for the contribution of linear terms in both the birth and death rates. I include the parameter δ to account for the stochastic relevance of the absolute values of the per capita birth and death rates; in the deterministic limit only their difference r affects the dynamics of the system. Parameter q describes where the intraspecies inhibition acts: a q near unity implies competition for resources and a decreased effective birth rate, whereas a low q near zero reflects more direct conflict, with intraspecies interactions resulting in greater death rates of organisms. It can be readily checked that $b_n - d_n$ recovers the right-hand side of equation 1.1 where, as per design, the new parameters q and δ do not appear. The choice of these parameters specifies a particular model and has consequences on the QPDF and MTE.

The model described above has one other notable feature. Except at $q = 0$, there is a population at which the competition brings the effective birth rate to zero. This is the maximum size the population

can achieve, and I define this cutoff as

$$N = \frac{1+\delta}{q}K. \tag{1.4}$$

Therefore I limit my calculations to the biologically relevant range $n \in [0, N]$. Already it is evident that the "hidden" parameters of δ and q have an effect on the system, as different values of the parameters will naturally define a range of states accessible in the model. Note that so long as $q \leq 1$ the death rate is positive semi-definite for the domain of interest. At $n = 0$ both the birth and death rates go to zero: this is the stochastic absorbing state.

1.3 Quasi-stationary Probability Distribution Function

A probability distribution function is a useful mathematical tool to describe the state of a dynamical system. I denote $P_n(t)$ as the probability that the population is composed of n organisms at time t. The evolution of the distribution in the single birth and death process is captured in the master equation

$$\frac{dP_n}{dt} = b_{n-1}P_{n-1}(t) + d_{n+1}P_{n+1}(t) - (b_n + d_n)P_n(t). \tag{1.5}$$

Note that ultimately at large times the probability of being at population size $n \neq 0$ decays to zero, as more and more of the probability gets drawn to the absorbing state. Although this is an important property of this model, it is difficult to describe any dynamics of our model with such a distribution. The approach to the true steady state is slow (on the order of the MTE; see next section below). Prior to reaching extinction, the system tends toward a quasi-stationary distribution. That is, after some decorrelation time, the system reaches a state that only changes very little as it leaks probability into the absorbing state at extinction.

I am interested in this conditional probability distribution function P_n^c: the probability distribution of the population conditioned on not being in the steady extinct state.

$$P_n^c = \frac{P_n}{1 - P_0}.$$

The dynamics of this conditional distribution are described in a slightly different master equation than equation 1.5:

$$\frac{dP_n^c}{dt} = b_{n-1}P_{n-1}^c + d_{n+1}P_{n+1}^c - \big(b_n + d_n - P_1^c d_1\big)P_n^c. \tag{1.6}$$

After an initial transient period, this conditional probability will stabilize to some steady $\tilde{P}_n^c$ for which $d/dt\,\tilde{P}_n^c = 0$. The steady state of this distribution is referred to as the quasi-stationary distribution (qpdf), not to be confused with the true stationary distribution of the population which is the state where $\tilde{P}_n(t \to \infty) = \delta_{n,0}$.

One way to obtain the quasi-stationary distribution is to exploit equation 1.6 in an algorithm which iteratively calculates the change in the distribution ΔP_n^c in an arbitrarily small time interval Δt until all change in the distribution is negligible [16]. Decreasing the time step Δt increases both the accuracy and the runtime, such that an arbitrarily accurate distribution takes a prohibitively long time to calculate. Instead I employ a different algorithm [139]: at steady state equation 1.6 can be rearranged to relate $\tilde{P}_{n+1}$ to $\tilde{P}_n$ and $\tilde{P}_{n-1}$; given that $b_0 = 0$ there is a lower cutoff and so the whole distribution can be written in terms of $\tilde{P}_1$, which is then solved by normalization. The former technique is shown in figure

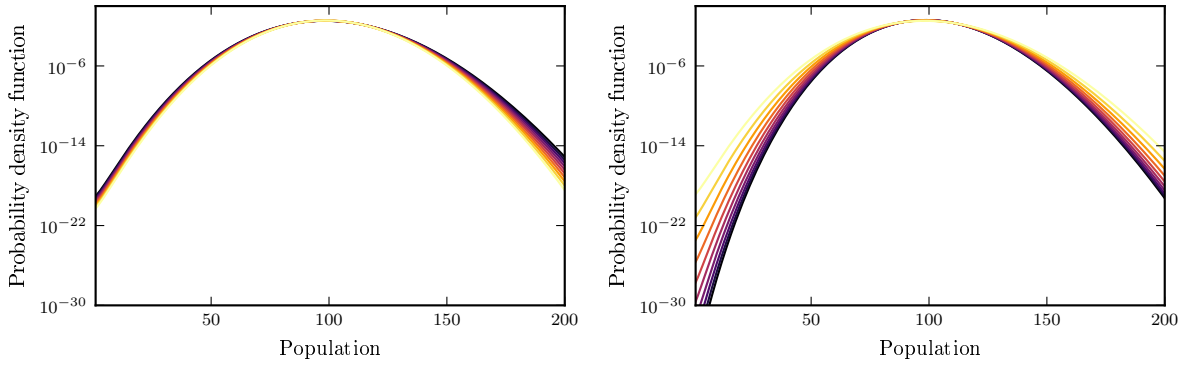

(a) *Probability distribution with* $\delta = 1.00$ *and* $K = 100$ (b) *Probability distribution with* $q = 0.06$ *and* $K = 100$

Figure 1.1: *Probability distribution of the population* The conditional probability distribution functions as found using the quasi-stationary distribution algorithm. Note that for each curve, the population cutoff N is outside the domain presented here. In 1.1a increasing lightness indicates an increase in q. Similarly, the lightness increase in 1.1b corresponds to an increase in δ

1.1, for different values of q and δ. Increasing the value of δ shifts the mode toward the anterior of the distribution and spreads the distribution out, increasing the variance. Decreasing q has a similar but lesser effect to increasing δ.

1.4 Exact Mean Time to Extinction

As described earlier, the system ultimately goes to the absorbing extinct state. The time in which this happens is a random variable, the mean of which is the mean time to extinction τ_e. In fact, in many cases the MTE nicely characterizes the distribution of exit times, which is typically observed to look roughly exponential. Because the absorbing point is deterministically repelling and, as the QPDF shows, the system spends most of its time near the deterministic fixed point, extinction events are rare, as are trajectories that get close to extinction. These extinction attempts can be considered as almost independent, since the decorrelation time is so much shorter than the time between attempts. The system has repeated, independent events that occur with at a constant rate; it is Poissonian, hence the distribution of extinction times is exponential and described by its mean, the MTE.

For one-species systems it is well known how to exactly solve the MTE for a birth-death process [139**? ?**]. The mean time of extinction, for a population of size n, is

$$\tau(n) = \frac{1}{d(1)} \sum_{i=1}^{n} \frac{1}{R(i)} \sum_{j=i}^{N} T(j) \tag{1.7}$$

where

$$R(n) = \prod_{i=1}^{n-1} \frac{b(i)}{d(i)} \quad \text{and} \quad T(n) = \frac{d(1)}{b(n)} R(n+1).$$

Combining equations 1.2 and 1.3 with the solution for the mean time to extinction 1.7 obtains a complicated analytical expression in the form of a hypergeometric sum. Little intuition can be gained from the mathematical expression, but the numerical results of the MTE, as shown in figure 1.2, are more

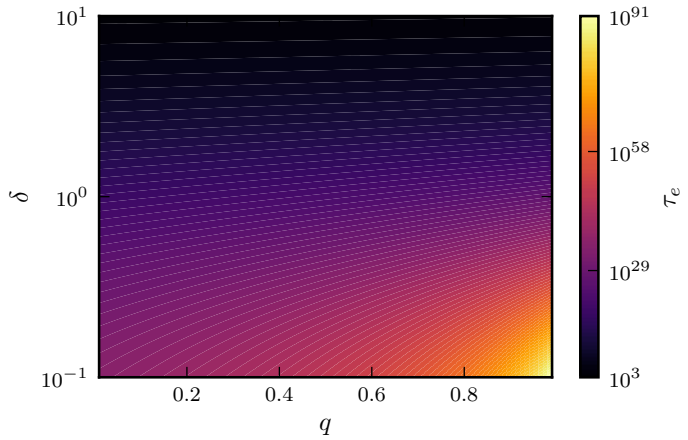

Figure 1.2: *Exploring the mean time to extinction in the parameter space* Recall that q shifts the nonlinearity between the birth and death rates: for $q = 0$ the nonlinearity is purely in the death rate, for $q = 1$ nonlinearity appears only in birth. The birth and death rates are increased simultaneously with δ.

interpretable.

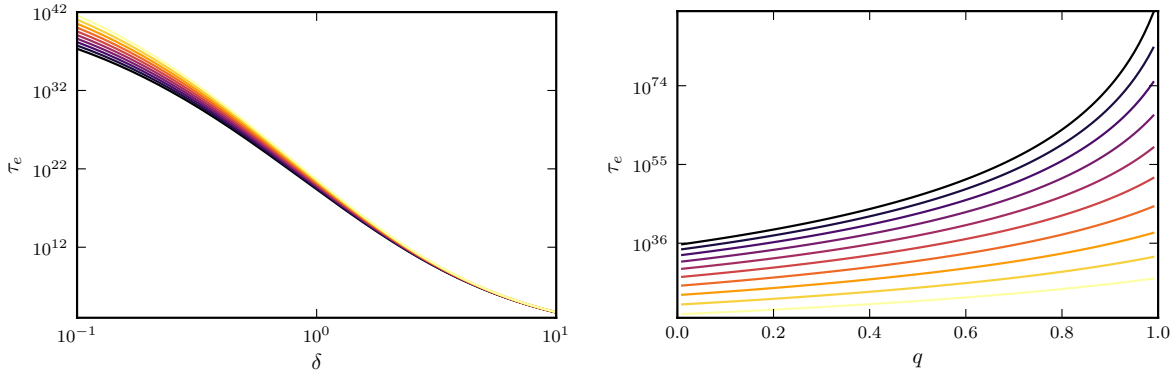

(a) *Varying* δ (b) *Varying* q

Figure 1.3: *Mean time to extinction for varying* δ *and* q Each line represents a slice in Figure 1.2: Figure 1.3a are vertical slices which show how, for different values of q, the δ affects τ. Similarly Figure 1.3b are horizontal slices which show how, for different values of δ, the q affects τ. As in Figure 1.1, lightness of the line indicates an increase of 1.3a q and 1.3b δ

A typical trajectory starting from n goes first to the deterministic fixed point K and fluctuates about that point before a large fluctuation leads to its extinction. Since the time for the population to reach carrying capacity is insignificant compared to the extinction time, the MTE is largely independent of the initial population, and I write $\tau(n) \approx \tau(K) \equiv \tau_e$ for all n. This approximation only fails for small n. It is well known that τ_e goes like e^K [142] and this is indeed what I observe. What is less well known is the dependence on the hidden parameters. It is evident that the MTE depends on the values of δ and q, parameters that appear in the births and deaths but do not appear in the deterministic equation. Increasing the scaling of the linear terms δ in birth and death rates has a tendency to decrease τ_e. On the other hand, shifting the nonlinearity from the death to the birth rate, in other words increasing q,

causes an increase in τ_e. Note however that the effect of q is magnified for smaller values of δ and weaker for larger values of δ: see figure 1.3.

1.5 Approximations

As shown above, for a one-species model it is possible to write down a closed form solution for the MTE τ_e. However, finding a general solution for the mean time to extinction given multiple populations, and therefore higher dimensions, is not as trivial. Nor can a nice analytic expression be found, even for a single species. Models of stochastic processes away from equilibrium are also difficult to study. Many approximations have been developed to accommodate these complications. These approximations make the calculations possible or reduce the computing runtime significantly; therefore it is important to know which of these tools to use and when they are applicable. Unfortunately the regime of parameter space in which each approximation is valid is not very well understood. Using the same model system of a single logistic species I shall evaluate these approximations and compare them to the above exact results, in order to gain insight into their utility.

The first approximation I will regard is the Fokker-Planck (FP) equation, which approximates the discrete populations as continuous, while still maintaining stochasticity. It is equivalent to writing a Langevin equation [**?**]. Starting from the master equation 1.5 and expanding the ± 1 terms as $P_{n\pm1} \approx P_n \pm \partial_n P_n + \partial_n^2 P_n$ we arrive at the popular Fokker-Planck equation:

$$\partial_t P_n(t) = -\partial_n\big((b_n - d_n)P_n(t)\big) + \frac{1}{2}\partial_n^2\Big((b_n + d_n)P_n(t)\Big). \tag{1.8}$$

In going from the master equation to FP I have used the Kramers-Moyal expansion [64]. Pawula theorem says that when employing the Kramers-Moyal expansion the only valid orders to stop the expansion are at two terms or infinite [**?**]. I have been cavalier; more precisely, we need a large parameter, which I denote K, to do the expansion. Typically in bio the large parameter is volume. Then $x = n/K$ is something like density, and is the parameter about which we expand, requiring that $|1/K| \ll 1$. Furthermore, the expansion requires that the rates W_n can be written in a form $W_n/K = w(x)$. The more pedagogical Fokker-Planck equation is then

$$\partial_t P(x,t) = -\partial_x\big((b(x) - d(x))P(x,t)\big) + \frac{1}{2K}\partial_x^2\Big((b(x) + d(x))P(x,t)\Big), \tag{1.9}$$

which is equivalent to equation 1.8 above for $b(x) = b_n/K$ and similarly for d. Instead of a difference differential equation for the probability, equation 1.8 is a partial differential equation for the probability density. The first term on the right hand side is called the drift term and corresponds to the dynamical equation at the deterministic limit, when fluctuations are neglected. The second term is the diffusion term and describes the magnitude of the effect of stochasticity on the system. A quasi-steady state can be calculated when the time derivative $\partial_t P_n(t)$ is small. That is,

$$\ln P_n^{ss} \propto \frac{2(b_n - d_n) - \partial_n(b_n + d_n)}{(b_n + d_n)}. \tag{1.10}$$

By analogy with Boltzmann statistics, the right-hand side of the above equation is sometimes referred to as a pseudo-potential [**?**]. Equation 1.8 can also be solved directly to give a MTE [64]. For ease of

reference, I leave the equation here:

$$\tau(n) = 2\int_0^n dy \frac{1}{\phi(y)} \int_y^\infty dz \frac{phi(z)}{B(z)} \tag{1.11}$$

In the above, $phi(x) = \exp\left[\int_0^x dn 2A(n)/B(n)\right]$, $A(n) = b_n - d_n$, and $B(n) = b_n + d_n$.

To simplify the situation further the birth and death rates can be linearized about a stable fixed point, which implies a Gaussian solution to the FP equation. More specifically, the drift term is replaced with $(n-n^*)\partial_n(b_n - d_n)|_{n=n*}$ (since $(b_n - d_n)|_{n=n*} = 0$) and the diffusion with $(b_n + d_n)|_{n=n*}$. We only expect this further approximation to hold near the fixed point. If we extend the domain to all space the solution is Gaussian, peaked near the fixed point.

Another method frequently utilized is the WKB approximation []. Generally, the WKB method involves approximating the solution to a differential equation with a large parameter (such as K) by assuming an exponential solution (an ansatz) of the form

$$¶_n \backsim e^{K\sum_i \frac{1}{K^i} S_i(n)}. \tag{1.12}$$

Starting again from the masters equation 1.5, one can immediately apply the ansatz in the probability distribution and solve the subsequent differential equations to different orders in $1/K$[14**?**].To leading order, only $S_0(n)$ is needed. This method is commonly referred to as the real-space WKB approximation, wherein we obtain a solution for the quasi-stationary probability distribution. Another method, known as the momentum-space WKB, is to write an evolution equation of the generating function of P_n, the conjugate of the master equation, and then apply the exponential ansatz [**?**]. The momentum-space WKB has been shown to differ from real-space WKB [**?**], and has gone out of favour. Real-space WKB remains popular. The quantity $S_0(n)$ can be interpreted as the action in a Hamilton-Jacobi equation. Its solution is $S_0(n) = \int_{n=0}^{n^*} \ln\left(\frac{b_n}{d_n}\right)$. From the pdf, the MTE is calculated via $\tau = \frac{1}{d_1 P_1}$ [**?**].

Rather than approximating the probability distribution function near the fixed point, a different approximation can be done to estimate the probability distribution function near the absorbing state $n = 0$. If the bulk of the probability mass is centered on K then the probability of being close to the absorbing state is small (note that this condition is similar to the quasi-stationary approximation, since the flux out of the system is proportional to the probability of being at a state close to 0). Furthermore, it is assume that the probability distribution function grows rapidly, away from the absorbing state, such that $P_{n+1} \gg P_n$, whereas neighbouring birth and death rates are of the same order [**?**]. Rewriting the master equation 1.5 as $\partial_t P_n = (b_{n-1}P_{n-1} - b_n P_n) + (d_{n+1}P_{n+1} - d_n P_n)$ one approximates the left hand side as zero and the right hand side as $(-b_n P_n) + (d_{n+1}P_{n+1})$. Rearranging this gives $P_n = \frac{b_{n-1}}{d_n} P_{n-1} = \prod_{i=2}^{n} \frac{b_{i-1}}{d_i} P_1$. P_1 can be found by ensuring the probability is normalized; despite the sum extending beyond the region for which $P_{n+1} \gg P_n$ is valid, the probability distribution generated from this small n approximation is qualitatively reasonable and is used, in conjunction with approximations that work near the fixed point, to verify numerical solutions [**?**].

As seen above, certain of these approximation methods permit the calculation of a quasi-stationary distribution. Figure 1.4 gives an instance of the quasi-stationary distribution as a function of n (or x) for a choice of the parameters q, δ and K for each technique. Note that with this scale of the figure the WKB approximation and the quasi-stationary algorithm are not distinguishable by eye, though there are indeed slight differences. In general, the ability of the techniques to successfully approximate the

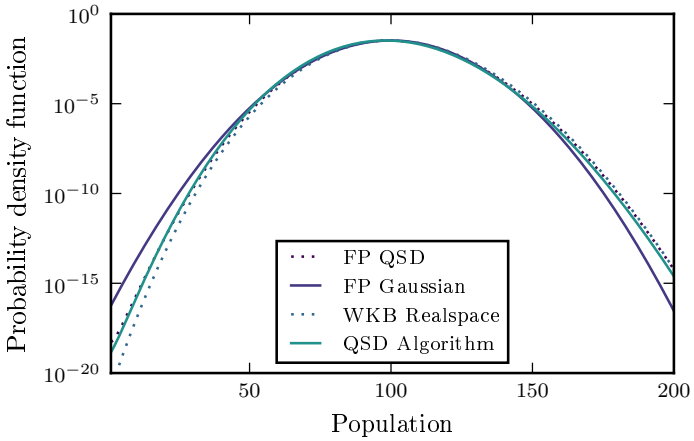

Figure 1.4: *Techniques for calculating a probability distribution function* A comparison of the different probability distribution approximations show how the described dynamics at equilibrium may differ for various techniques.

quasi-stationary distribution depends heavily on the region of parameter space. What I observe is that for large K the celebrated FP approximation is valid in all cases except for low δ and q. For small K it is a poor approximation except low δ and high q. The WKB method fares better, appearing to be reasonable everywhere in q, δ, K parameter space. All other approximations match near the fixed point but fail elsewhere.

It is also possible to obtain the mean time to extinction from these distributions. As described earlier, the quasi-stationary probability distribution leaks from P_n, a non-extinct population, to P_0. As since this is a single step process (with the population only changing by one individual per event), the only transition from which it can reach the absorbing state is through a death at P_1: all population extinctions must go through this sole state. The flux of the probability to the absorbing state is thus given by the expression $d(1)P_1$, hence the approximation [**?** **?**]

$$\tau_e \approx \frac{1}{d(1)P_1}. \tag{1.13}$$

This same equation can be applied to different methods and algorithms that have produced quasi-stationary distributions.

Having calculated the MTE using each approximation, I can now compare the results to the exact solution and verify their accuracy in the parameter space of q, δ, and K. These results are summarized in Figure 1.5. As with the probability distribution function, the difference between the solution of the approximations and equation 1.7 is dependent on q, δ and K. Most of the solutions tend to converge at very low K, though this is unsurprising as the techniques should all approach zero as K decreases and the initial condition of K approaches the final absorbing state at 0. With increasing K the divergence of each approximation becomes more evident. I find that while no approximation works well for large δ, many of them recover the correct scaling in K, albeit off by a factor. For all other parameter regimes, small n and the WKB approximation are both reasonable approximations for the exact results.

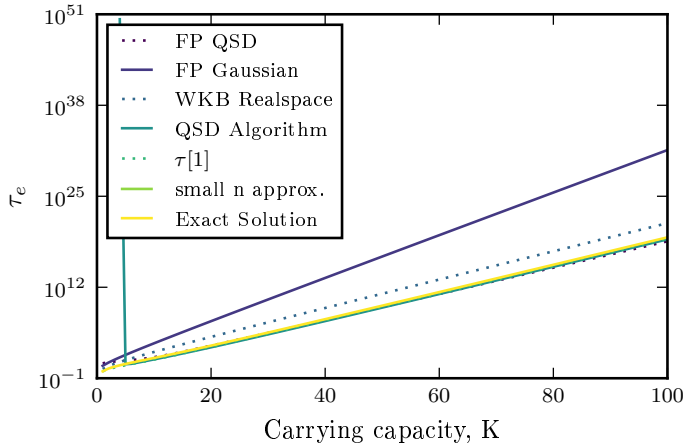

Figure 1.5: *Techniques for calculating the mean time to extinction* Plotted as a function of the carrying capacity, a comparison of the ratio of the MTE of different techniques to that of the 1D sum reveals the ranges for which they are more accurate for approximating τ_e.

1.6 Discussion

What is the justification for the use of q and δ in the birth and death rates? These parameters are products of the assumptions made in constructing the mathematical framework that change the behaviour of the models without affecting the deterministic dynamics. The parameter δ gives a scale for the linear per capita birth and death rates individually (rather than their difference r). This scaling differentiates systems with low birth and death rates from those with high turnover, even when the two models would have the same average dynamics. Whereas the deterministic dynamics includes only the difference of birth and death and will not distinguish between populations with high or low turnover, the size of the birth and death rates is still of relevance. For example, the probability of extinction of a system with linear birth and death rates starting from population n_0 goes as $(b_n/d_n)^{n_0}$ [139]. In this context, the model with high turnover will differ from one with low turnover as the ratio b_n/d_n will depend on the scale, that is to say, on δ.

Additionally, q determines where the quadratic dependence lies, whether more in the birth or death rate. By having the nonlinearity in the birth, one is assuming that the competition, modelled by the quadratic term, slows down the birth rate, for instance in the form of quorum sensing [135]. If it were present in the death the supposition is that the competition instead kills off individuals, for example with illness spreading more rapidly in denser populations []. Although I have worked with a $q \in [0, 1]$, there is no mathematical reason why q could not take values outside this range. Negative values of q would increase both rates, meaning that the density dependence would in fact be beneficial for the birth rates, as in the Allee effect [], and of further significance for the death rates. All $q > 1$ has the opposite effect of negatively impacting both rates, signifying that population density would reduce both the birth and death rates.

Figure **??** summarizes the numerical results of equation 1.7 into a heat map of the mean time to extinction as a function of the two hidden parameters q and δ. For the range of q and δ explored, I find that the MTE changes similarly upon decreasing q and increasing δ, although it depends more sensitively on δ. It is not trivially apparent from the form of the exact analytical solution that the linear

contribution to the rates should be more significant. However, one can get an intuition for why this might be the case. At small populations, the linear term is of order δ (for $\delta \geq 1$) and the quadratic terms is of order q/K, hence the linear term dominates the small population end of the distribution. It is exactly this portion of the distribution that affects the MTE, as seen in equation 1.13.

These qualitative results can be readily intuited by considering the effect each of these parameters has on the distribution, see Figure **??**. A broader probability distribution function corresponds to a shorter MTE, as probability more readily leaks from the quasi-steady state solution to extinction. I find that decreasing δ sharpens the peak of the distribution and slightly shifts the mode posteriorly. As before, the reverse is true for varying q: similar tendencies are observed when q is instead decreased. As the population is allowed more variance about the carrying capacity, states further from the fixed point will be explored more frequently, increasing the probability that the system can stochastically go extinct. Varying the parameters has another effect on the probability distribution, as the parameters determine the maximum population size, restricting the possible states to those less than the population cutoff. It is readily checked, however, that this change in maximum population size has little to no effect on the MTE, by setting manual cutoffs in the numerical analysis and comparing the results to the true MTE. In any case, the mean extinction time of a single, self-interacting logistic species is now known, for all coefficients for first and second order terms.

Regarding the approximations, the best candidate in most regimes appears to be the WKB approximation. It generalizes to multiple dimensions without conceptual difficulty. Mathematically, at higher dimensions WKB necessitates solving a Hamiltonian system, in order to find a likely route to extinction along which to integrate; an analytic solution cannot be derived in general, and a symplectic integrator is necessary to find the numeric trajectory []. Nevertheless, in this one-dimensional case I find an analytic expression for the mean time to extinction using the WKB approximation to be

(1.14)

We can contrast this with the Gaussian approximation to the Fokker-Planck equation, which always gives an analytic result:

$$\tau_{\text{FP gaussian}} = \frac{2}{1+2\delta}\sqrt{2\pi K(1+\delta-q)} \tag{1.15}$$

Both formulae are dominated by their exponential dependence on K. This is to be expected, as the true solution with $\delta, q = 0$ increases as $\frac{1}{K}e^K$ [108]. It is the prefactor multiplying with the carrying capacity in the exponential that is of critical importance in determining the qualitative behaviour of the MTE. Lacking an analytical form for this prefactor in the exact solution, we can compare these prefactors in each approximation. The Gaussian Fokker-Planck solution has a prefactor $\frac{1}{2(1+\delta-q)}$, so we expect it to underestimate τ_e in the low parameter regime. To lowest order in δ and q the WKB approximation has a prefactor of $1 - 1/K$, which nicely matches the expected limit of 1. The WKB approximation matches well for all δ and q values, as seen in Figures 1.4 and 1.5. The other technique that successfully approximates the true probability distribution and mean extinction time is the small n approximation. It assumes the probability distribution grows rapidly, which is justified for small n and large K. Since the mean extinction time depends only on P_1 this technique gives a reasonable approximation for τ_e. I also note that inverting the transition matrix, as will be done in the following chapters, gives results practically identical to the analytic results.

How can the MTE be probed in a lab setting? For experimentalists the difficulty of measuring a

birth or death rate alone, as it changes with something like population density, varies with the system of interest. However, as previously discussed, measuring the average dynamics alone is insufficient. It is possible experimentally to corroborate some of the claims made in this chapter. For a bacterial species the birth rate could be inferred by the amount of reproductive byproduct present in a sample, for instance factors involved in DNA replication or cell division. The death rate is easily inferred from the birth rate and the average dynamics, or it can be measured using radioisotopes [**?**]. With these two rates and a couple of 96 well plates it should be a routine procedure to probe the quasi-steady state population probability distribution. A patient experimentalist could also verify the dependence of the MTE on δ and q.

The use of approximations is widespread and necessary when using mathematics to model real systems. One takeaway message of this chapter is that one must be mindful in their modelling. I find that FP, WKB, and small n are largely suitable in the models considered here, in that they recover the correct exponential scaling of the MTE with carrying capacity. The biggest caveat is that FP fails for low values of δ and q, and at low K. I will nevertheless use the Fokker-Planck equation to motivate some results in the next chapter, despite selecting a model with $\delta, q = 0$. Other techniques do not fare so well. It is common knowledge that various approximations have situations in which they are more or less applicable. Mindfulness in modelling not only refers to the method of solution, but to the choice of model itself. Historically the choice of model seemed to be one of taste or mathematical convenience [5, 6, 15, 72, 136, 138, 140, 142**?**]. So long as the correct deterministic results were given, the choice of model was not discussed. I have shown that stochastic assumptions have significant qualitative and quantitative effects on at least two metrics of interest in mathematical biology, including the MTE. This does not invalidate the results of past research, but it does imply that the results are valid only for the hidden parameters chosen at that time, and anyone looking to extend or generalize the results should be wary. Going forward armed with the knowledge that not all stochastic models are created equal, I argue that one should give careful regard to the biology of relevance when selecting a model. Our decisions must be informed by the real world if we are to make models that properly capture this biology.

Chapter 2

Going from Two Species to One

This chapter is based on a paper written by me and my supervisor Anton Zilman, which will be published in a Royal Society journal [16].

2.1 Introduction

The previous chapter treated the tractable problem of a single species undergoing only intraspecies interactions. Adding a second species complicates both the mathematics and the biology, but offers possible resolutions to the problem of biodiversity. Competitive exclusion suggests that only one species will persist in each ecological niche [**?**], but ecosystems like the ocean surface seem to have more species than there are niches [80]. Niche and neutral models both address this "paradox of the plankton" but a resolution remains elusive. Further study is required.

Deterministically, ecological dynamics of mixed populations have commonly been described using a dynamical system of the numbers of individuals of each species and the concentrations of the limiting factors [9, 10, 127]. Steady state coexistence typically corresponds to a stable fixed point in such dynamical system, and the number of stably coexisting species is typically constrained by the number of limiting factors. In some cases, deterministic models allow coexistence of more species than limiting factors, for instance when the attractor is a limit cycle rather than a point [10, 169]. Particularly pertinent for this chapter is the case when the interactions of the limiting factors and the target species have a redundancy that results in the transformation of a stable fixed point into a marginally stable manifold of fixed points. Then the stochastic fluctuations in the species numbers become important [8, 10, 27, 36, 156, 180]. I will return to the mathematical formulation of these concepts later.

Stochastic effects, arising either from the extrinsic fluctuations of the environment [86**?**], or the intrinsic stochasticity of individual birth and death events within the population [13, 40, 44, 54, 58, 62, 68, 114, 190], modify the deterministic picture. As in the previous chapter, I focus on this latter type of stochasticity, known as demographic noise. Demographic noise causes fluctuations of the populations abundances around the deterministic steady state until a rare large fluctuation leads to extinction of one of the species [40, 114**?**]. In systems with a deterministically stable coexistence point, the mean time to extinction is typically exponential in the population size [15, 85, 140, 142], as was seen in the previous chapter. Exponential scaling is commonly considered to imply stable long term coexistence for typical biological examples with relatively large numbers of individuals [81, 142].

By contrast, in systems with a neutral manifold that restore fluctuations off the manifold but not along it, mean extinction timescales as a power law with the population size, indicating that the coexistence fails in such systems on biologically relevant timescales [41, 92, 114, 133]. This type of stochastic dynamics parallels the stochastic fixation in the classical Moran-Fisher-Wright model that describes strongly competing populations with fixed overall population size [31, 61, 133, 159, 162, 170, 187**?**].

As is reviewed below, a broad class of dynamical models of multi-species populations interacting through limiting factors can be mapped onto the generalized Lotka-Volterra model. Lotka-Volterra models allow one to conveniently distinguish between various interaction regimes, such as competition or mutualism, and which have served as paradigmatic models for the study of the behavior of interacting species [8, 27, 36, 40, 44, 54, 58, 62, 91, 114, 180, 190]. Remarkably, the stochastic dynamics of LV type models is still incompletely understood, and has recently received renewed attention motivated by problems in bacterial ecology and cancer progression [31, 40, 58, 89, 170, 177]. There has also been the observation that for certain parameter values that the stochastic 2D generalized Lotka-Volterra model exhibits similar dynamics to the Moran model [40, 44, 114, 190]. How the system transitions from the typical LV results of MTE scaling exponentially with system size to the algebraic times of the Moran model is the main result of this chapter. The results outline the conditions of niche overlap and carrying capacity that allow two species to coexist (and conversely, those that will lead to relatively quick fixation).

In this chapter, I analyze a model of two competing species with the emphasis on the transition from deterministic coexistence to stochastic fixation. I use the master equation and first passage formalism that enables numerically solution to arbitrary accuracy in all regimes. First I will provide a definition of ecological niche [do I?!?] and a derivation of the competitive LV model, and examine its regimes of deterministic stability. Then I will introduce the stochastic description of the LV model and analyze fixation times as a function of the niche overlap between the two species. These results will be compared to known analytic limits, included here for completeness. I will make further comparisons to the Fokker-Planck and WKB approximations before concluding with a general discussion of the results.

2.2 Long-term stability of deterministic interacting populations

Quite generally, the dynamics of a system of N asexually reproducing species that interact with each other only through M limiting factors (such as food, soluble signaling and growth/death factors, toxins, metabolic waste) and experience no immigration can be described by the following system of equations for the species $x_1, ..., x_N$ and the limiting factor densities $f_1, ..., f_M$ [9, 10, 127]:

$$\dot{x}_i = \beta_i(\vec{f})x_i - \mu_i(\vec{f})x_i, \tag{2.1}$$

where $\vec{f}$ is the state of all factors that might affect the per capita birth rate $\beta_i(\vec{f})$ and the death rate $\mu_i(\vec{f})$ of the species i.

The density of a factor j in the environment, f_j, follows its own dynamical production-consumption equation

$$\dot{f}_j = g_j(\vec{f}, \vec{x}) - \lambda_j(\vec{f}, \vec{x})f_j \tag{2.2}$$

where g_j is a production-consumption rate that includes both the secretion and the consumption by

the participating species as well any external sources of the factor f_j, and λ_j is its degradation rate. Alternatively, for some abiotic constrains such as physical space or amount of sunlight, the concentration of the factor f_j can be set through a conservation equation of a form [10, 127] $f_j = c_j(\vec{f}, \vec{x})$.

The fixed points of the $N + M$ equations (2.1) and (2.2) determine the steady state numbers of each of the N species and the corresponding concentrations of the M limiting factors. However, the structure of equations (2.1) imposes additional constraints on the steady state solutions: at a fixed point $\beta_i(\vec{f}) = \mu_i(\vec{f})$ for each of the N species, which determines the steady state concentrations of the M limiting factors $\vec{f}$. However, if $N > M$, the system (2.1) of N equations is over-determined and typically does not have a consistent solution, unless the fixed point populations of $N - M$ of the species are equal to zero [9, 10, 60, 127, 156]. This reasoning provides a mathematical basis for the competitive exclusion principle, whereby the number of independent niches is determined by the number of limiting factors, and a system with M resources can sustain at most M species in steady state.

Nevertheless, as mentioned in the introduction, the number of species at the steady state can exceed the number of limiting factors, when the N equations for the species are not independent and thus provide less than N constraints on the solutions. In this case, at steady state the populations of the non-independent species typically converge onto a marginally stable manifold on which each point is stable with respect to off-manifold perturbations but is neutral within the manifold [8, 33, 54, 114, 127]. I return to this point in the following sections within the discussion of the Lotka-Volterra model.

2.3 Minimal model of interacting species and the derivation of 2D LV model

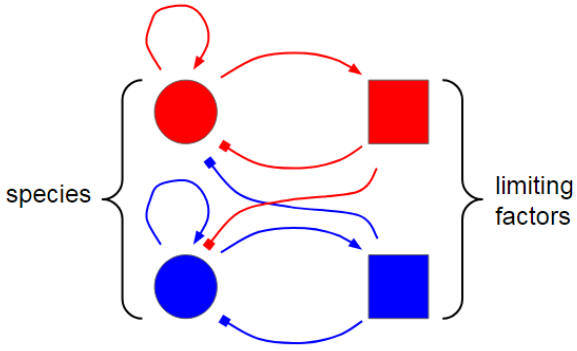

Figure 2.1: *A simple two species two resource model that derives the Lotka-Voltera model* Each of the two species (here, red and blue circles) reproduces (arrows to self) and produces a toxin (arrows to limiting factors, respectively red and blue squares) which inhibits its own growth (square-ending lines to self) and the growth of the other (square-ending lines to other colour).

As a minimal example, in this section I introduce a model of two interacting species whose dynamics is constrained by two secreted factors. Each species x_i has basal per capita birth rate β_i, death rate μ_i, and each generates the secreted soluble factors t_j at rates g_{ji}. Each factor t_i is degraded at a rate λ_i, and affects the death rate of each bacterium linearly with the efficacy e_{ij}. Positive e_{ij} may correspond to metabolic wastes, toxins or anti-proliferative signals [83, 123, 158, 177, 188**?**], while negative e_{ij} would describe growth factors or secondary metabolites [123, 185**?**]. The model kinetics is encapsulated in

the following equations for the turnover of the species numbers:

$$\begin{aligned}\dot{x}_1 &= \beta_1 x_1 - \mu_1 x_1 - e_{11} t_1 x_1 - e_{12} t_2 x_1 \\ \dot{x}_2 &= \beta_2 x_2 - \mu_2 x_2 - e_{21} t_1 x_2 - e_{22} t_2 x_2,\end{aligned} \tag{2.3}$$

and the equations for the production and the degradation of the secreted factors:

$$\begin{aligned}\dot{t}_1 &= g_{11} x_1 + g_{12} x_2 - \lambda_1 t_1 \\ \dot{t}_2 &= g_{21} x_1 + g_{22} x_2 - \lambda_2 t_2.\end{aligned} \tag{2.4}$$

Figure 2.1 gives a pictoral representation of the interactions of the two species (cirlces) and their associated toxins (squares), albeit with $g_{12} = g_{21} = 0$.

It is useful to recast Equations (2.3), (2.4) defining vectors $\vec{x} = (x_1, x_2)$ and $\vec{t} = (t_1, t_2)$, so that

$$\dot{\vec{x}} = \hat{R}\hat{X}\left(\vec{1} - \hat{E}\vec{t}\right) \quad \text{and} \quad \dot{\vec{t}} = \hat{L}\left(\hat{G}\vec{x} - \vec{t}\right), \tag{2.5}$$

where we have the matrices $\hat{X} = \begin{pmatrix} x_1 & 0 \\ 0 & x_2 \end{pmatrix}$, $\hat{L} = \begin{pmatrix} \lambda_1 & 0 \\ 0 & \lambda_2 \end{pmatrix}$, $\hat{R} = \begin{pmatrix} r_1 & 0 \\ 0 & r_2 \end{pmatrix} \equiv \begin{pmatrix} \beta_1 - \mu_1 & 0 \\ 0 & \beta_2 - \mu_2 \end{pmatrix}$, $\hat{G} = \begin{pmatrix} g_{11}/\lambda_1 & g_{12}/\lambda_1 \\ g_{21}/\lambda_2 & g_{22}/\lambda_2 \end{pmatrix}$, and $\hat{E} = \begin{pmatrix} e_{11}/r_1 & e_{12}/r_1 \\ e_{21}/r_2 & e_{22}/r_2 \end{pmatrix}$.

In many experimentally relevant systems, such as communities of microorganisms and cells, the timescale of production, diffusion, and degradation of secreted factors is on the order of minutes [21], whereas cell division and death occurs over hours [112, 157], and the dynamics of the turnover of the secreted factors can be assumed to adiabatically reach a steady state $\vec{t^*}$ given by $\vec{t^*} = \hat{G}\vec{x}$ [14, 41, 156]. In this approximation the dynamical equations for the species number reduce to

$$\dot{\vec{x}} = \hat{R}\hat{X}\left(\vec{1} - (\hat{E}\hat{G})\vec{x}\right). \tag{2.6}$$

Written explicitly, this becomes the familiar generalized two-species competitive Lotka-Volterra system [27, 40, 44, 50, 54, 113, 118, 190]:

$$\begin{aligned}\dot{x}_1 &= r_1 x_1 \left(1 - \frac{x_1 + a_{12} x_2}{K_1}\right) \\ \dot{x}_2 &= r_2 x_2 \left(1 - \frac{a_{21} x_1 + x_2}{K_2}\right),\end{aligned} \tag{2.7}$$

where $\frac{1}{K_i} = \frac{e_{ii} g_{ii}}{r_i \lambda_i} + \frac{e_{ij} g_{ji}}{r_i \lambda_j}$ and $\frac{a_{ij}}{K_i} = \frac{e_{ii} g_{ij}}{r_i \lambda_i} + \frac{e_{ij} g_{jj}}{r_i \lambda_j}$. The turnover rates r_i set the timescales of the birth and death for each species, and K_i are known as the carrying capacities. The interaction parameters a_{ij} provide a mathematical representation of the intuitive notion of the niche overlap between the species [2, 38, 119, 167]. When $a_{ij} = 0$, species j does not affect the species i, and they occupy separate ecological niches. At the other limit, $a_{ij} = 1$, the species j compete just as strongly with species i as species i does within itself, and both species occupy same niche. We refer to the a_{ij} as the niche overlap parameters.

The number of deterministically viable species is typically constrained by the number of limiting factors [10], as described in the previous section. Namely, if both matrices $\hat{E}$ and $\hat{G}$ are non-singular

and invertible, the solutions to Equation (2.5) are that one (or both) of the species is zero or else $\vec{x}^* = (EG)^{-1}\vec{1}$. The latter solution corresponds to the coexistence of the two species.

When the matrix $(\hat{E}\hat{G})$ is singular ($a_{12}a_{21} = 1$), the coexistence fixed point $\vec{x}^* = (EG)^{-1}\vec{1}$ does not exist, and the Equations (2.5) are satisfied only if the population of one (or both) of the species is zero. Biologically, this condition corresponds to the complete niche overlap between two species, whereby only one species can survive in the niche. (Of note, exclusion of one species by the other can also occur in non-singular cases, as discussed in the next section.) Nevertheless, even in the complete niche overlap case, multiple species can deterministically coexist within one niche if the matrix $(\hat{E}\hat{G})$ possesses a further degeneracy, $K_1/K_2 = a_{12} = 1/a_{21}$, corresponding to an additional symmetry in the interactions of the species with the constraining factors, as illustrated in the next paragraph.

These mathematical notions can be understood in a biologically illustrative example, when the matrix $\hat{E}$ is singular, so that $\det(\hat{E}) = 0$. Any singular 2×2 real matrix can be written in the general form $\hat{E} = \begin{pmatrix} \alpha & \alpha\beta \\ \alpha\gamma & \alpha\beta\gamma \end{pmatrix}$, where α, β and γ are arbitrary real numbers [**?**]. In this case Equation (2.3) becomes

$$\begin{aligned} \dot{x}_1 &= r_1 x_1\big(1 - \alpha\,(t_1 + \beta t_2)\,\big) \\ \dot{x}_2 &= r_2 x_2\big(1 - \gamma\alpha\,(t_1 + \beta t_2)\,\big), \end{aligned} \tag{2.8}$$

so that both secreted factors effectively act as one factor with concentration $t \equiv t_1 + \beta t_2$. With $\gamma \neq 1$ this corresponds to the classic notion of two species and only one limiting factor. The two equations cannot be simultaneously satisfied and the only solution of Equations (2.8) is either $x_1 = 0$ or $x_2 = 0$ (or both). This is one example of competitive exclusion due to competition within a single niche. Finally, when $\gamma = 1$ (corresponding to $a_{12} = 1/a_{21} = K_1/K_2$), both the species and the secreted factors are functionally identical, and the Equations (2.8) allow multiple solutions lying on the line in phase space defined by $\vec{x}^* = \hat{G}^{-1}\vec{t}^*$ and $1 = \alpha\,(t_1^* + \beta t_2^*)$ [44, 127]; in this case many different mixtures of the two species can be deterministically stable, depending on the initial conditions. However, as discussed in the next section, this line of fixed points is unstable with respect to perturbations along the line, and stochastic effects become important. These derivations above provide a mathematical definition and a biological illustration of the niche overlap between two interacting species, and can be extended to a general case of N species interacting via M factors, as shown in the Supplementary Information. In the next two sections, I study how the niche overlap affects the stability of the species coexistence in deterministic and stochastic cases.

2.4 Deterministic stability of the Lotka-Volterra model

In this section, I examine the behavior of the deterministic Equations (2.7), which have four fixed points:

$$O = (0,0) \quad A = (0,K_2) \quad B = (K_1,0) \quad C = \Big(\frac{K_1 - a_{12}K_2}{1 - a_{12}a_{21}}, \frac{K_2 - a_{21}K_1}{1 - a_{12}a_{21}}\Big). \tag{2.9}$$

The origin O is the fixed point corresponding to both species being extinct, and is unstable with positive eigenvalues equal to r_1 and r_2 along the corresponding on-axis eigendirections. The single species fixed points A and B are stable on-axis (with eigenvalues $-r_1$ and $-r_2$, respectively), but are unstable with respect to invasion if point C is stable, reflected in the positive second eigenvalue equal to $r_2(1 -$

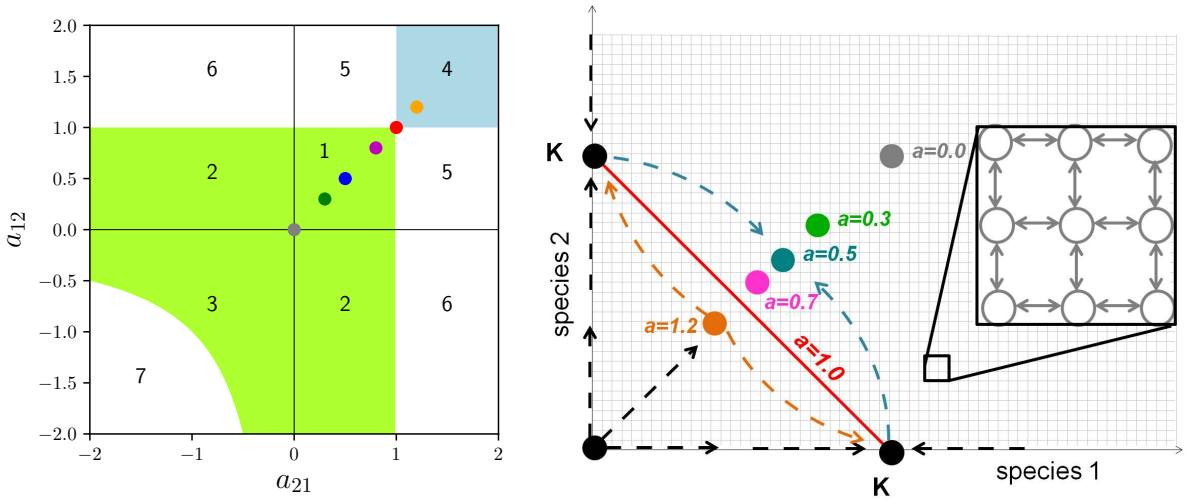

Figure 2.2: *Left: stability phase diagram of the coexistence fixed point for* $K_1 = K_2 = K$. The coexistence fixed point $C = \left(\frac{K_1 - a_{12}K_2}{1-a_{12}a_{21}}, \frac{K_2 - a_{21}K_1}{1-a_{12}a_{21}}\right)$ is stable in the green region and unstable in the blue region; in the white regions it is non-biological. Colored dots indicate the parameter range studied in the paper. The numbered regions correspond to different biological different regimes; see text. For the degenerate case $a_{12} = a_{21} = 1$, indicated by the red dot, the coexistence fixed point is replaced by a line of marginal stability, shown in the Right Panel. *Right: phase space of the coupled logistic model.* Colored dots show C at the indicated values of the niche overlap a. The fixed point is stable for $a < 1$. At $a = 0$ the two species evolve independently. As a increases, the deterministically stable fixed point moves toward the origin. At $a = 1$ the fixed point degenerates into a line of marginally stable fixed points, corresponding to the Moran model. The dashed lines illustrate the deterministic flow of the system: black is for $a = 0.5$, and orange for $a = 1.2$. The zoom inset illustrates the stochastic transitions between the discrete states of the system. Fixation occurs when the system reaches either of the axes. See text for details.

$a_{21}K_1/K_2$) and $r_1(1-a_{12}K_2/K_1)$, respectively. Fixed point C corresponds to the coexistence of the two species and is stable in the green shaded region in the left panel of Figure 2.2, which shows the stability diagram of the system for $K_1 = K_2$. [40, 46, 137].

The different regions of the phase space in Figure 2.2 have different biological interpretations [1**?**]. Parasitism, or predation/antagonism, occurs in regions 2 and 6 of (a_{12}, a_{21}) space, where $a_{12}a_{21} < 0$, with one species gaining from a loss of the other. In the strong parasitism regime (region 6), where the positive a_{ij} is greater than one, the parasite/predator drives the prey to extinction deterministically, and the only stable point is the predator's fixed point (A or B). Conversely, weak parasitism (region 2) allows coexistence of both species despite the detriment of one to the benefit of the other [40**?**].

The regions with both $a_{ij} < 0$ correspond to mutualistic/symbiotic interactions between the species [40, 46, 137**?**]. Weak mutualism (region 3) is mathematically similar to weak competition in that it results in stable coexistence. Strong mutualism (region 7) results in population explosion. Detailed study of this regime lies outside of the scope of the present work (but see [132]).

The quadrant with both $a_{12} > 0$ and $a_{21} > 0$ corresponds to the competition regime. At strong competition with either a_{12} or a_{21} greater than one (regions 4 and 5 in the left panel in Figure 2.2), either one of the species deterministically outcompetes the other (region 5) or the system possesses two single-species stable fixed points A and B with separate basins of attraction (region 4). The complete niche overlap regime of the underlying model of Equations (2.5) and defined by $\det[\hat{E}\hat{G}] = 0$ is contained

within region 4, and is given by the line $a_{12}a_{21} = 1$. These regimes correspond to the classical competitive exclusion theory, together with the strong parasitism case (region 6). By contrast, weak competition (region 1) where both $0 < a_{ij} < 1$ results in the stable coexistence at the mixed point C. In the special case $a_{12} = a_{21} = 1$ (shown by the red dot) the stable fixed point degenerates into a neutral line of stable points, defined by $x_2 = K - x_1$, as shown in the right panel of Figure 2.2. Each point on the line is stable with respect to perturbations off line, but any perturbations along the line are not restored to their unperturbed position [33, 127]. This line correspond to the singular case, discussed in the previous section, where the two species are functionally identical with respect to the action of the secreted factors (*eg.* $e_{11}/r_1 = e_{12}/r_1$ and $e_{22}/r_2 = e_{21}/r_2$ in Equations (2.5)). The stochastic dynamics along this line correspond to the classical Moran model as discussed below, and in the following I refer to this line as the Moran line.

The right panel of Figure 2.2 shows the phase portrait of the system, in the symmetric case of $K_1 = K_2 \equiv K$, $r_1 = r_2 \equiv r$, and $a_{12} = a_{21} \equiv a$, where neither of the species has an explicit fitness advantage. This equality of the two species, also known as neutrality, serves as a null model against which systems with explicit fitness differences can be compared. In this thesis, I focus on species coexistence in the weak competition regime, finding the scaling of the mean time to fixation due to stochasticity. The asymmetric case is also treated, with results qualitatively similar to the symmetric case.

2.5 The stochastic Lotka-Volterra model

Stochasticity naturally arises in the dynamics of the system from the randomness in the birth and death times of the individuals - commonly known as the demographic noise [13, 56, 144, 176]. Competitive interactions between the species can affect either the birth rates (such as competition for nutrients) or the death rates (such as toxins or metabolic waste), and in general may result in different stochastic descriptions [7, 16], as was discussed in the previous chapter. In this chapter, I follow others [44, 62, 114] in considering the case where the inter-species competition affects the death rates, so that the per capita birth and death rates b_i and d_i of species i are:

$$\begin{aligned} b_i/x_i &= r_i \\ d_i/x_i &= r_i \frac{x_i + a_{ij}x_j}{K_i}. \end{aligned} \tag{2.10}$$

In terms of the previous chapter, this corresponds to choosing $\delta = 0$ and $q = 0$. In the deterministic limit of negligible fluctuations the model recovers the mean field competitive Lotka-Volterra Equations (2.7) [114].

The system is characterized by the vector of probabilities $P(s, t|s^0)$ to be in a state $s = \{x_1, x_2\}$ at time t, given the initial conditions $s^0 = (x_1^0, x_2^0)$: $\vec{P}(t) \equiv \big(\dots, P(s, t|s^0), \dots\big)$ [134]. The forward master equation describing the time evolution of this probability distribution is [176]

$$\frac{d}{dt}\vec{P}(t) = \hat{M}\vec{P}(t), \tag{2.11}$$

where $\hat{M}$ is the (semi-infinite) transition matrix. I do not include the absorbing states in my transition matrix, and the master equation 2.11 as written does not preserve probability, as some of it leaks into fixation.

Because the approximate analytical and semi-analytical solutions of the master Equation (2.11) often do not provide correct scaling in all regimes ([14, 16, 55]; see also the previous chapter), I analyse the master equation numerically in order to recover both the exponential and polynomial aspects of the mean time to fixation. To enable numerical manipulations, I introduce a reflecting boundary condition at a cutoff population size $C_K > K$ for both species to make the transition matrix finite [30, 134] and enumerate the states of the system with a single index [134] via the mapping of the two species populations (x_1, x_2) to state s as

$$s(x_1, x_2) = (x_1 - 1)C_K + x_2 - 1, \tag{2.12}$$

where s serves as the index for our concatenated probability vector, uniquely enumerating all the states. In this representation, the non-zero elements of the sparse matrix $\hat{M}$ are $\hat{M}_{s,s} = -b_1(s) - b_2(s) - d_1(s) - d_2(s)$ along the diagonal, $\hat{M}_{s,s+1} = d_2(s+1)$ and $\hat{M}_{s+1,s} = b_2(s)$ at ± 1 off the diagonal, and $\hat{M}_{s,s+C_K} = d_1(s+C_K)$ and $\hat{M}_{s+C_K,s} = b_1(s)$ off-diagonal at $\pm C_K$. Some diagonal elements are modified to ensure the reflecting boundary at $x_i = C_K$.

Numerical results obtained from the Gillespie algorithm are accurate, assuming a sufficient number are averaged over [66]. Unfortunately even for a system size as small as $K = 20$ some of the simulations took over ten million steps before fixating. A tau-leaping implementation helps [29], but the problem remains that this fixation is a slow process and simulations of large K will be prohibitively long. As shown above, the distribution of fixation times is roughly exponential. Any simulations that do not finish will be from the tail end of the distribution but will have the largest contribution to the mean time, hence cannot be ignored.

Inverting the truncated transition matrix, as has been done in this chapter, is a much faster computational problem, and is hindered by insufficient RAM rather than interminable runtimes. Changing the cutoff means that the solution can be arbitrarily precise. In the left panel of figure 2.3, the direct solution from inverting the truncated transition matrix compares favourably with the Gillespie simulations.

To ensure accuracy of the mean times to 0.1% or better I choose $C_K = 5K$. This is largely excessive and even $C_K = 2K$ is sufficient for all but the smallest carrying capacities, for which it is least important to be accurate. The sparse matrix LU decomposition algorithm is implemented with the C++ library Eigen [**?**].

2.6 Mean fixation time in the classical Moran model

Here I derive the mean fixation time for the Moran model [133], which will be used later as a limiting case of the Lotka-Volterra dynamics. Previous authors have already shown that this is the limit [40, 44, 114], and the fixation time for the Moran model is already known [133]. I only include it here for completeness. The Wright-Fisher model gives similar results for large K, but is less intuitable, dealing as it does with a whole generation at a time, rather than one birth and one death.

In the classical Moran model, at each time step, an individual is chosen at random to reproduce. In order to keep the population constant, another one is chosen at random to die. The probabilities that the number of individuals of species 1 increases or decreases by one in one time step are [133]:

$$b_M(n) = f(1-f) = (1-f)f = d_M(n) = \frac{n}{K}\left(1 - \frac{n}{K}\right) = \frac{1}{K^2}n(K-n), \tag{2.13}$$

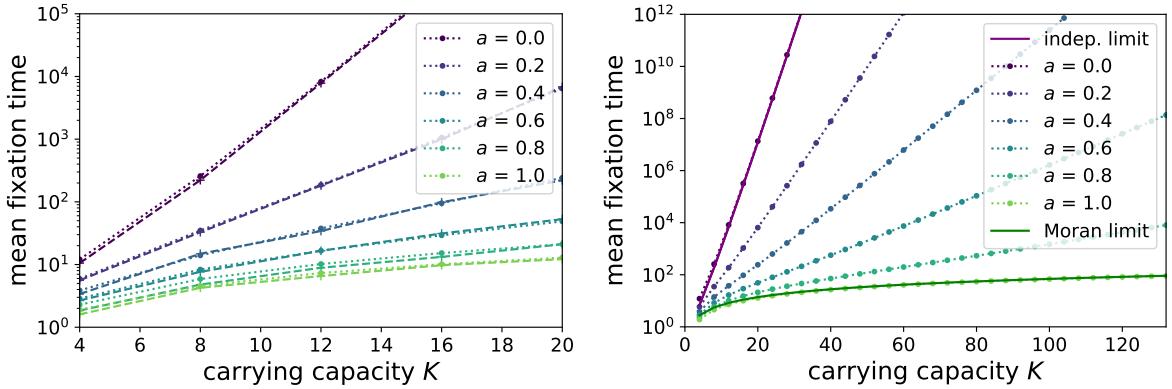

Figure 2.3: *Dependence of the fixation time on carrying capacity and niche overlap. Left:* Dotted lines come from directly solving the backwards master equation by inverting the transition matrix as per equation 2.22, after a cutoff has been applied to the matrix to make it finite. Dashed lines connecting crosses are each an average of a hundred realizations of the stochastic process, as simulated using the Gillespie algorithm with tau-leaping [29, 66]. The simulations and direct solution are in good agreement, as one would expect. *Right:* The same direct solution data as in the left panel are extended to larger carrying capacities. The lowest line, $a = 1$, recovers the Moran model results in solid green with the fixation time algebraically dependent on K for $K \gg 1$. For all other values of a, the fixation time is exponential in K for $K \gg 1$. At $a = 0$ the systems acts as two independent stochastic logistic systems, and matches that limit as shown with the solid purple line.

where n is the number and f is the fraction of species 1 in the system (of total system size K). The mean fixation time, $\tau(n)$, starting from some initial number n of species 1 is described by the following backward master equation [139]:

$$\tau(n) = \Delta t + d_M(n)\tau(n-1) + (1 - b_M(n) - d_M(n))\,\tau(n) + b_M(n)\tau(n+1),$$

where Δt is the time step. Substituting the values of the 'birth' and 'death' probabilities of species 1 from equation (2.13) we get

$$\tau(n+1) - 2\tau(n) + \tau(n-1) = -\frac{\Delta t}{b_M(n)} = -\Delta t \frac{K^2}{n(K-n)}.$$

At $K \gg 1$, the Kramers-Moyal expansion in $1/K$ results in

$$\frac{\partial^2 \tau}{\partial n^2} = -\Delta t\, K \left(\frac{1}{n} + \frac{1}{K-n}\right).$$

Integrating, using the boundary conditions $\tau(0) = \tau(K) = 0$, gives

$$\tau(n) = -\Delta t\, K^2 \left(\frac{n}{K} \ln\left(\frac{n}{K}\right) + \frac{K-n}{K} \ln\left(\frac{K-n}{K}\right)\right). \tag{2.14}$$

For the initial condition analogous to the coexistence point, $n = K/2$, this gives

$$\tau = \Delta t\, K^2 \ln(2).$$

Recall that the Moran model counts one time unit Δt every birth and death pair of events. The correspondence between the Moran model and the related Wright-Fisher model occurs when the Moran model has undergone a number of births and deaths equal to the (fixed) population size of Wright-Fisher, often called the generation time [**?**]. The time scale regarded is important. Similarly, for comparison between Moran and the coupled logistic model, one needs to match the time scales. First, note that the birth and death events can be treated as independent under the assumption that a single birth or death does not change the rates significantly, an assumption which is valid far from the axes. Then the probability of the next birth event happening around time t is $f(t)dt = b\,e^{-b\,t}dt$, and similarly $g(t)dt = d\,e^{-d\,t}dt$. Then define the probability of the birth happening by *by* time t is $F(t) = \int_0^t f(t')dt'$, and similarly $G(t) = 1 - e^{-d\,t}$. Assuming independence, a birth and a death event have happened by time t with probability $F(t)G(t)$, and the distribution of this time is given by $\partial_t[F(t)G(t)]$. The average time of a birth and death is then

$$\begin{aligned}\Delta t &= \int_0^\infty t\partial_t[FG]dt = \int_0^\infty t\partial_t[FG] = \int_0^\infty t\left(f(t)+g(t)-(b+d)e^{-(b+d)t}\right)\\ &= \frac{1}{b}+\frac{1}{d}-\frac{1}{b+d} = \frac{b^2+bd+d^2}{b(b+d)d}.\end{aligned}$$

In principle this should be averaged over all combinations of the two species giving birth and dying, weighted by the probabilities of each pairing. It should also account for the probability of being at a particular state, as the state affects the rates. To simplify this I provide a lower bound by assuming that most of the time is spent near the initial state for the Moran limit, $(K/2, K/2)$, such that $b_i\,(K/2, K/2) = d_i\,(K/2, K/2) = K/2$. This gives

$$\Delta t = \frac{3}{2}\frac{1}{b} = \frac{3}{2}\frac{1}{K/2} = \frac{3}{K} \tag{2.15}$$

and therefore

$$\tau = 3\ln(2)\,K. \tag{2.16}$$

The fixation time of the Moran model agrees well with the results of the coupled logistic model for complete niche overlap, as shown in the left panel of figure 2.4.

2.7 Fixation time of the coupled logistic model in the independent limit

Here I calculate the mean fixation time in the independent limit of the coupled logistic model given a distribution of extinction times for a single logistic model. The fixation occurs when either of the species goes extinct. Denoting the probability distribution of the extinction times for either of independent species as $p(t)$ and its cumulative as $F(t) = \int_{s=0}^t p(s)ds$, the probability that *either* of the species goes extinct in the time interval $[t, t+dt]$, is the probability of species 1 going extinct while species 2 has not plus the probability that species 2 goes extinct while species 1 has not, since these are the two possibilities. That is,

$$p_{min}(t)dt = \Big(p(t)\,(1-F(t)) + (1-F(t))\,p(t)\Big)dt = 2p(t)\,(1-F(t))\,dt. \tag{2.17}$$

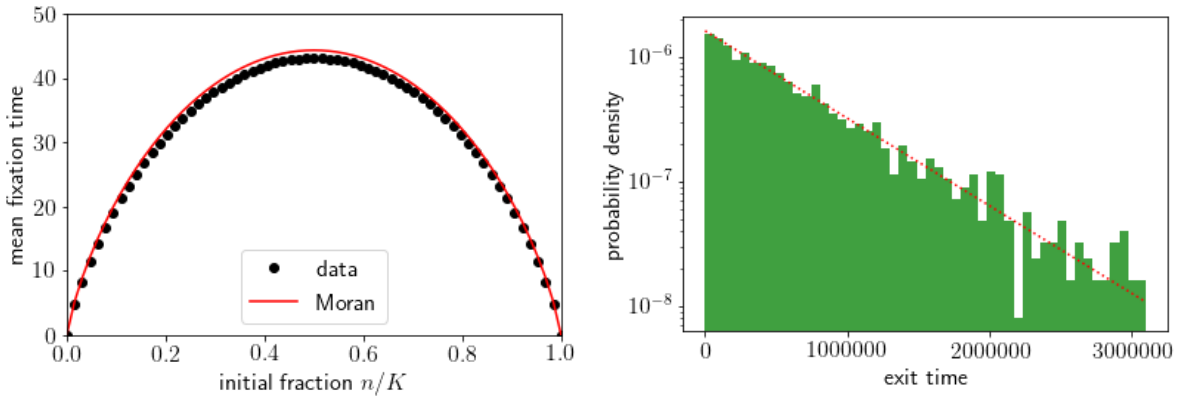

Figure 2.4: *Exploration of the niche overlap limits of the coupled logistic model. Left:* The coupled logistic model agrees with the Moran model in the limit of complete niche overlap, $a = 1$. Fixation time varies with initial fraction of the species in the population. The fixation time for the Moran model is in red and the coupled logistic model for $a = 1$ is in black. The population size of the Moran model is set equal to the carrying capacity $K = 64$ of the corresponding coupled logistic model. *Right:* The extinction time distribution of a one-dimensional logistic model is dominated by a single exponential tail. The bulk of the probability density is modelled by an exponential distribution with the same mean, shown in the red dotted line. Data are generated using using the Gillespie algorithm for $K = 16$. For higher carrying capacities the assumption of exponentially distributed times becomes even more accurate. This informs my two-dimensional independent limit $a = 0$, as the minimum of two exponential distribution is an exponential distribution.

The mean time to fixation $\langle t \rangle$ is

$$\langle t \rangle = \int_0^\infty dt\, t\, p_{min}(t). \tag{2.18}$$

As shown in the right panel of figure 2.4, the probability distribution of fixation times of a single species is dominated by the exponential tail. It can be approximated as

$$p(t) = \alpha e^{-\alpha t}, \quad F(t) = 1 - e^{-\alpha t} \tag{2.19}$$

with $\frac{1}{\alpha} \simeq \frac{1}{K} e^K$ from the previous section. Finally, I obtain for the mean time to fixation

$$\langle t \rangle = \int_0^\infty dt\, t\, 2\alpha e^{-2\alpha t} = \frac{1}{2\alpha}. \tag{2.20}$$

which leads to the equation $\tau \simeq \frac{1}{2K} e^K$.

2.8 Fixation time as a function of the niche overlap

In this section I calculate the first passage times to the extinction of one of the species and the corresponding fixation of the other, induced by demographic fluctuations, starting from an initial condition of the deterministically stable coexistence point. The master Equation (2.11) has a formal solution obtained by the exponentiation of the matrix: $\vec{P}(t) = e^{\hat{M}t}\vec{P}(0)$. However, direct matrix exponentiation, as well as direct sampling of the master equation using the Gillespie algorithm [29, 66], are impractical since the fixation time grows exponentially with the system size. However, the moments of the first

passage times can be calculated directly without explicitly solving the master equation [73]. The mean residence time in any state s during the system evolution is

$$\langle t(s^0)\rangle_s = \int_0^\infty dt\ P(s,t|s^0) = \int_0^\infty dt\ (e^{\hat{M}t})_{s,s^0} = -(\hat{M}^{-1})_{s,s^0}. \tag{2.21}$$

The final equality in the previous equation is obtained integration by parts and requires that all the eigenvalues of the transition matrix $\hat{M}$ are negative, a fact that is evident by its construction: since the master equation conserves probability (which is bounded by one), none of the eigenvalues can be positive; since the steady state absorbing states have been removed, there are no zero eigenvalues. Thus, the mean time to fixation starting from a state s^0 is [82]

$$\tau(s^0) = -\sum_s \langle t(s^0)\rangle_s = -\sum_s \left(\hat{M}^{-1}\right)_{s,s^0}. \tag{2.22}$$

This expression can be also derived using the backward equation formalism [82]. The matrix inversion was performed using LU decomposition algorithm implemented with the C++ library Eigen [**?**], which has algorithimic complexity of the calculation scaling algebraically with K. Increasing the cutoff C_K enables calculation of the mean fixation times to an arbitrary accuracy.

The right panel of figure 2.3 shows the calculated fixation times with the initial condition at the deterministically stable coexistence fixed point as a function of the carrying capacity K for different values of the niche overlap a. In the limit of non-interacting species ($a = 0$), each species evolves according to an independent stochastic logistic model, and the probability distribution of the fixation times is a convolution of the extinction time distributions of a single species, which are dominated by a single exponential tail [74, 140, 142]. Mean extinction time of a single species can be calculated exactly as in the previous chapter, and asymptotically for $K \gg 1$ it varies as $\frac{1}{K}e^K$ [108] giving for the overall fixation time in the two species model $\tau \simeq \frac{1}{2K}e^K$ as in Equation (2.20). This analytical limit is shown in figure 2.3 as a solid purple line and agrees well with the numerical results of Equation (2.22). From the biological perspective, for sufficiently large K, the exponential dependence of the fixation time on K implies that the fluctuations do not destroy the stable coexistence of the two species.

In the opposite limit of complete niche overlap, $a = 1$, any fluctuations along the line of neutrally stable points are not restored, and the system performs diffusion-like motion that closely parallels the random walk of the classic Moran model [8, 40, 44, 54, 58, 90, 114, 190]. The Moran model shows a relatively fast fixation time scaling algebraically with K [114, 133], $\tau \simeq \ln(2)K^2\Delta t$; see Equation (2.16). The fixation time predicted by the Moran model is shown in figure 2.3 as a solid green line and shows excellent agreement with my exact result. The relatively short fixation time in the complete niche overlap regime implies that the population can reach fixation on biologically realistic timescales.

The exponential scaling of the fixation time with K persists for incomplete niche overlap described by the intermediate values of $0 < a < 1$. However, both the exponential and the algebraic prefactor depend on the niche overlap a. The exponential scaling is expected for systems with a deterministically stable fixed point [14, 55, 58, 62, 142], as indicated in [40, 54, 114] using Fokker-Planck approximation and in [62] using the WKB approximation. However, the Fokker-Planck and WKB approximations, while providing the qualitatively correct dominant scaling, do not correctly calculate the scaling of the polynomial prefactor and the numerical value of the exponent simultaneously [16, 90, 142], as was shown in the previous chapter. For large population sizes and timescales, effective species coexistence will be

typically observed experimentally whenever the fixation time has a non-zero exponential component.

To quantitatively investigate the transition from the exponentially stable fixation times to the algebraic scaling in the complete niche overlap regime, I use the ansatz

$$\tau(a, K) = e^{h(a)} K^{g(a)} e^{f(a)K}. \tag{2.23}$$

In the Moran limit, $a = 1$, I expect $f(1) = 0$, $g(1) = 1$, and $h(1) = \ln\big(\ln(2)\big)$ as follows from equation (2.16). In the independent species limit with zero niche overlap, $a = 0$, equation (2.20) suggests $f(0) = 1$, $g(0) = -1$, and $h(0) = -\ln(2)$. The left panel of figure 2.5 shows the ansatz functions $f(a)$, $g(a)$, and $h(a)$, obtained by numerical fit to the fixation times as a function of K shown in Figure 2.3. The numerical results agree well with the expected approximate analytical results for $a = 0$ and $a = 1$ with small discrepancies attributable to the approximate nature of the limiting values. Notably, $f(a)$, which quantifies the exponential dependence of the fixation time on the niche overlap a, smoothly decays to zero at $a = 1$: only when two species have complete niche overlap ($a = 1$) does one expect rapid fixation dominated by the algebraic dependence on K. In all other cases the mean time until fixation is exponentially long in the system size [74, 142]. Even two species that occupy *almost* the same niche ($a \lesssim 1$) effectively coexist for $K \gg 1$, with small fluctuations around the deterministically stable fixed point.

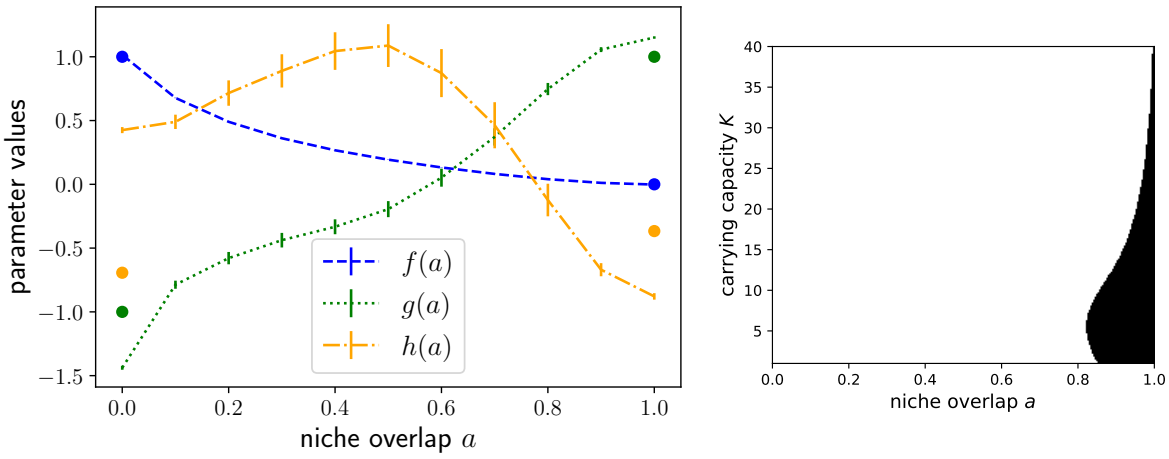

Figure 2.5: *Niche overlap controls the transition from coexistence to fixation. Left:* Blue line: $f(a)$ from the ansatz of Equation (2.23) characterizes the exponential dependence of the fixation time on K; it smoothly approaches zero as the niche overlap reaches its Moran line value $a = 1$. Green line: $g(a)$ quantifies the scaling of the pre-exponential prefactor $K^{g(a)}$ with K. Yellow line: $h(a)$ is the multiplicative constant. Dashed bars represent a 95% confidence interval. The dots at the extremes $a = 0$ and $a = 1$ are the expected asymptotic values from equations (2.16) and (2.20), which varies from $g(a) = -1$ for the independent processes to $g(a) = 1$ in the Moran limit. *Right:* In part of the parameter space, fixation is always fast. The white area shows where two species are expected to effectively coexist, while the black shading identifies the regime where fixation is faster than a similarly-sized Moran model. Fixation is estimated by extrapolating the ansatz parameter fits to the a, K parameter space.

2.9 Co-existence versus fixation in parameter space

I make the claim that when biological system sizes are large, a fixation time that scales exponentially with carrying capacity effectively implies coexistence. This is typically the case. However, some systems have only a few competing members, as in nascent cancers or plasmids in a single cell. I want to get a better sense of when the exponential scaling is relevant, especially since for those systems with almost complete niche overlap the exponential scaling is slow. To this end I compare the expected mean fixation time with that of the Moran model. The ansatz $e^{h(a)}K^{g(a)}e^{f(a)K}$ is fit to the data and then used to estimate the fixation time at a variety of parameter values. This time is compared to the fixation time of a Moran model with the same carrying capacity. In the right panel of figure 2.5 the shaded region represents those parameter combinations for which the estimated fixation is faster than the corresponding Moran model. For example, a carrying capacity of about 35 organisms is sufficient to allow for effective coexistence of two species which are not more than 99% identical in their niches. This is a small population size in most biological contexts. Even for systems with a smaller carrying capacity, unless the two species are more similar they are expected to coexist for long times before fixation.

2.10 Analysis of the Fokker-Planck approximation in this context

The most common approximation to the master equation is Fokker-Planck, which assumes the state space is continuous. I attempt its use here to get an analytic estimate of the dependence of fixation time on K and a. We shall see that its utility is only marginal, though with some further approximations and an application of Kramers' theory I get my desired estimate.

The Fokker-Planck approximation to the coupled logistic system studied herein takes its traditional form [139]:

$$\begin{aligned}\frac{dP}{dt} &= -\partial_1[(b_1-d_1)P] - \partial_2[(b_2-d_2)P] + \frac{1}{2}\partial_1^2[(b_1+d_1)P] + \frac{1}{2}\partial_2^2[(b_2+d_2)P] \\ &= -\sum_i \partial_i F_i P + \sum_{i,j}\partial_i\partial_j D_{ij} P \end{aligned} \tag{2.24}$$

where F is the force vector and D is the diffusion matrix (in this case diagonal). Here, under symmetric conditions and nondimensionalization by r, $F_1 = \frac{x_1}{K}(K - x_1 - ax_2)$ and $D_{11} = \frac{x_1}{K}(K + x_1 + ax_2)$, with similar terms for species 2.

In general, Equation (2.24) cannot be reduced to diffusion in a potential $U(\vec{x})$ with an equilibrium distribution function $P(\vec{x}) \sim \exp(U(\vec{x}))$. The condition of zero flux at equilibrium, $J_i = F_i P - 1/2\sum_j \partial_j D_{ij} P = 0$, would require [64]

$$\partial_i \log P = \sum_k (D^{-1})_{ik}\big(2F_k - \sum_j \partial_j D_{kj}\big) \equiv -\partial_i U,$$

However, for consistency it also requires $\partial_j\left(-\partial_i U\right) = \partial_i\left(-\partial_j U\right)$ [64]. It is easy to show that this is not upheld for the two directions unless $a_{12} = a_{21} = 0$ and the system can be decomposed into two one-dimensional logistic systems.

Instead, I define the pseudo-potential as:

$$U(x_1, x_2) \equiv -\ln\left[P_{ss}(x_1, x_2)\right]. \tag{2.25}$$

where $P_{ss}(x_1, x_2)$ is a quasi-stationary probability distribution function [192]. I calculate $P_{ss}(x_1, x_2)$ in the approximation to the Fokker-Planck Equation (2.24) linearized about the deterministic coexistence fixed point. The linearized equation is

$$\partial_t P = -\sum_{i,j} A_{ij}\partial_i(x_j - x_j^*)P + \frac{1}{2}\sum_{i,j} B_{ij}\partial_i\partial_j(x_i - x_i^*)(x_j - x_j^*)P \tag{2.26}$$

where $A_{ij} = \partial_j F_i|_{\vec{x}=\vec{x}^*}$ and $B_{ij} = D_{ij}|_{\vec{x}=\vec{x}^*}$. The quasi-equilibrium solution to Equation (2.26) is $P_{ss} = \frac{1}{2\pi}\frac{1}{|C|^{1/2}}\exp[-(\vec{x}-\vec{x}^*)^T C^{-1}(\vec{x}-\vec{x}^*)/2]$, a Gaussian centered on the coexistence point and with a variance given by the covariance matrix $C = B \cdot A^{-1}/2$ in the symmetric case $a_{12} = a_{21} = a$, $K_1 = K_2 = K$ [176]. In this case the diagonal term of C is $\frac{1}{1-a^2}K$ and gives the variance of a species about its mean value. The off-diagonal, which corresponds to the covariance between the two species, is $-\frac{a}{1-a^2}K$. Thus the Pearson correlation coefficient between the two species is $-a$. That is, they are maximally anti-correlated when $a = 1$, lying along the line $x_1 + x_2 = K$ - the Moran line.

For the initial condition at the coexistence fixed point and assuming that the system escapes towards fixation once it reaches one of the axial fixed points $(0, K)$ or $(K, 0)$, from Equation (2.25) the well depth is proportional to carrying capacity K, being

$$\Delta U = \frac{(1-a)}{2(1+a)}K. \tag{2.27}$$

In a Kramers' type approximation, the escape time from the pseudo-potential well scales as $\sim \exp(\Delta U)$ [74], reproducing the exponential scaling of the extinction time with K, observed numerically. Moreover, the Fokker-Planck approximation also shows that the exponential scaling disappears as niche overlap a approaches unity, in accord with the numerical results above. The correlation between the two species goes to negative one in this parameter limit, such that they are entirely anti-correlated. Whereas the well has a single lowest point at the coexistence fixed point for partial niche overlap, at $a = 1$ the potential shows a trough of constant depth going between the two axial fixed points. This is the Moran line, along which diffusion is unbiased; diffusion away from the Moran line is restored, as the system is drawn toward the bottom of the trough. Because everywhere along the Moran line is equally likely, the probability cannot be normalized, and the linearization approximation fails. This is to be expected, as it is an expansion about a fixed point, but the fixed point is replaced by the Moran line in the Moran limit of $a = 1$.

2.11 Breaking the parameter symmetries

I have addressed the symmetric case of $K_1 = K_2 \equiv K$ and $a_{12} = a_{21} \equiv a$. The result of exponential scaling of the fixation time except when the Moran line exists is true even when some symmetries are broken. However, the evidence is not as clear as in the symmetric case.

Panel A of figure 2.6 shows the dependence of the fixation time on the niche overlap a_{21} while keeping $a_{12} = 0.5$ for $K_1 = K_2 \equiv K$; using the similar ansatz, I apply the same $\tau = e^{h(a_{21})}K^{g(a_{21})}e^{f(a_{21})K}$. As the

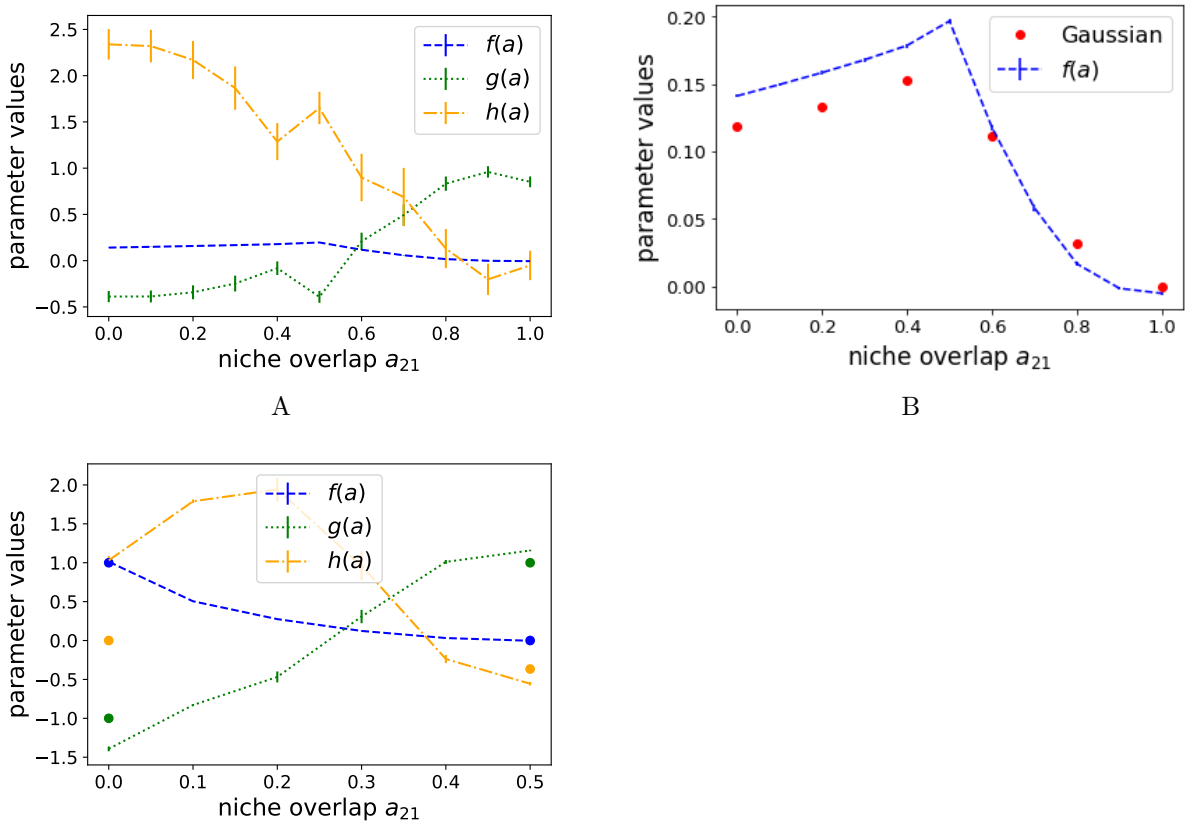

Figure 2.6: *Breaking the parameter symmetries. Panel A:* As in figure 2.5, lines come from fitting the ansatz of equation 2.23 to data generated from equation 2.22. In this case the niche overlap symmetry is broken and $a_{12} = 0.5$. The exponential dependence on carrying capacity is non-zero except at $a_{21} = 1$, at which point the "coexistence" fixed point is coincident with the fixed point on the x-axis. *Panel B:* The ansatz fit from panel A is compared with the Gaussian well depth at the same parameter values. The non-zero exponential dependence is observed in the Gaussian approximation as well. *Panel C:* The symmetry is broken in carrying capacity, such that $K_2 = 2K_1$. The ansatz is fit to K_1. The exponential dependence is non-zero except at the appearance of the Moran line at $a_{21} = 1/2$. The extreme points are the expected asymptotic values.

niche overlap a_{21} changes from 0 to 1, the location of the coexistence fixed point shifts from $(K/2, K/4)$ to $(K, 0)$. Accordingly, the fixation time starting from the fixed point maintains its exponential scaling with carrying capacity up until $a_{21} = 1$, where the fixed time is equal to zero, as reflected in the shape of the of $h(a_{21})$. Notably, in this asymmetric case the exponential scaling function $f(a_{21})$ is much weaker compared to the symmetric case, partially because the fixed point is located closer to an axis that in the symmetric case even at $a_{21} = 0$. Panel B of Figure 2.6 shows the comparison of the results of the ansatz fit with the estimates of the exponential part of the fixation time using Kramers'/Fokker-Planck pseudo-potential described in the previous section that explains the observed trends of $f(a_{21})$. The Gaussian pseudo-potential shows a similar trend to the data, though quantitatively it remains incorrect.

Next let us consider breaking the symmetry such that the Moran line can still be recovered. The carrying capacity symmetry is broken, such that $K_2 = 2K_1$. The two species are still independent when $a_{12} = a_{21} = 0$, but in this case the Moran line exists when $a_{12} = 2$ and $a_{21} = 1/2$. Figure **??** shows the

results when the symmetry is broken both in the carrying capacity and the niche overlap. It shows the change in the fixation time as a function of the niche overlap a_{21} for $K_2 = 2K_1 \equiv K$ while the niche overlaps change along the line where $a_{12} = 4a_{21}$, starting from the independent case $a_{12} = a_{21} = 0$ to $a_{12} = 2$ and $a_{21} = 1/2$ where the system reaches its corresponding Moran line. The observed behaviour is very similar to that shown in the symmetric case, with the exponential dependence transitioning smoothly to zero at the Moran line.

I uphold the conclusion that at the Moran line will fixation be fast; when the system parameters are even slightly off those niche overlap values which balance the carrying capacities and allow for the Moran line to exist, the fixation is exponential in the carrying capacity, to the point that the two species effectively coexist. I include the caveat that fixation will also be fast when the coexistence fixed point is close to one axis, as evinced with the broken niche overlap symmetry above.

2.12 Route to Fixation

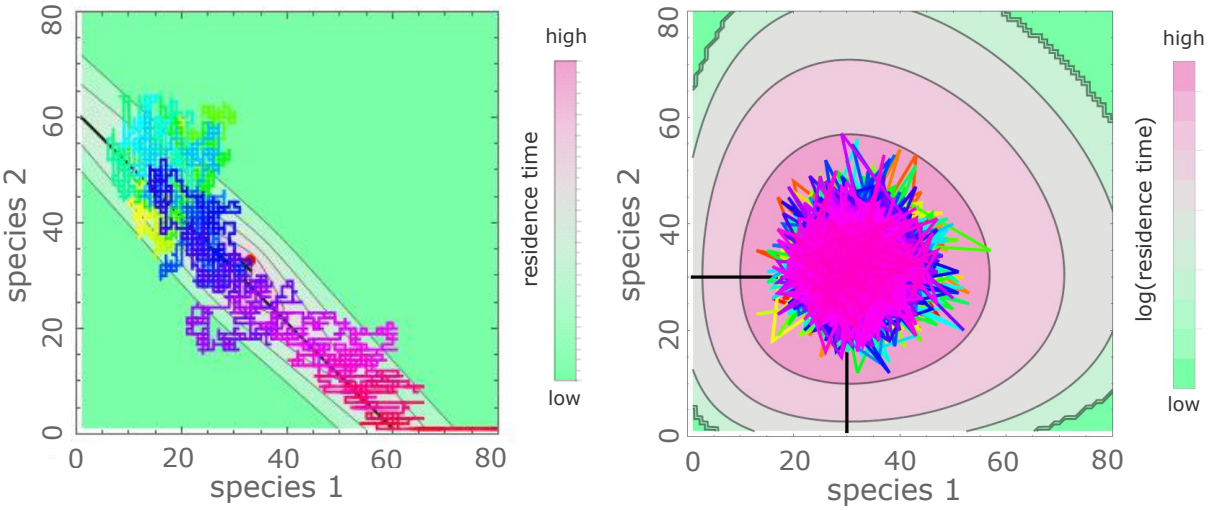

Figure 2.7: *The system samples multiple trajectories on its way to fixation.* Contour plot shows the average residency times at different population states of the system, with pink indicating longer residence time, deep green indicating rarely visited states. The colored line is a sample trajectory the system undergoes before fixation; color coding corresponds to the elapsed time with orange at early times, purple at the intermediate times and red at late stages of the trajectory. The red dot shows the deterministic coexistence point. See text for more details. *Left*: Complete niche overlap limit, $a = 1$, for $K = 64$. *Right*: Independent limit with $a = 0$ and $K = 32$.

To gain deeper insight into the fixation dynamics, in this section I calculate the residency times in each state during the fixation process [73], given by Equation (2.21), reproduced here:

$$\langle t(s^0)\rangle_s = \int_0^\infty dt P(s,t|s^0,0) = \hat{M}^{-1}_{s,s^0}.$$

This gives the mean total time the system resides in state s, given that it starts in state s^0. As with the fixation times, the dependence on the initial state is weak, so long as that initial state is not near an axis. Whereas I previously analyzed the fixation time scaling, the residency times themselves proffer some insight into the system. The results are shown as a contour plot in Figure 2.7, where pink corresponds

to the high occupancy sites and green to the rarely visited ones, for two different niche overlaps, one at and the other far from the Moran limit. The set of states lying along the steepest descent lines of the contour plot, shown as the black line, can be thought of as a "typical" trajectory [62, 90, 124]. However, even for two species close to complete niche overlap the system trajectory visits many states far from this line. This departure is even greater for weakly competing species, where the system covers large areas around the fixed point before the rare fluctuation that leads to fixation occurs [68]. These deviations from a "typical" trajectory are related to the inaccuracy of the WKB approximation in calculating the scaling of the pre-exponential factor [14, 68, 108]; see also the previous chapter.

This occupancy landscape can be qualitatively thought of as an effective Lyapunov function/effective potential of the system dynamics [192], although the LV system does not possess a true Lyapunov function - an issue that also arises in the Fokker-Planck approximation [40, 192]. One way to deal with this issue is the linearization in the Fokker-Planck section above (section 2.10). This allows one to easily solve the Fokker-Planck equation in any system with an attractive deterministic fixed point. More pertinently, linearizing the Fokker-Planck equation, as in Equation 2.26 described above, allows one to get an estimate of the depth of the pseudo-potential: $\frac{(1-a)}{2(1+a)}K$. This provides an intuitive underpinning for the general exponential scaling in the incomplete niche overlap regime: the fixation process can be thought of as the Kramers'-type escape from a pseudo-potential well [**?**]. The Kramers result is dominated by $\tau \simeq \exp(\text{well depth})$, corresponding to the dominant scaling $\tau \simeq \exp(f(a)K)$. As a increases and the species interact more strongly, the potential well becomes less steep, resulting in weaker exponential scaling. In the complete niche overlap limit, the pseudo-potential develops a soft direction along the Moran line that enables relatively fast escape towards fixation. This is what is seen in the residence time graph; in the Moran limit, the states along the line connecting the coexistence fixed point to the two axial fixed points are visited much more frequently than those off it. Outside of the Moran limit, it is rather the states in a cloud around the coexistence point that enjoy long residence times.

In linearizing the FP equation I also arrived at the Pearson correlation coefficient between the two species: $-a$. They are anti-correlated, and this anti-correlation becomes complete as niche overlap approaches one. In state space this corresponds to the system lying on the Moran line. Thus we expect the pseudo-potential to become less steep as a increases, eventually developing a level trough along the Moran line that enables relatively fast escape toward fixation. Though I am unaware of any direct connection, this disappearance is also mimicked in the deterministic coexistence point eigenvalue associated with the $(1, -1)$ direction, which goes to zero as niche overlap goes to one, as $-\frac{1-a}{1+a}$.

2.13 Discussion

Maintenance of species biodiversity in many biological communities is still incompletely understood. The classical idea of competitive exclusion postulates that ultimately only one species should exist in an ecological niche, excluding all others. Although the notion of an ecological niche has eluded precise definition, it is commonly related to the limiting factors that constrain or affect the population growth and death. In the simplest case, one factor corresponds to one niche, which supports one species, although a combination of factors may also serve as a niche, as discussed above. The competitive exclusion picture has encountered long-standing challenges as exemplified by the classical "paradox of the plankton" [37, 80] in which many species of plankton seem to co-habit the same niche; in many other ecosystems the biodiversity is also higher than appears to be possible from the apparent number

of niches [37, 76, 116, 125, 168].

Competitive exclusion-like phenomena can appear in a number of popular mathematical models, for instance in the competition regime of the deterministic Lotka-Volterra model, whose extensive use as a toy model enables a mathematical definition of the niche overlap between competing populations [2, 38, 119, 167]. Another classical paradigm of fixation within an ecological niche is the Moran model (and the closely related Fisher-Wright, Kimura, and Hubbell models) that underlies a number of modern neutral theories of biodiversity [3, 76, 97, 114, 126, 133**?**]. Unlike the deterministic models, in the Moran model fixation does not rely on deterministic competition for space and limiting factors but arises from the stochastic demographic noise. Recently, the connection between deterministic models of the LV type and stochastic models of the Moran type has accrued renewed interest because of new focus on the stochastic dynamics of the microbiome, immune system, and cancer progression [8, 11, 14, 40, 44, 114, 156, 178].

Much of the recent studies of these systems employed various approximations, such as the Fokker-Planck approximation [40, 44, 54, 58, 114], WKB approximation [62, 90] or game theoretic [8] approach. The results of these approximations typically differ from the exact solution of the master equation, especially for small population sizes [14, 16, 55, 90, 142], as was discussed in more detail in the previous chapter. In this chapter, I have interrogated stochastic dynamics of a system of two competing species using a numerically arbitrarily accurate method based on the first passage formalism in the master equation description. The algorithmic complexity of this method scales algebraically with the population size rather than with the exponential scaling of the fixation time, (as is the case with the Gillespie algorithm [66]) enabling us to capture both the exponential behaviour and the algebraic prefactors in the fixation/extinction times for both small and large population sizes. This accuracy is needed in order to observe the transition from slow, exponentially dominated processes to the algebraically fast fixation of the Moran limit.

Stochastic fluctuations allow the system to escape from the deterministic coexistence fixed point towards fixation. If the escape time is exponential in the (typically large) system size, in practice it implies effective coexistence of the two species around their deterministic coexistence point. If the time is algebraic in K, as in degenerate niche overlap case (closely related to the classical Moran model), the system may fixate on biological timescales [93, 133]. For those biological systems with small characteristic population sizes, exponential scaling does not dominate the fixation time; power law and prefactor become more relevant. Figure **??** shows that a niche overlap as low as 0.8, for a carrying capacity around 6, has rapid fixation, more rapid than a corresponding Moran model. The transition between the exponential scaling of effective coexistence time to the rapid stochastic fixation in the Moran limit is governed by the niche overlap parameter, which for example can be derived in terms of the dynamics and interactions of the species and their secreted growth and death factors.

While I find that the fixation time is exponential in the system size unless the two species occupy exactly the same niche, the numerical factor in the exponential is highly sensitive to the value of the niche overlap, and smoothly decays to zero in the complete niche overlap case. These results can be understood by noticing that the escape from a deterministically stable coexistence fixed point can be likened to Kramers' escape from a pseudo-potential well [23, 54, 74, 142], where the mean transition time grows exponentially with well depth [142]. Approximating the steady state probability with a Gaussian shows that this well depth is proportional to $K(1-a)$ and disappears when $a = 1$. With complete niche overlap the system develops a "soft" marginally stable direction along the Moran line that enables algebraically fast escape towards fixation [40, 54]. Similar to the exponential term, the

exponent of the algebraic prefactor is also a function of the niche overlap, and smoothly varies from -1 in the independent regime of non-overlapping niches to $+1$ in the Moran limit.

Niche overlap between two species, the similarity in how they interact with their shared environment, is of critical importance in determining whether they will coexist. For typically large biological populations, effective coexistence occurs when escape time grows exponentially with the carrying capacity, which is the case for even slightly mismatched niches. Any niche mismatch leads to species which tend to exist for long times near their respective carrying capacities; in effect, niche models are apt even for large niche overlap. Only when niche overlap is complete will fixation be relatively rapid, algebraic in K. This has important implications for understanding the long term population diversity in many systems, such as human microbiota in health and disease [43, 98, 143], industrial microbiota used in fermented products [186], and evolutionary phylogeny inference algorithms [26, 159]. My results show that the generalized Lotka-Volterra model serves well as an extension to neutral models for problems such as maintenance of drug resistance plasmids in bacteria [67], strain survival in cancer progression [11], or the generation of coalescent or phylogenetic trees [97, 159, 162]. The theoretical results can also be tested and extended based on experiments in more controlled environments, such as the gut microbiome of a *c. elegans* [178], or in microfluidic devices [78].

Chapter 3

Going from One Species to Two

The first half of this chapter is based on a paper written by me and my supervisor Anton Zilman, which will be published in a Royal Society journal [16].

3.1 Introduction

The previous chapter regarded an ecosystem with two competing species, and asked questions about the mean time until one of the species goes extinct and the other fixates in the system. In this chapter I aim to look at the reverse problem; starting with a stable system with one species, what is the probability and timescale that a second one will enter and establish itself, given some overlap between the niches of the extant and immigrating species. First I would like to motivate the problem and discuss where a new species entering a system might come from.

Invasion, in one form or another, is a relevant factor in a variety of biological contexts. When a new allele arises in a population of genes it acts as an invader, and if it is successful it contributes to the genetic diversity of the population This is the situation considered by Kimura and Crow as they analyzed the probability of a single mutant or immigrant allele to fixate [49, 93**?**]. Invasion is also of relevance in biodiversity. The biodiversity of an island increases as immigrants from a neighbouring mainland enter (and decreases as species go locally extinct); the balance of these forces was one of the historic contributions of MacArthur and Wilson [117**?**]. More generally, the biodiversity of an ecosystem is maintained by invaders generated by speciation, as per Hubbell's neutral theory, which predicts the abundance distribution of species [76]. Bearing these historical precedents in mind, I do not distinguish from where a new strain or species might enter in my modelling below; mutation, speciation, and immigration are all viable. What is important to my research is that a distinctive second species is attempting to invade an already occupied system. Whether the invader is under selection [92] or the system is neutral [76**?**], the literature regards cases where the system is constrained to the Moran line, to constant population size. What has *not* been done is to look at an invasion attempt into an established niche when the invader has partial niche overlap with the established species.

By using the two species Lotka-Volterra model from the previous chapter I can study invasion in the neutral case where the system is allowed to fluctuate off the Moran line, or even when the two species should happily coexist in the deterministic limit, *i.e.* with partial niche overlap and a single stable coexistence fixed point. I do this by continuing to use the truncated transition matrix inverse to solve

the backward master equation for arbitrary accuracy. Furthermore, the literature typically argues that invasion attempts are sufficiently rare that when an invader arrives it will either successfully invade or die off before another member of the same strain invades. Indeed, this is one of my assumptions when using the Lotka-Volterra model below. But this need not be the case, depending on the immigration rate (see, for example, [69]); I also analyze the Moran model with an immigration term, which allows for repeated concurrent invaders of the same species. In either case I do not worry about effects like clonal interference or multiple mutations [52], since the mutations are either rare or equivalent in my models. Anyway, immigration is more appropriate than mutation for the introduction of invaders, since it is unlikely to have the same mutation recurring independently, unless there is a common mutation pathway or if we categorize all equivalent mutants into one category of invader. In this chapter I shall investigate how the success probability and mean times scale with niche overlap, carrying capacity, and immigration rate, and in so doing I shall uncover critical combinations of these parameters as they affect the scaling of the mean times and the shape of the steady state population probability distribution. Having increased niche overlap leads to lesser chance of invasion and greater times before the attempt resolves. In the Moran model with immigration, the steady state distribution changes from unimodal to bimodal around when the inverse immigration rate of a strain is equal to the expected population of that strain in the system.

There are a few steps needed to get to these conclusions. Within the generalized Lotka-Volterra model there is some ambiguity in the definition of a successful invasion, which I will discuss in the next section before providing a definition. And since there is a chance of success or failure, I shall also find the mean times conditioned on the outcome of that attempt. In the previous chapter because of the initial conditions each species was equally likely to go extinct first. In this chapter's case, it is possible (and indeed true) that an invasion attempt that is ultimately successful will take a long time, whereas one that is unsuccessful fails quickly. These are the conditional mean times, and their scaling with carrying capacity will be analyzed, since exponential scaling implies that the event effectively does not happen. In order to extend these results to the circumstance of repeated concurrent invaders in the Moran limit I analyze the Moran model with an immigration term. I find the steady state probability distribution analytically to allow for an investigation of the critical parameter combinations that change the concavity of the curve. Along with the probability distribution I find the mean time to fixation, both unconditioned and conditioned on whether the species first fixates or goes extinct in the system. The application is in neutral theories like that of Hubbell [76]; I find the qualitatively different regimes of the probability distribution, which can be extended to abundance distributions. Neutral theories of the maintenance of biodiversity argue that no species truly establishes itself, and biodiversity is maintained by transient species in the system. Calculation of the steady state number of species requires the time that these transient species exist in the system. My results hold both for a species in an ecosystem (hence its relevance to conservation biology, where biodiversity is a marker of ecosystem robustness) [24, 71, 130, 151] and a gene in a population (hence its use in calculating heterozygosity, which confers resilience to environmental changes) [87, 94, 105, 149]. There are also more practical applications, like the susceptibility of a microbiome ecosystem like the gut or lungs to invasion, say from salmonella or pneumococcus [45, 59, 98, 103, 161, 174**?**].

3.2 Defining Invasion in the 2D Lotka-Volterra Model

As before, I employ the symmetric generalized LV model with niche overlap a and carrying capacity K. I study the case where the system starts with $K-1$ individuals of the established species and 1 invader. This initial condition corresponds to a birth of a mutant. An initial condition of K established organisms and the 1 invader gives similar results. The species' dynamics are described by the birth and death rates defined by Equations (2.10) from the previous chapter, which I reproduce here:

$$\begin{aligned} b_i/x_i &= r_i \\ d_i/x_i &= r_i \frac{x_i + a_{ij}x_j}{K_i}. \end{aligned}$$

An invasion is unsuccessful if the invading species dies out before establishing itself in the system. There are many ways to define what it means for a species to be established, and I will outline one such definition below. Deterministically the system would grow to asymptotically approach the coexistence fixed point; deterministically, all invasion attempts are successful, and stochasticity is required for non-trivial invasion probabilities. In a stochastic system, the populations could very easily fluctuate *near* the fixed point without touching that exact point. This would overestimate the time to establishment, or even misrepresent a successful invasion as unsuccessful if the system gets near the fixed point without reaching it but then goes extinct. Indeed, there is even a chance the established species dies out before the system reaches the coexistence fixed point, which would be counted as an unsuccessful invasion. For these reasons a successful invasion should not be defined as the system arriving at the coexistence point. The same arguments hold for a defined region near the fixed point (for instance, within three birth or death events, or within a circle of radius ε): the region might by chance be avoided for a time even after the invader is more populous than the original species, which could even go extinct before the invader. Inspired by the observation that in the symmetric case, the coexistence fixed point has the same population of each species, I consider the invasion successful if the invader grows to be half of the total population without dying out first. So long as the invader population matches that of the established species, regardless what random fluctuations may have made that population to be, the invasion is a success. I denote the probability of a invader success as $\mathcal{P}$.

Along with the probability of a successful invasion attempt, I am interested in the timescales involved. As such, I will consider conditional mean times, conditioned on either success or failure of the invasion attempt. The mean time to a successful invasion is written as τ_s, and the mean time of a failed invasion attempt as τ_f. More generally, invasion probability and the successful and failed times starting from an arbitrary state s^0 are denoted as $\mathcal{P}^{s^0}$, $\tau_s^{s^0}$ and $\tau_f^{s^0}$, respectively.

Similar to Equation (2.22) in a previous chapter, the invasion probability can be obtained from [82, 139]

$$\mathcal{P}^{s^0} = -\sum_s \hat{M}^{-1}_{s,s^0}\alpha_s \tag{3.1}$$

and the times from

$$\Phi^{s^0} = -\sum_s \hat{M}^{-1}_{s,s^0}\mathcal{P}^s, \tag{3.2}$$

where α_s is the transition rate from a state s directly to extinction or invasion of the invader and $\Phi^{s^0} = \tau^{s^0}\mathcal{P}^{s^0}$ is a product of the invasion or extinction time and probability. Similar equations describe τ_f [82, 139]. As in the previous chapter, I truncate the transition matrix and invert it in order to solve

these equations.

3.3 Invasion probability and times into the Lotka-Volterra model

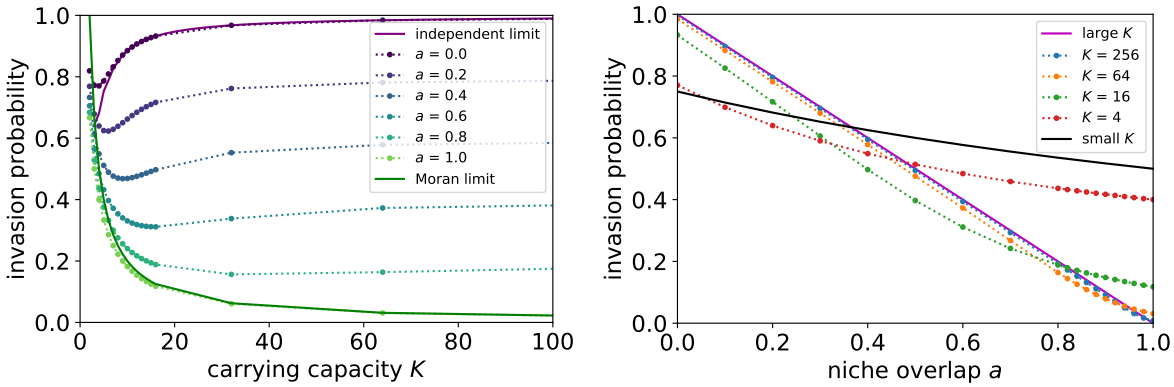

Figure 3.1: *Probability of a successful invasion. Left:* Solid lines show the numerical results, from $a = 0$ at the top to $a = 1$ at the bottom. The purple solid line is the expected analytical solution in the independent limit. The green solid line is the prediction of the Moran model in the complete niche overlap case. Data come from equation 3.2 and are connected with dotted lines to guide the eye. *Right:* The red data show the results for carrying capacity $K = 4$, and suggest the solid black line $\frac{b_{mut}}{b_{mut}+d_{mut}}$ is an appropriate small carrying capacity limit. Successive lines are at larger system size, and approach the solid magenta line of $1 - d_{mut}/b_{mut} \approx 1 - a$.

Figure 3.1 shows the calculated invasion probabilities as a function of the carrying capacity K and of the niche overlap a between the invader and the established species. In the complete niche overlap limit, $a = 1$, the dependence of the invasion probability on the carrying capacity K closely follows the results of the classical Moran model, $\mathcal{P}^{s^0} = 2/K$ [133], shown in the blue dotted line in the left panel, and tends to zero as K increases. In the other limit, $a = 0$, the problem is well approximated by the one-species stochastic logistic model starting with one individual and evolving to either 0 or K individuals; the exact result in this limit is shown in black dotted line, referred to as the independent limit [139]. In the independent limit, $a = 0$, the invasion probability asymptotically approaches 1 for large K, reflecting the fact that the system is deterministically drawn towards the deterministic stable fixed point with equal numbers of both species. As K gets large, fluctuations are minimal and the system becomes more deterministic. Interestingly, the invasion probability is a non-monotonic function of K and exhibits a minimum at an intermediate/low carrying capacity, which might be relevant for some biological systems, such as in early cancer development [11] or plasmid exchange in bacteria [67].

For the intermediate values of the niche overlap, $0 < a < 1$, the invasion probability is a monotonically decreasing function of a, as shown in the right panel of Figure 3.1. For large K, the outcome of the invasion is typically determined after only a few steps: since the system is drawn deterministically to the mixed fixed point, the invasion is almost certain once the invader has reproduced several times. At early times, the invader birth and death rates (2.10) are roughly constant, and the invasion failure can be approximated by the extinction probability of a birth-death process with constant death d_{mut} and birth b_{mut} rates. The invasion probability is then $\mathcal{P} = 1 - d_{mut}/b_{mut} \approx 1 - a$. This heuristic estimate is in excellent agreement with the numerical predictions, shown in the right panel of Figure 3.1 as a purple

dashed and the blue lines respectively. Similarly, for small K either invasion or extinction typically occurs after only a small number of steps. The invasion probability in this limit is dominated by the probability that the lone mutant reproduces before it dies, namely $\frac{b_{mut}}{b_{mut}+d_{mut}} = \frac{K}{K(1+a)+1-a}$, as shown in black dotted line in the right panel of Figure 3.1.

The upper panels of figure 3.2 show the dependence of the mean time to successful invasion, τ_s, on K and a. Increasing K can have potentially contradictory effects on the invasion time, as it increases the number of births before a successful invasion on the one hand, while increasing the steepness of the potential landscape and therefore the bias towards invasion on the other. Nevertheless, the invasion time is a monotonically increasing function of K for all values of a. In the complete niche overlap limit $a = 1$ the invasion time scales linearly with the carrying capacity K, as expected from the predictions of the Moran model, $\tau_s = \Delta t K^2(K-1)\ln\left(\frac{K}{K-1}\right)$ with $\Delta t \simeq 1/K$, as explained above. The quantitative discrepancy arises from the breakdown of the $\Delta t \simeq 1/K$ approximation off of the Moran line. For all values $0 \leq a < 1$ the invasion time scales sub-linearly with the carrying capacity, indicating that successful invasions occur relatively quickly, even when close to complete niche overlap, where the invading mutant strongly competes against the stable species. In the $a = 0$ limit of non-interacting species, the invading mutant follows the dynamics of a single logistic system with the carrying capacity K, resulting in the invasion time that grows approximately logarithmically with the system size, as shown in the upper left panel of figure 3.2 as a purple line. This result is well-known in the literature, often stated without reference [108, 145]. It is easy to see: by writing $\tau_s = \int dt = \int_{x_o}^{x_f} dx \frac{1}{\dot{x}}$ for initial state $x_0 = 1$ and final state $x_f = (1-\epsilon)K$ with small ϵ and large K we get

$$\begin{aligned}\tau_s &= \frac{1}{r}\int_{x_o}^{x_f} dx \frac{K}{x(K-x)} = \frac{1}{r}\int_{x_o}^{x_f} dx \left(\frac{1}{x} - \frac{1}{K-x}\right) = \frac{1}{r}\ln\left[\frac{x}{K-x}\right]|_{x_o}^{x_f} = \frac{1}{r}\ln\left[\frac{x_f(K-x_o)}{x_o(K-x_f)}\right] \\ &\approx \frac{1}{r}\ln\left[\frac{(1-\epsilon)K}{\epsilon}\right] \approx \frac{1}{r}\left(\ln[K] - \ln[\epsilon]\right)\end{aligned}$$

and so expect the invasion time to grow logarithmically with carrying capacity.

Unlike the mean times conditioned on success, the failed invasion time, shown in the lower left panel of figure 3.2, is non-monotonic in K. The analytical approximations of the Moran model and the of two independent 1D stochastic logistic systems recover the qualitative dependence of the failed invasion time on K at high and low niche overlap, respectively. All failed invasion times are fast, with the greatest scaling being that of the Moran limit. For $a < 1$ these failed invasion attempts appear to approach a constant timescale at large K.

The dependence of the time of an attempted invasion (both for successful and failed ones) on the niche overlap a is different for small and large K, as shown in the right panels of figure 3.2. For small K both τ_s and τ_f are monotonically decreasing functions of a, with the Moran limit having the shortest conditional times. In this regime, the extinction or fixation already occurs after just a few steps, and its timescale is determined by the slowest steps, namely the mutant birth and death. Thus $\tau \approx \frac{1}{b_{mut}+d_{mut}} = \frac{K}{K+1+a(K-1)}$, as shown in the figure as the solid cyan line. By contrast, at large K, the invasion time is a non-monotonic function of the niche overlap, increasing at small a and decreasing at large a. This behavior stems from the conflicting effect of the increase in niche overlap: on the one hand, increasing a brings the fixed point closer to the initial condition of one invader, suggesting a shorter timescale; on the other hand, it also makes the two species more similar, increasing the competition that hinders the invasion.

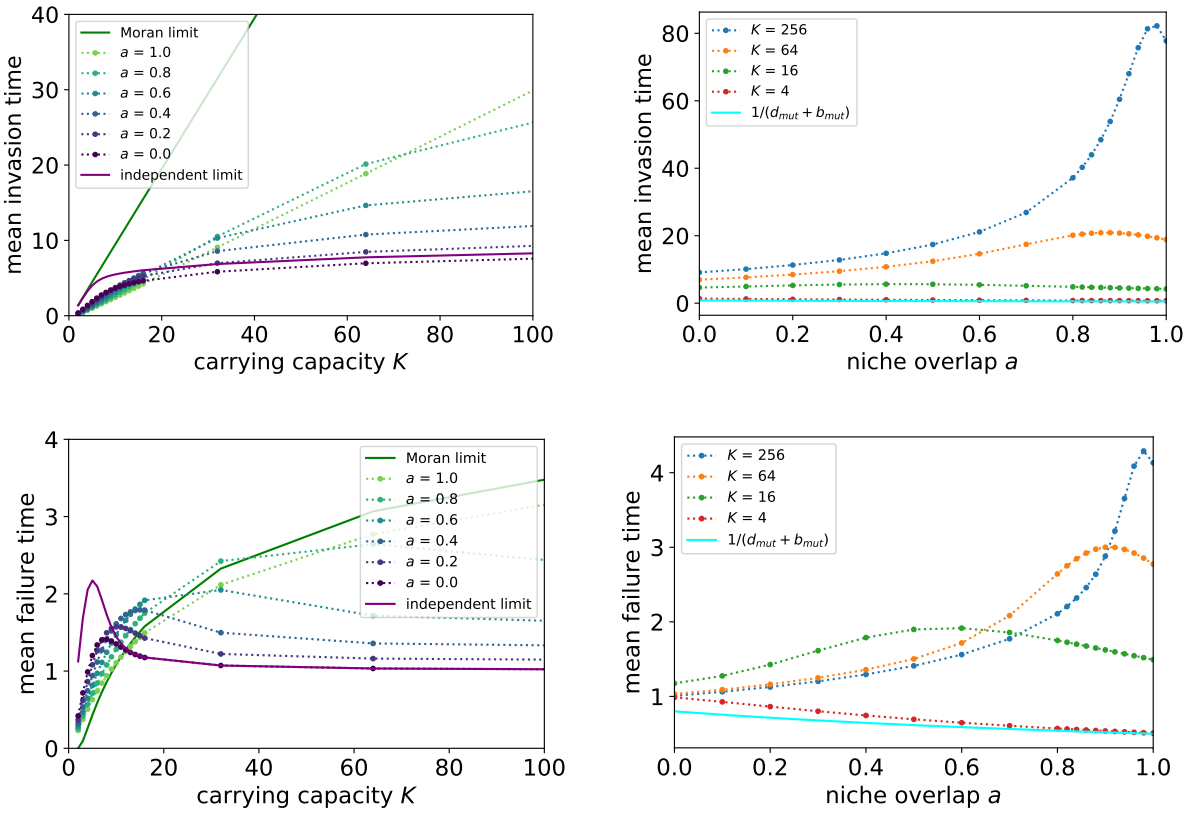

Figure 3.2: *Mean time of a successful or failed invasion attempt. Upper Left:* Dotted lines connect the numerical results of invasion times conditioned on success, from $a = 0$ at the bottom being mostly fastest to $a = 1$ being slowest. The solid green line shows for comparison the predictions of the Moran model in the complete niche overlap limit, $a = 1$; see text. The solid purple line correspond to the solution of an independent stochastic logistic species, $a = 0$, and overestimates the time at small K but fares better as K increases. *Upper Right:* The red line shows the results of successful invasion time for carrying capacity $K = 4$, and successive lines are at larger system size, up to $K = 256$. The cyan line is $1/(b_{mut} + d_{mut})$ and matches with small K. *Lower Panels:* Same as upper panels, but for the mean time conditioned on a failed invasion attempt.

3.4 Discussion of one attempted invasion

Unlike the fixation times of the previous chapter, invasions into the system do not show exponential scaling in any limit. Indeed, all scaling with K is sublinear except in the complete niche overlap limit for successful invasion times. The timescale of a successful invasion varies between linear and logarithmic in the system size. The mean time of an unsuccessful invasion is even faster than logarithmic, and for large K it becomes independent of K. Curiously, these failed invasion attempts are non-monotonic, at intermediate carrying capacity and niche overlap values. As for the probabilities, the likelihood of a failed invasion attempt grows linearly with niche overlap, for sufficiently large K. For complete niche overlap the invasion probability goes asymptotically to zero, but it is low even for partially mismatched niches.

High niche overlap makes invasion difficult due to strong competition between the species. In this regime, the times of the failed invasions become important because they set the timescales for transient species diversity. If the influx of invaders is slower than the mean time of their failed invasion attempts,

most of the time the system will contain only one settled species, with rare "blips" corresponding to the appearance and quick extinction of the invader. On the other hand, if individual invaders arrive faster than the typical times of extinction of the previous invasion attempt, the new system will exhibit transient coexistence between the settled species and multiple invader strains, determined by the balance of the mean failure time and the rate of invasion [37, 53, 76]. Full discussion of diversity in this regime is beyond of the scope of the present work. The weaker dependence of the invasion times on the population size and the niche overlap, as compared to the escape times of a stably coexisting system to fixation, imply that the transient coexistence is expected to be much less sensitive to the niche overlap and the population size than the steady state coexistence. Curiously, both niche overlap and the population size can have contradictory effects on the invasion times (as discussed in the previous section) resulting in a non-monotonic dependence of the times of both successful and failed invasions on these parameters.

For species with low niche overlap, the probability of invasion is likely, and for large K decreases monotonically as $1 - a$ with the increase in niche overlap, independent of the population size K. The mean time of successful invasion is relatively fast in all regimes, and scales linearly or sublinearly with the system size K and is typically increasing with the niche overlap a.

The fixation times of two coexisting species, discussed in the previous chapter, determine the timescales over which the stability of the mixed populations can be destroyed by stochastic fluctuations. Similarly, the times of successful and failed invasions set the timescales of the expected transient coexistence in the case of an influx of invaders, arising from mutation, speciation, or immigration. Our results provide a timescale to which the rate of immigration or mutation can be compared. If the influx of invaders is slower than the mean time of their failed invasion attempts, each attempt is independent and has the invasion probability we have calculated. In the extreme case of this, that is, if the time between invaders is even longer than the fixation times calculated in the previous chapter, then serial monocultures are expected. If the rate in is greater than the mean failure time, the system will diversify. The balance between mutation or immigration coming into the system and these invaders failing to establish themselves determines how diverse a system will be. With different strains of invaders arising faster than the time it takes to suppress the previous invasion attempt, the new strains interact with one another in ways beyond the scope of this thesis, leading to greater biodiversity.

3.5 Known Moran model results

We can get an idea of what it would be like to have a new immigrant come in before the previous invasion attempt is over by considering a Moran model with immigration. This would correspond to the complete niche overlap limit, such that the population size is roughly constrained to the Moran line. In the following sections I solve steady state and dynamical properties of the Moran model with immigration. Compared to the Moran limit of the Lotka-Volterra system it is easier to treat, has well established literature results against which to compare, and offers analytic solutions.

The previous results in this chapter have related to a single organism attempting to invade a system wherein another species is already established. The number of invader progeny fluctuates and ultimately it either dies out or occupies half of the total population, as per my definition of a successful invasion. But recall the island model of MacArthur and Wilson, in which a mainland system, which is large, is considered to be static, while a much smaller island system's dynamics are regarded, occasionally including immigration from the mainland. If the immigration rate is large then the invaders will receive

reinforcements from the mainland in their attempt to establish themselves on the island system of interest. Rather than using the Lotka-Volterra model as I did above, I choose to model this process with the simpler Moran model with immigration, which allows for analytic calculation. The cost of the model's tractability is that it is constrained to neutrality; after I have derived my results I will comment on how a deviation with neutrality might shift the results. I will be able to find the expected population of a focal species, how the model parameters qualitatively change how the population is distributed, and the characteristic times of the system. The Moran model without immigration is the basis for the neutral models of Kimura [148**?** **?**] and Hubbell [20, 76], as well as coalescent theory [26, 57, 97]. Slightly different models, with selection and without the chance of repeat immigrants, have been addressed by others [26, 35, 42, 50, 107, 146, 154, 173]. With immigration, the model was analyzed by McKane *et al.* [131] to find the probability distribution exactly and the time evolution approximately. In the following section I will confirm their probability distribution and use the fact that it is analytic to calculate the critical parameter combination at which the distribution qualitatively changes shape. I also find the first passage times analytically and link the Moran model with immigration to the results of a single invader as studied earlier in this chapter. But first I must review the Moran model and some quantities that can be calculated from it.

In the classic Moran model, each iteration or time step involves a birth and a death event. Each organism is equally likely to be chosen (for either birth or death), hence a species is chosen according to its frequency, $f = n/N$, where N is the total population and n is the number of organisms of that species. We focus on one species of population n, which will be referred to as the focal species. Note that $N - n$ represents the remainder of the population, and need not all be the same species, so long as they are not the focal species [25]. The focal species increases in the population if one of its members gives birth (with probability f) while a member of a different species dies (with probability $1 - f$); that is, in time step Δt the probability of focal species increase is $b(n) = f(1 - f)$. Similarly, decrease in the focal species comes from a birth from outside the focal group and a death from within, such that the probability of decrease is $d(n) = (1 - f)f$. By commutativity of multiplication, increase and decrease of the focal species are equally likely, with

$$b(n) = d(n) = n(N - n)/N^2. \tag{3.3}$$

Each time step, the chance that nothing happens is $1 - (b(n) + d(n)) = f^2 + (1 - f)^2$.

Note that, unlike in previous chapters where I used b and d as rates, here these are not rates, rather they are the probability of an increase or decrease of the focal species in one time step. I use the same notation not to be confusing but to hint at an approximation I employ in the following sections. Taking Δt to be infinitesimal, $b(n)\Delta t$ and $d(n)\Delta t$ serve as probabilities of birth and death of the focal species during this small time interval. This creates a continuous time analogue to the Moran model, with b and d serving as rates. The timescale is now in units of Δt, which is only relevant if one were to compare with other models, which I do not. With this approximation I can employ the formulae explored in chapter 1 for quantities like quasi-stationary probability distribution and mean time to extinction.

For reference, I include the mean and variance of a focal population as a function of time [93, 130, 133], so that I may later compare with the immigration case. If the system starts with n_0 individuals of the focal species, then on average there should be n_0 individuals in the next time step as well. Therefore the mean population as a function of time is $\langle n \rangle(t) = n_0$. Since the extremes of $n = 0$ and $n = N$ are absorbing, the ultimate fate of the system is in one of these two states, despite the mean being constant.

The variance starts at zero for this delta function initial condition. After k time steps the variance is

$$V_k = n_0(N-n_0)\big(1-(1-2/N^2)^k\big).$$

For finite N the variance goes to $N^2\, f_0(1-f_0) = n_0(N-n_0)$ at long times. This is easy to intuit: there is probability f_0 that the system ended in $n=N$, and probability $(1-f_0)$ of ending at $n=0$, since at long times the system has fixated at one end or the other. Notice that as $N\to\infty$ the variance, a measure of the fluctuations, goes to zero, and the system becomes deterministic, as any change of $\pm 1/N$ in the frequency of the focal species becomes meaningless.

The mean and variance characterize the distribution of outcomes that could occur when running an ensemble of identical trials of the same system. This is the the ensemble average denoted by $\langle\cdot\rangle$. Any individual trajectory, any individual realization, will take its own course, independent of any others, and after fluctuations will ultimately end up with either the focal species dying (extinction) or all others dying (fixation). Both of these cases are absorbing states, so once the system reaches either it will never change. Since a species is equally likely to increase or decrease each time step, the model is akin to an unbiased random walk [64], and therefore the probability of extinction occurring before fixation is just

$$E(n) = 1 - n/N = 1 - f. \tag{3.4}$$

The first passage time, however, does not match a random walk, as there is a probability of no change in a time step, and this probability varies with f.

The unconditioned first passage time can be found using the techniques outlined in chapter 1. As a reminder, I define the unconditioned first passage time $\tau(n)$ as the time the system takes, starting from n organisms of the focal species, to reach either fixation *or* extinction. It can be calculated by regarding how the mean from one starting position n relates to the mean of its neighbours.

$$\tau(n) = \Delta t + d(n)\tau(n-1) + (1-b(n)-d(n))\,\tau(n) + b(n)\tau(n+1) \tag{3.5}$$

Substituting in the values of the increase and decrease rates and rearranging this gives

$$\tau(n+1) - 2\tau(n) + \tau(n-1) = -\frac{\Delta t}{b(n)} = -\Delta t\frac{N^2}{n(N-n)}.$$

Similar to the Fokker-Planck approximation, I approximate the LHS of the above with a double derivative (ie. $1 \ll N$) to get $\frac{\partial^2\tau}{\partial n^2} = -\Delta t\, N\left(\frac{1}{n}+\frac{1}{N-n}\right)$. Double integrate and use the bounds $\tau(0)=0=\tau(N)$ gives

$$\tau(n) = -\Delta t\, N^2\left(\frac{n}{N}\ln\left(\frac{n}{N}\right) + \frac{N-n}{N}\ln\left(\frac{N-n}{N}\right)\right). \tag{3.6}$$

Note that it was not necessary to use the large N approximation, there is an exact solution [133],

$$\tau(n) = \Delta t\, N\left(\sum_{j=1}^{n}\frac{N-n}{N-j} + \sum_{j=n+1}^{N}\frac{n}{j}\right) \tag{3.7}$$

though it is less clear how this scales with N and f.

3.6 Steady state properties of Moran model with immigration

In section (3.4) I argued that qualitatively different steady states are expected depending on a comparison of the timescales of immigration/mutation/speciation and invasion attempts. If new species enter the system faster than they go extinct, the number of extant coexisting species, and hence the biodiversity, should increase to some steady state. Conversely, if extinction is much more rapid than speciation, a monoculture of one single species is expected in the system. Whether the monocultural system consists of the same species over multiple invasion attempts or whether it experiences sweeps, changing from a monoculture of one species to the next, depends on the probability of a successful invasion [37, 39, 52**?**]. Results can easily be simulated, but to get better insight into the role of the parameters on the results I look for analytic solutions, and as such I treat a simplified model, that of the Moran model with immigration.

The Moran model with immigration is akin to the Hubbell model [76]. His work reinvigorated the debate between niche and neutral mechanisms of biodiversity maintenance. Early numerical solution of the Hubbell model was done by Bell [19]. Ultimately, it is simply a Moran model with immigration, where the immigrant species is never from one of the extant species (from Hubbell's perspective, the newcomers arise via speciation rather than immigration or simple mutation). Hubbell composed his theory to describe species abundance curves, rather than my interests of the population probability distribution or lifetime of a single species. By an abundance curve I mean a Preston plot, a plot of the number of species that belong in bins of exponentially increasing population size [76]. This contrasts with the stationary probability distribution of the population (or abundance) of a single species. With regard to this latter concept there was some pioneering work done by Crow and Kimura [49, 96], who had to assume both continuous time (as do I) and continuous population densities (which I do not), arriving at numerical results for the distribution. There now exist more modern techniques, and I highlight the work of McKane *et al.* [130], which follows techniques similar to Hubbell but calculates the single species distribution. The difference between my work and that of McKane *et al.* is that I find the critical value of parameters such that the distribution changes qualitatively. There also remains a gap in the literature in that no one, to the best of my knowledge, has considered the conditional first passage time conditioned on the focal species going extinct or else fixating in the system.

One experimental motivation for this work is work from the Gore lab [178], measuring the gut microbiome of bacteria-consuming *C. elegans* grown in a 50-50 environment of two strains of fluorescently-labeled but otherwise identical *E. coli*. After an initial colonization period, each nematode has a stable number of bacteria in their gut, presumably from a balance of immigration, birth, and death/emigration. The researchers find the population distribution depending on the comparison of two experimental timescales, those of establishment and fixation time conditioned on a successful invasion. In this section I calculate the stationary probability distribution of a single species [**?**], analyzing the critical parameter choices that change its qualitative form. Later, I find the probability of first reaching extinction versus fixation and the first passage times conditioned on these two possibilities.

Just as before, the Moran model focuses on one species of n organisms, called the focal species, with the remaining $N - n$ organisms being of a different strain (or strains). Again I define a fractional abundance $f = n/N$ of the species on which I focus. The Moran population is treated as a rapidly evolving population, with immigrants coming from a more static metapopulation of larger size and diversity. As with the Moran population, the metapopulation contains the focal species and other species, with new parameters m, M and g being analogous to n, N and f. That is, an immigrant

into the Moran population is a member of the focal species with probability g, and of another species with probability $1-g$. The metapopulation contains $m = g\,M$ members of the focal species out of M total organisms. In principle g should be a random number drawn from the probability distribution associated with an evolving metapopulation, but for $M \gg N$ one can treat it as fixed. In practice, I am assuming that the metapopulation changes much slower than the Moran population [**?**]. In the context of the Gore experiment [178], the system of interest is the nematode gut, and the metapopulation is the environment in which the nematode lives (and eats). The consumption of one bacterium will influence the gut microbiome while having a negligible effect on the external environment. In a more general setting, the system of interest is a small island receiving immigrants from a larger mainland; the arrival of one immigrant on the island can be impactful even when the loss of that same emigrant is negligible to the mainland.

Each step of the Moran model involves one birth and one death. As before, the focal species dies with probability f. Immigration is incorporated by having a fraction ν of the birth events be replaced by immigration events. The regular Moran model has the focal species increasing in population with probability $f(1-f)$; this is now modified to occur only a fraction $(1-\nu)$ of the time, and there is also a contribution $\nu g(1-f)$ that increases the focal population when an immigrant enters (fraction ν) of the focal species (fraction g) when a death of a non-focal species occurs (fraction $1-f$). As before, I take the time interval Δt of each step to be infinitesimal, such that b and d are rates, which are:

transition	function	value
$n \to n+1$	$b(n)$	$f(1-f)(1-\nu) + \nu g(1-f)$
$n \to n-1$	$d(n)$	$f(1-f)(1-\nu) + \nu(1-g)f$
$n \to n$	$1-b(n)-d(n)$	$\left(f^2+(1-f)^2\right)(1-\nu) + \nu\left(gf+(1-g)(1-f)\right)$

Note that the rates of increase and decrease of the focal species are no longer the same as each other (as they are in the classical Moran model); there is a bias in the system, toward having a population of gN. Notice that setting the immigration rate ν to zero recovers the classic Moran model.

If a new mutant or immigrant species is unlikely to enter again (ie. if $g \simeq 0$) then the model corresponds to the Moran model with selection [26, 35, 42, 50, 107, 146, 154, 173], which I will not explicitly treat, though it is included in the general treatment below. Also included here results similar to those of the Moran limit of section 3.4 above, with a single immigrant entering the community and then either successfully invading or going (locally) extinct. Since there is immigration from the static metacommunity, the system will never truly fixate, as there will always be immigrants of the 'extinct' species to be reintroduced to the population. Rather, the system will settle on a stationary distribution of P_n, the probability of having n organisms of the focal species. The process has the master equation $\frac{d\,P_n(t)}{dt} = P_{n-1}(t)b(n-1) + P_{n+1}(t)d(n+1) - \big(b(n)+d(n)\big)P_n(t)$, the difference equation of which can be solved in steady state to give

$$\widetilde{P}_n = \frac{q_n}{\sum_{i=0}^{N} q_i} \tag{3.8}$$

where

$$q_0 = \frac{1}{b(0)} = \frac{1}{\nu g}$$
$$q_1 = \frac{1}{d(1)} = \frac{N^2}{(N-1)(1-\nu)+\nu N(1-g)}$$
$$q_i = \frac{b(i-1)\cdots b(1)}{d(i)d(i-1)\cdots d(1)} = \frac{1}{d(i)}\prod_{j=1}^{i-1}\frac{b(j)}{d(j)}, \qquad \text{for } i > 1$$

recalling that $\frac{b(i)}{d(i)} = \frac{i(N-i)(1-\nu)+\nu N g(N-i)}{i(N-i)(1-\nu)+\nu N(1-g)i}$. The unnormalized steady-state probability q_n can be written compactly as

$$q_n = \frac{N^2\Gamma(N)\Gamma\left(n+\frac{gN\nu}{1-\nu}\right)\Gamma\left(N-n+1+\frac{(1-g)N\nu}{1-\nu}\right)}{\big(n(N-n)(1-\nu)+(1-g)nN\nu\big)\Gamma(n)\Gamma(N-n+1)\Gamma\left(1+\frac{gN\nu}{1-\nu}\right)\Gamma\left(N+\frac{(1-g)N\nu}{1-\nu}\right)}$$

and the sum of these is the normalization

$$\sum q_i = \frac{1}{g\nu}\frac{\Gamma[1-\frac{N(1-g\nu)}{1-\nu}]\Gamma[N+1-\frac{N}{1-\nu}]}{\Gamma[N+1-\frac{N(1-g\nu)}{1-\nu}]\Gamma[1-\frac{N}{1-\nu}]}$$

which follows formally from the definition of the hypergeometric function ${}_2F_1$. See also [**?**]. See figure 3.3 for a visualization of the steady-state probability distribution for different immigration rates. When immigration is frequent the distribution is drawn near the middle and is peaked at $g\,N$, which is the most common population to occur. This high likelihood of having a moderate population is contrasted with the case when immigration is rare. Instead of a unimodal distribution with the focal species existing at some moderate value, the species is most likely to be locally extinct, unless immigration is most often from the focal species ($g > 0.5$), in which case the species is most likely to be found as the dominant, fixated species in the system. These qualitatively different outcomes suggest some critical parameter combination that divides them, which is discussed below.

While the time dependent population probability distribution is difficult to calculate before it attains the steady state [**?**], the mean and variance of the distribution are more tractable at all times. If the mean μ at some time step k has $\mu_k = n_k$ individuals, then after one time step $\mu_{k+1} = n_k - d(n_k) + b(n_k) = n_k + \nu(g - f_k)$ individuals. That is, $\mu_{k+1} - \mu_k = \nu(g - \mu_k/N)$. This is solved by

$$\mu_k = \langle n\rangle(k) = gN\left(1-(1-n_0)(1-\nu/N)^k\right). \tag{3.9}$$

At long times the mean fraction f approaches g, the fraction of the focal species in the metapopulation. Finding the variance involves solving a difficult difference equation; to get the an approximation of the variance, I consider the continuous time analogue to the model by taking Δt to be infinitesimal, as described previously. First, the above difference equation of the mean is written as a differential equation $\partial_t\mu(t) = \langle b(n) - d(n)\rangle = \nu\,(g - \mu(t)/N)$, which has solution $\mu(t) = gN + (\mu_0 - gN)e^{-\nu t/N}$, and

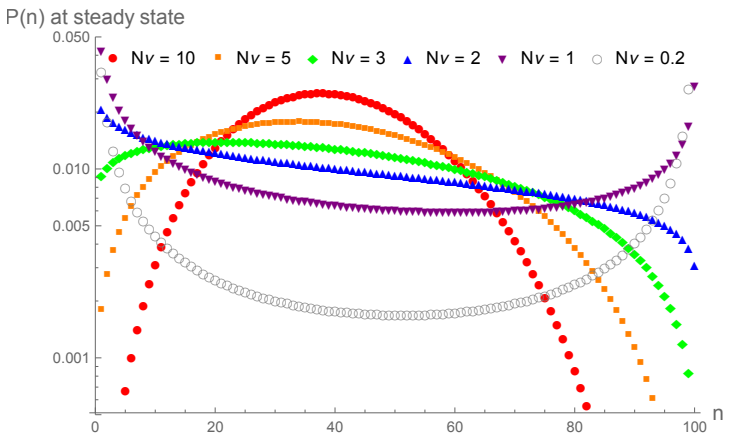

Figure 3.3: *PDF of stationary Moran process with immigration.* Metapopulation focal fraction is $g = 0.4$, local system size $N = 100$, immigration rate ν is given by the colour. Notice that the curvature of the distribution inverts around $\nu = 2/N$. For high immigration rate the distribution should be centered near the metapopulation fraction $g\,N$ whereas for low immigration the system spends most of its time fixated.

the timescale is set by N/ν. The dynamical equation for the second moment is

$$\begin{aligned}\partial_t\langle n^2\rangle &= 2\langle nb(n) - nd(n)\rangle + \langle b(n) + d(n)\rangle \\ &= 2\nu\left(g\mu - \langle n^2\rangle/N\right) + 2(1-\nu)\left(N\mu - \langle n^2\rangle\right)/N^2 + \nu(\mu + gN - 2\mu g)/N\end{aligned}$$

which is an inhomogeneous linear differential equation. Recalling that $\sigma^2(t) = \langle n^2\rangle(t) - \mu^2(t)$ I solve the above equation and write the variance as

$$\sigma^2(t) = \sigma^2(\infty) + A\exp\{-\frac{\nu}{N}t\} - B\exp\{-2\frac{\nu}{N}t\} + C\exp\{-\frac{2}{N}\left(\nu + \frac{(1-\nu)}{N}\right)t\}$$

where $A = \big(1 + g\nu - g(1-\nu)/N\big)N^2\frac{\mu_0 - gN}{N\nu + 2(1-\nu)}$, $B = (gN - \mu_0)^2$, and C is an integration constant; $C = \sigma^2(0) - \sigma^2(\infty) + (gN - \mu_0)^2 + (gN - \mu_0)(2-\nu)(1-2g)/\big(N\nu + 2(1-\nu)\big)$ if the initial variance is $\sigma^2(0)$.

$$\sigma^2(\infty) = g(1-g)N^2\frac{1}{1 + \nu(N-1)} \tag{3.10}$$

is the long time, steady state variance of the system. The variance also has a timescale set by N/ν, after which the steady state variance is approached. The steady state variance is plotted in the left panel of figure 3.4.

Notice that for $g = 0$ or $g = 1$ the long term variance $\sigma^2(\infty)$ asymptotically tends to zero. This contrasts with the results of the Moran model without immigration, which has a nonzero variance. Without immigration there is a nonzero chance of ending up with the focal species fixated or extinct, with fixation ultimate probability equal to initial fractional abundance. Having a supply of immigrants destabilizes one of these absorbing states; for instance for $g = 0$ the ultimate fate is none of the focal species. This is true even if the initial population fraction was almost entirely of the focal species. If immigration is rare the system may temporarily fixate with the focal species, but with the repeated invasion attempts eventually a non-focal species will fixate, after which the system cannot recover the

focal species. Ultimately there is only one fate, hence no variance.

For $g \notin \{0, 1\}$ I would first like to consider the low immigration case when the time $1/\nu$ between immigration events is longer than the timescale of the classic Moran model, which scales proportional to N. In this case we recover similar results to the no immigration case of the Moran model. Instead of $f_0(1 - f_0)N^2$ from the Moran model we get $\sigma^2(\infty) \approx g(1 - g)N^2$, with the metapopulation focal species abundance g acting analogously to the initial abundance f_0. This is easy to intuit. Because the immigration events are rare, each time an immigrant arrives it does so into a system that has already fixated into a monoculture, either of the focal species or without the focal species. A fraction g of the events the immigrant is of the focal species; this is akin to having multiple independent iterations of a classic Moran model, hence the appearance of g as the initial abundance analogue.

In the other extreme, immigration happens much more rapidly than the fixation time of the classic Moran model. When $N\nu \gg 1$ the system is still evolving when a new immigrant is introduced, which acts to keep the probability distribution near g and away from fixation. In this limit the long term variance tends to $\sigma^2(\infty) \approx g(1 - g)N/\nu$. For a fixed system size N, increasing the immigration rate decreases the variance, as the system is drawn more toward the metapopulation abundance and away from the extremes of focal species fixation or extinction.

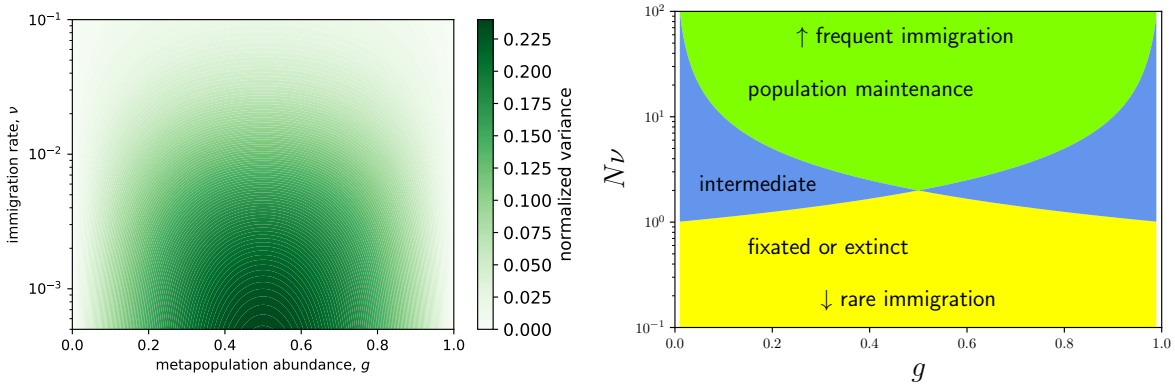

Figure 3.4: *Mapping the parameter space of the Moran model with immigration. Left:* The heat map shows the steady state variance of a focal species' population probability distribution $\sigma^2(\infty)$ in the Moran model with immigration, normalized by N^2. System size is $N = 100$. As immigration probability ν is increased the variance decreases monotonically. Variance is optimal in metapopulation focal species fractional abundance g for $g = 0.5$ as at this fraction there is the greatest likelihood of an immigrant not matching the most populous species in the system. *Right:* Parameter space is divided into the qualitatively different regimes of the system based on the system size N, the immigration rate ν, and the focal species metapopulation abundance g. When immigration is frequent (green region) the focal species is likely to be maintained at a moderate population by new immigrants. When immigration is rare (yellow region) the steady state of the system is either an absence or monoculture of the focal species. There is an intermediate regime (blue region) for which the focal species is present but not fixated.

To the best of my knowledge, these observations on the variance of a Moran model with immigration are novel. The variance limits, and indeed figure 3.3, suggest that there are at least two parameter space regimes of the Moran model with immigration. At low immigration rate the system undergoes a series of monocultures punctuated by the occasional immigrant [52]. It spends most of its time resting in the fixated state, rarely seeing a new immigrant which quickly either dies out or takes over in a new fixation. When immigration is frequent the system follows the metapopulation and is maintained at moderate

population in the system. Deviations away from the metapopulation abundance are suppressed and the probability of having n focal organisms gathers near the mean value gN. These regimes will be investigated further in the following paragraphs.

Like the mean, another way to characterize the distribution is the extremum, which for large immigration rate corresponds to the mode of the system. The extremum occurs at the n for which $\partial_n \widetilde{P}_n = 0$. For ease of analysis it is notable that $\partial_n \widetilde{P}_n = \partial_n \left(q_n / \sum_i q_i\right) = \partial_n q_n = q_n \partial_n \ln(q_n)$ and therefore I can instead calculate the value which gives $\partial_n \ln(q_n) = 0$. First,

$$\begin{aligned}\ln(q_n) = 2\ln[N] - \ln\left[n(N-n)(1-\nu) + (1-g)nN\nu\right] + \ln[(N-n)!] + \ln\left[\left(n - 1 + \frac{\nu g N}{1-\nu}\right)!\right] \quad (3.11)\\ + \ln\left[\left(N - n + \frac{\nu(1-g)N}{1-\nu}\right)!\right] - \ln[(N-n)!] - \ln[(n-1)!] - \ln\left[\left(\frac{\nu g N}{1-\nu}\right)!\right] - \ln\left[\left(N - 1 + \frac{\nu(1-g)N}{1-\nu}\right)!\right].\end{aligned}$$

I have employ the Stirling approximation $\ln[x!] = x\ln[x] - x + O(1/x)$. Setting $\partial_n \ln[q_n] = 0$ and collecting all the non-logarithmic terms to the right-hand side gives

$$\begin{aligned}\ln\left[\frac{(N-n)(n-1+\nu g N/(1-\nu))}{(n-1)(N-n+\nu(1-g)N/(1-\nu))}\right] &= \frac{-2n + N(1-\nu-g\nu)/(1-\nu)}{n\left(-n + N(1-\nu-g\nu)/(1-\nu)\right)}\\ = \ln\left[\frac{(1-f)(f-\gamma+\epsilon g)}{(f-\gamma)(1-f+\epsilon(1-g))}\right] &= \gamma\frac{1-2f-\epsilon g}{f\,(1-f-\epsilon g)} \qquad (3.12)\end{aligned}$$

where $\gamma = 1/N$ and $\epsilon = \nu/(1-\nu)$, and recalling that $f = n/N$. The parameters γ and ϵ are typically small, so I perform an expansion in them. For this expansion the lowest order in these parameters is $O(\gamma)$, followed by $O(\epsilon\gamma)$. The left-hand side has an infinite series in ϵ starting at $O(\epsilon^1)$, before picking up $O(\epsilon\gamma)$ terms. Keeping only the $O(\epsilon^1)$ terms from the left and $O(\gamma^1)$ terms from the right gives

$$f^* = \frac{1 - g\epsilon/\gamma}{2 - \epsilon/\gamma}. \qquad (3.13)$$

This analysis agrees with the observation that there are multiple regimes in parameter space. When immigration is large, $\epsilon/\gamma \approx N\nu \gg 1$, and the maximum or mode of the distribution matches with the mean. The bulk of the probability is centred near gN. But in the opposite limit, when the probability is concentrated at zero and one, the minimal value is half way between these two.

The question remains, how does the distribution switch between these two qualitatively different regimes as ν changes. First, note that there is in fact an intermediate regime, as shown by the blue line $N\nu = 2$ in figure 3.3. The probability need not only be concentrated near both extremes or near gN: for moderate values of immigration there is the possibility that the curvature near one edge of the domain is positive while it is negative near the other. To this end, I calculate whether the ratio of $\widetilde{P}_0/\widetilde{P}_1$ is greater than one for g (assuming $g < 0.5$) and for the symmetric case $g \leftrightarrow 1-g$ (rather than also considering $\widetilde{P}_N/\widetilde{P}_{N-1}$ as a function of g). There are three regimes, with two critical parameter combinations dividing them. At the lower division,

$$\frac{\widetilde{P}_0}{\widetilde{P}_1} - 1 = \frac{q_0}{q_1} - 1 = \frac{N - \nu N^2 g - \nu N g - 1 + \nu}{\nu N^2 g} \approx \frac{N - \nu N^2 g}{\nu N^2 g} < 0 \qquad (3.14)$$

which implies the probability distribution is concave down when $N\nu > 1/g$. By symmetry the other bound is at $1/(1-g)$, below which the distribution is concave down. It turns out these same bounds can

be found by requiring $0 < f^* \approx \frac{1-gN\nu}{2-N\nu} < 1$, since only when the extremum f^* is inside the domain can the distribution have a consistent curvature; when the extremum is outside the domain the distribution is monotonic (between 0 and N) and therefore in the intermediate regime. The regimes are shown in the right panel of figure 3.4.

To recapitulate, when the immigration rate is low, specifically $N\nu < \min\big(1/g, 1/(1-g)\big)$, the Moran model with immigration will have its focal species either fixated or extinct most of the time. In the case of frequent immigration, with $N\nu > \max\big(1/g, 1/(1-g)\big)$, the focal species is maintained at moderate abundance in the system, spending most of its time near the average value gN, with a fraction of the focal species equal to the faction in the metacommunity from which the system receives its immigrants. Qualitatively, these regimes correspond to the system spending most of its time as a monoculture or as having multiple species present, respectively. And there is a third, intermediate regime for $N\nu$ between $1/g$ and $1/(1-g)$ for which the system is often fixated to one extreme but not the other (of $f = 0, 1$), with occasional fluctuations bringing the system away from this extreme. If the metapopulation is equally likely as not to provide an immigrant of the focal species ($g = 0.5$) then there are only the two qualitative regimes of low and high immigration rate.

Regarding the results of the Gore lab [178] one observes two qualitatively different regimes. In those experiments, $g = 0.5$ and $N = 35,000$ for wild type worms or $4,700$ for the immune-compromised strain. They vary the external bacterial concentration, of which ν should be a monotonically increasing function (ranging from $0.1/N \lesssim \nu \lesssim 100/N$). At low bacterial concentration (and therefore low ν), the system has a bimodal population probability distribution dominated by peaks at extinction and fixation. At high bacterial concentration the distribution is more peaked toward the middle. My research predicts that the immune-compromised worms should require a greater external bacterial concentration before the bimodal to unimodal transition is observed when compared to the wild type. The evidence from the data is not obvious.

I had previously written that $N\nu \gg 1$ was the condition of frequent immigration. One also needs to make the comparison between $N\nu$ and $1/g$ to predict, for the focal species, whether it is expected to be locally extinct most of the time (for $N\nu < 1/g$) or maintained at the fractional abundance g (for $N\nu > 1/g$). Of course, how the focal species' metapopulation abundance compares to $N\nu$ is not indicative of how the rest of the (non-focal) species will compare. The metapopulation is expected to contain many species, thus when any one of them is the focal species it is likely that the associated g is small. For each species i that $N\nu > 1/g_i$ we expect it to exist in the system, and so the number of species with g_i's greater than $1/(N\nu)$ gives a estimate of the expected number of species extant in the system when immigration is frequent. To this extent, the distribution of g_i's in the metapopulation prescribes the biodiversity of the local system.

3.7 Dynamical properties of Moran model with immigration

Figure 3.3 gives the probability distribution of the species of interest at steady state, but does not allow us to infer anything about the timescales or dynamics of the system. We can guess that if immigration is common the system will fluctuate about its mean, and if immigrants are rare the system will be in a fixated state punctuated by occasional invasion attempts. Starting from the focal species at an intermediate abundance, I want to find the probability of locally fixating before going extinct, and the timescales of these conditions, recognizing that both local fixation and extinction are temporary states,

since there is always another immigrant on the way. By local I mean in the system, rather than in the metapopulation, which does not evolve. As is standard practice, we take $b(0) = d(N) = 0$, which allows us to find the mean time the system first reaches focal species fixation or extinction [139]. Unlike in the coupled logistic model considered earlier, in this model this mean first passage time is affected by the continual influx of immigrants, and depends on immigration rate ν and focal fraction g.

The technique I employ follows that laid out in the chapter 1 [139]. Define the temporary extinction probability E_i as the probability that the focal species goes extinct in this modified system with absorbing states at $n = 0$ and $n = N$, *i.e.* the system reaches the former before the latter, given that it starts at $n = i$. Then $E_i = \frac{b(i)}{b(i)+d(i)} E_{i+1} + \frac{d(i)}{b(i)+d(i)} E_{i-1}$. Further define $S_i = \frac{d(i)\cdots d(1)}{b(i)\cdots b(1)}$. Then

$$E_i = \frac{\sum_{j=i}^{N-1} S_j}{1 + \sum_{j=1}^{N-1} S_j}. \tag{3.15}$$

See figure 3.5 for the graphical representation of the results. As with the stationary distribution, the extinction probabilities can be written explicitly in terms of N, ν, and g, but graphical interpretation is easier than understanding such a complicated expression. See the appendix.

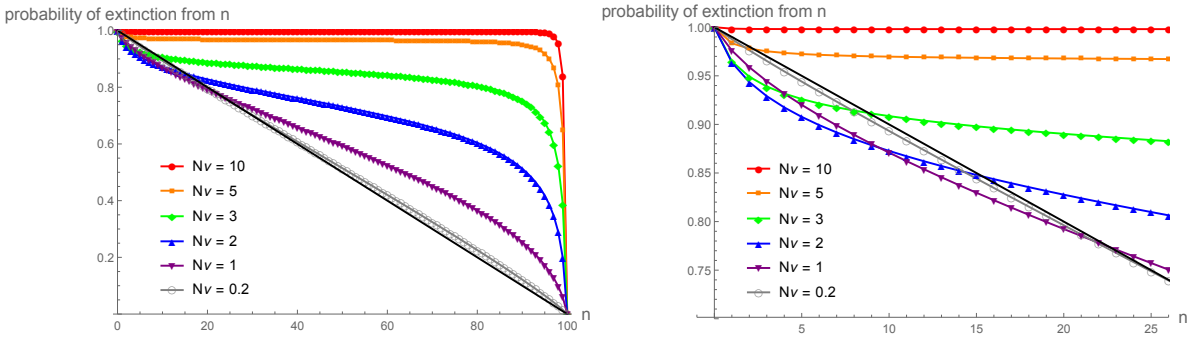

Figure 3.5: *Probability of the focal species reaching temporary extinction before fixation, as a function of initial population. Left:* Metapopulation focal fraction is $g = 0.4$, local system size $N = 100$, immigration rate ν is given by the colour. Lines are included to guide the eye. The black line is the regular Moran result without immigration. *Right:* Same as the left panel but focused on the small n, to show that immigration acts to lower the probability of extinction as compared to the Moran model for some f less than g, even though $g < 0.5$ and more often than not the immigrant is not from the focal species.

Unsurprisingly, when immigrants of the focal species are uncommon ($g < 0.5$) the temporary extinction probability E_i is generally increased compared to the Moran model without immigration. The exception, as highlighted in the right panel of figure 3.5, is observed for some n/N values less than g, when the focal fraction in the metapopulation is notably greater than in the local system; in this case the immigration acts to stabilize the population, lessening the probability of extinction before fixation. Unlike with the steady state results, the different trends for the extremes of $N\nu$ compared to $1/g$ and $1/(1-g)$ are less pronounced. Certainly for large immigration rate and population size, for $g < 0.5$ the temporary extinction is almost certain, as is fixation for $g > 0.5$. But all parameter combinations (with $g \neq 0, 1$) result in a leveling of the probability as compared to the Moran model (in black).

Unconditioned First Passage Time

Similar to the extinction probabilities, we can write the unconditioned mean first passage time to either

temporary fixation or extinction of the focal species [139]:

$$\tau[i] = \sum_{k=1}^{N-1} q_k + \sum_{j=1}^{i-1} S_j \sum_{k=j+1}^{N-1} q_k. \tag{3.16}$$

At $n = 0$ the focal species has temporarily gone extinct and at $n = N$ it has fixated; for both of these cases we get $\tau[n] = 0$ since the system has already attained one of these extremes. The closed analytical expression is cumbersome and shown in the appendix; the results are graphically summarized in the left panel of figure 3.6. Immigration acts to stabilize the system, drawing the focal fraction towards g and hence away from the extremes, at which temporary fixation or extinction occurs. Thus a higher immigration rate is expected to increase the mean time until fixation when compared to the regular Moran model. What is more, immigration skews this unconditioned first passage time for initial focal fractions away from g. Figure 3.6 shows an example with $g = 0.4$. At small n the focal species is more likely to go extinct before it fixates, thus the largest contribution to the unconditioned time is from the mean time conditioned on extinction. Immigration may help delay the inevitable, but the effect is not great, as the majority immigrants do not increase the focal species population. At large n, however, fixation is the main contributor to the unconditioned time. Most of the immigrants act in opposition to fixation of the focal species, greatly increasing the time to either fixation or extinction. I once again remind the reader that since the metapopulation continues to send immigrants into the system, both fixation and extinction of the focal species are temporary.

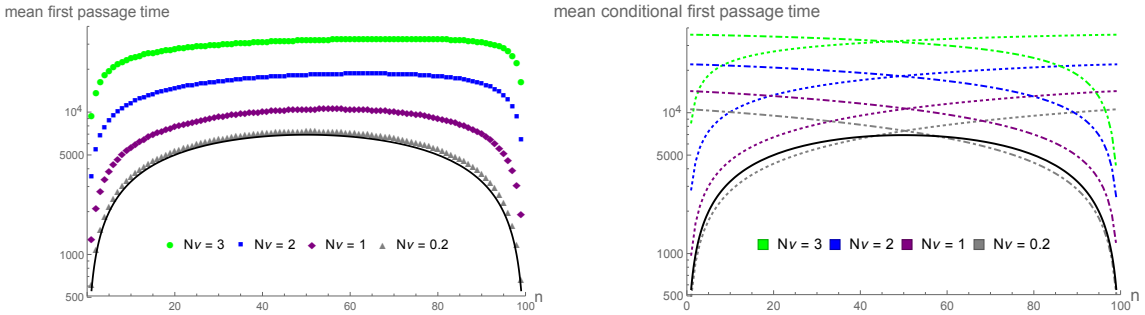

Figure 3.6: *Mean first passage times depending on initial population. Left:* Unconditioned mean time to first reaching either fixation or extinction, from a given starting population of the focal species. Focal immigration fraction is $g = 0.4$, system size is $N = 100$, and immigration rate ν is coloured as before. The black line shows regular Moran results without immigration. Immigration acts to increase the first passage time, and the effects are greatest away from gN. *Right:* Same as the left panel but for conditioned first passage times. Times conditioned on reaching fixation first are given as dashed, and those conditioned on extinction first are dotted. Note that the curves follow their corresponding unconditioned times from the left panel when the occurrence is probable but are much longer when improbable.

Conditioned First Passage Times

In interpreting the unconditioned mean time I made reference to the times conditioned on local focal fixation or extinction. With the clock stopping when the focal population first reaches 0 or N individuals, I calculate the conditional times, respectively to extinction and to fixation. The extinction probability is given by equation 3.15. Equation 3.2 gives the general equation for solving the conditional time, but it can be written more clearly, following the notation of the fixation probability and unconditioned time,

as

$$\phi_n = \phi_1 + \sum_{j=1}^{n-1} \left(\phi_1 - \sum_{i=1}^{j} q_i E_i \right) S_j. \tag{3.17}$$

Here $\phi_i \equiv E_i \theta_i$ (not a dot product, just multiplication of elements), where θ_i is the conditional extinction time [82]. The boundary conditions are both zero, since $E_N = 0$ as does θ_0 [139]. These boundary conditions allow me to rearrange the previous equation to get

$$\phi_1 = \frac{\sum_{j=1}^{N-1} \sum_{i=1}^{j} q_i E_i}{1 + \sum_{j=1}^{N-1} S_j}. \tag{3.18}$$

Equation 3.7 substituted into equation 3.7 allows us to solve for ϕ_n, and therefore the conditional time θ_n. One arrives at the graph shown in the right panel of figure 3.6. The conditional times mostly match the unconditioned time, except near the rare events that do not much contribute to the average. For instance, a low focal species population close to zero is more likely to go extinct and will only rarely fixate. Naturally, the rare fixation takes much longer than the common extinction, the latter of which tends to dominate the unconditioned time.

3.8 Discussion

In the research presented above, even though not all species are equal to each other, their interactions have been symmetric. That is, no species has been given an explicit fitness advantage. The complete neutrality of Hubbell comes when the species not only interact with each other symmetrically but also interact with other species as strongly as they interact with themselves.

My results of the coupled logistic and Moran with immigration models allow for predictions on the dynamic behaviour of a system with one extant species upon attempted invasion of a second, the focal species. Suppose the focal species population starts in state $n = 0$, before any mutations have arisen or immigrants have entered. At a rate νg there will be an attempted invasion by the focal species. Once the invader arrives the dynamics and its ultimate fate depend on how much its niche overlaps with the species currently present in the system. It will be most excluded by those with high population and those with large niche overlap. In the research above I have considered the case of only one extant species upon the arrival of an invader. For species with low niche overlap, the probability of invasion is likely, and for large K decreases monotonically as $1 - a$ with the increase in niche overlap, independent of the population size K. The invader is least likely to be successful in the Moran limit when niche overlap is complete. For invaders that are mutants of the extant wild type species, this $a = 1$ is the niche overlap they are most likely to experience, and so the more similar a mutant is to the wildtype, the less likely it is to reach half the population size, which is how I have defined a successful invasion.

Whether or not a mutant invasion is successful, the timescale is longest when niche overlap is high. The times of successful and failed invasions into a stable population set the timescales of the expected transient coexistence in the case of an influx of invaders, arising from mutation, speciation, or immigration [32, 52, 76]. The mean time of successful invasion is relatively fast in all regimes, and scales linearly or sublinearly with the system size K. By contrast, high niche overlap makes invasion difficult due to strong competition between the species. In this regime, the times of the failed invasions become particularly salient because they set the timescales for transient species diversity. We must compare the

rate of invasion attempts νg to the time to success or failure of an invasion attempt. If the influx of invaders is slower than the mean time of their failed invasion attempts, most of the time the system will contain only one settled species, with rare "blips" corresponding to the appearance and quick extinction of the invader [37, 53, 76]. Recent research from the Gore lab shows that these transient species can have lasting effects on the distribution of extant species [**?**], but I do not study the structure of the surviving species here. On the other hand, if individual invaders arrive faster than the typical times of extinction of the previous invasion attempt, they will buoy the population in the system, maintaining its presence. I deal with both of these cases, high or low immigration rate, using the Moran model with immigration when the niche overlap is $a = 1$. For incomplete niche overlap, once a species successfully invades it will persist for long times, based on the results of chapter 2.

Within the Moran model with immigration I have explicitly considered the cases of high and low immigration rate. When immigration is sufficiently high, such that $N\nu > \max\big(1/g, 1/(1-g)\big)$, the focal species is maintained at steady state most often at a fractional abundance equal to that in the metapopulation from which the immigrants arrive. For low immigration rate, specifically $N\nu < \min\big(1/g, 1/(1-g)\big)$, the focal species spends the bulk of its time either temporarily extinct or else fixated in the local system (rather than in the metapopulation). One way to characterize biodiversity is by the number of different species that reside in a system [76, 125**? ?**]. An estimate of the expected number of species in a system, at least when immigration is frequent, is given by the number of g_i's greater than $1/(N\nu)$, where g_i is the fractional abundance of species i in the static large metapopulation that provides immigrants to the system.

For incomplete niche overlap, the number of species in a system, as well as their abundances, depends on how their K_i's are distributed. This can be connected back to theories of the apportionment of resources common to niche theories of biodiversity [111, 116, 172]. Calculating the abundance curve of systems will less than complete niche overlap is outside of the scope of this thesis. I can, however, make qualitative arguments on how a lesser niche overlap would affect Hubbell's abundance curve, given that the Hubbell model is similar to the Moran model with immigration. Those species in disparate niches will exist at their local carrying capacity, and will not be suppressed by their neighbours, thus there should be more species at higher abundance, higher mean population. Only those species that have a naturally low carrying capacity and those that have high niche overlap with others in the system will be found at low abundance or in a transient state. Based on my results, an observed species abundance curve that shows more species at high abundance but lesser at low abundance when compared to the prediction of Hubbell is a signature of a non-neutral ecosystem influenced by niche differences.

Chapter 4

Conclusion

4.1 Limitations and caveats

Some of the assumptions underlying the theories outlined in this thesis might fail. That said, they can at least serve as a minimal working model, from which deviations can be noted and explained. A comparison of experimental data against my predictions would illuminate the way in which that particular system differs from my simple model and the assumptions underlying it. While there is a broad range of experiments to which my results would apply, there are also a number of ways they could fall short, and I discuss these complications here.

For the bulk of this thesis I have assumed the species interactions are symmetric, with true neutrality as the limiting case of complete niche overlap. The symmetry implies no species has an explicit fitness advantage, and is relevant when there is no selective pressure in a system. Selection due to differing fitnesses tends to lead to greater fixation probabilities and faster fixation times than the unselective case. It is hard to believe that two species that occupy even partially overlapping niches would not have a fitness difference between them such that one of them is favoured (but see [77, 163]). This dissonance is especially potent if two species evolved in different systems and are optimized for different conditions before one of them immigrates to the environment of the other. I have largely been silent on where new strains might arise from. On the molecular level, mutation is most likely to come from single nucleotide polymorphisms, which has three common outcomes: most often, the mutation is deleterious and selected against; often the mutation is synonymous and therefore neutral; occasionally the mutation is beneficial. Synonymous mutations should obey the Moran limit of my results, but to have symmetric partial niche overlap the mutant must use a resource less effectively than the wild type strain while simultaneously not decreasing the mutant's basal growth rate. Intuitively this should require at least two mutations; one to decrease the usage efficacy and a second to improve a different resource usage to compensate. The idea is not so far-fetched, however, since most enzymes have some activity on a variety of substrates (typically optimized for one compound), it is not inconceivable that a mutation should decrease the catalytic activity of an enzyme on one substrate while simultaneously improving it for another.

One conceit of this thesis is that most of the parameters, like turnover rate r, carrying capacity K, and niche overlap a, are phenomenological. Often these parameters can be connected to real physical quantities, as I demonstrated in chapter 2 with the example of two bacterial strains producing antibacterial toxins. Niche overlap, for example, was an amalgam of the basal birth and death rates, the toxin

production and degradation rates, and the death rate increases due to the presence of toxins. Deriving the phenomenological parameters from physical and biological quantities is case dependent and is outside the scope of this thesis. Phenomenological parameters see wide use in the literature; nevertheless an astute reader should be wary whenever they are presented.

At times I have suggested that those organisms not from the focal species could be all from some second species or from a variety of non-focal species. For incomplete niche overlap this means that those non-focal species all occupy the same niche as each other and have the same overlap with the focal species, a situation which is unlikely. Lumping all non-focal species together is more justified under the assumptions of the Moran and Hubbell models, that in some way each species affects the others as strongly as itself. Neutral theory apologists have made such arguments [77, 163]. My results are more readily applied to those systems wherein only two species might coexist.

One of my major assumptions is that species are well-mixed, such that each organism has a chance of interacting with every other organism in the system. I have also allowed for self-interactions, but this is of secondary import. The well-mixed assumption is more valid for some systems than others. It seems to work well with mobile organisms like animals or tree seeds [76], or mobile bacteria in a fluid [**?**]. There are situations for which it is clearly not applicable, where spacial arrangement matters. Then there are situations for which it is unclear. One of the motivating questions for this thesis is the paradox of the plankton, how come there are so many species of plankton that seem to coexist in a seemingly small niche with little variety of resources. One resolution of this paradox is that spatial effect act to stabilize the competing populations, and that otherwise they would collapse to only a few species coexisting [165]. Briefly, the idea is that in different patches a given species might go extinct, while elsewhere it is flourishing, and migration between the patches is what supports the global continued existence of each species.

Another caveat of my research is that I have regarded demographic fluctuations while ignoring environmental noise. In reality both sources of stochasticity should contribute, to varying degrees. Typically, environmental fluctuations are of larger magnitude and therefore lead to larger variances and faster first passage times [142]. However, this depends on the particular experimental or biological setup. It is also worth noting that an experimentalist can act to minimize environmental noise, but demographic stochasticity is inherent to any system of finite population and therefore cannot be removed. There are many other simplifications I have employed to make my research questions tractable. For instance, I have assumed that reproduction is (or can at least be effectively treated as being) asexual. As such I can make no comment on how demographic stochasticity and interspecies competition should affect heterozygosity. I have also not considered any life stages or structured populations. Genotypically an organism has died when it can no longer reproduce, yet it still can compete for resources. There are many ways that my research could be made more realistic or otherwise extended. I discuss some such examples in my Next Steps section. The results of this thesis come from very simple models, which can nevertheless capture qualitative behaviours in extinction rates and coexistence phase diagrams.

4.2 Experimental tests

The research presented in previous chapters were theoretical in nature. However, experimental tests are possible for some of the claims. I will now present some experiments that were attempted with relevance to the theoretical work I have done. I will also propose other sets of experiments that would test my

results.

It is possible, for instance, to experimentally corroborate some of the claims made in the first chapter. As previously discussed, measuring the average dynamics of a population increasing and decreasing is insufficient on its own to predict its eventual stochastic demise. Instead, each of the birth and death rates must be measured. For example, in a bacterial species the birth rate can be inferred by the uptake and usage of radioisotope-doped nucleotides in nucleic acid synthesis [99]. The death rate can also be measured using radioisotopes [**?**], and both birth and death can be tracked by following one or a few cells [109, 182, 184**? ?**]. These two rates, and their dependence on neighbour density, constitute all that are required to make predictions in an experiment where the environment is tightly controlled. The quasi-steady state population probability distribution could be measured by having multiple parallel replicates or by having just the one population but repeatedly measuring the population to collect statistics on the distribution. The experimentalist would have to wait for the system to relax back to its quasi-steady state between measurements, but some preliminary work suggests that this is a fast process, on the order of a generation [**?**]. At sufficiently low carrying capacity it would be possible to verify the dependence of the MTE on δ and q. Unless the mean population size were very small, a measurement of the MTE would not be possible.

The extinction times from the last few chapters are long, and not just those that scale exponentially with the carrying capacity. Even the relatively fast results of the Moran model, which scale linearly with K, will be longer than is experimentally viable for typical biological populations and timescales. The fastest reproducing model organism is the *E. coli* bacterium, which reproduces every twenty minutes in ideal conditions [112**?**]. A carrying capacity as low as 10^3 would show fixation in the Moran limit in a week, but the complete extinction of the population (as described in the first chapter) would take longer than life has existed on the Earth. For example, the famous long running experiments by Lenski [112] would take something like 10^{10^8} years for one of their vials to have all the bacteria die out due to demographic fluctuations. A typical bacterial density is $10^6 - 10^8$ per millilitre. Larger organisms tend to have lesser densities but also slower bithrates. Moran results, specifically those propounded by Kimura, have been measured experimentally [95, 96].

The most promising work on small populations has been with microfluidic devices [182, 184**? ?**]. Often these researchers ask different questions to those that I address in this thesis, and typically are more interested with the particular species or mechanisms at hand rather than species persistence and extinction in general. Nevertheless, with their setups they are well positioned to study the dynamics of a small population. Some labs can even observe a single individual cell over the span of generations; if they can maintain a population of one, surely they can maintain a few.

With lab space provided by Josh Milstein at the University of Toronto, and inspired by similar designs [**?**], some undergraduate students and I attempted to build a microfluidic device that would constrain a bacterial population to a population on the order of tens or a few hundred. The challenge was to design a device that allowed for the population to receive a constant small influx of nutrients in a confined space (hence a small carrying capacity) without flushing them out of the system too quickly. The flow rate could not be too slow, however, as it was the mechanism by which the bacteria would be well mixed. Otherwise the bacteria would be spatially arranged and death (in this case, being flowed out of the system) would not be random but depend on proximity to the main channel. It later turned out that this was indeed the case, which was problematic both in that it would not allow for competition of species (instead simply favouring the one farthest from the mouth of the chamber) and it would not

allow for extinction of a single species (as the death rate dropped to negligible magnitude for bacteria in far back positions). Nevertheless the bacteria grew and were maintained. Further investigation of this system, both in experimental refinement and theoretical modelling, is warranted.

One manifestation of the theories I have analyzed in this thesis was done by the Gore lab, growing bacteria in the guts of nematodes [178]. These *C. elegans* worms are grown in an environment filled with red- and green-tagged *E. coli* bacteria that are otherwise identical. The bacteria invade the nematode guts by infrequently surviving the eating process and then slowly reproducing to colonize the system. As the bacteria have the same reproductive rate and chance of entering the gut unscathed this is an experimental realization of the Moran model with immigration from chapter 3 with $g = 0.5$. The researchers use a version of the two-dimensional Lotka-Volterra model in the Moran limit to simulate their data, compared to the more analytically tractable model of the Moran model with immigration that I propose. The data are sparse but both theories appear to fit nicely.

4.3 Applications of the theory

The experimental realizations outlined above exhibit very controlled situations where my research could be applicable. The obvious application of the theories investigated in this thesis is to biological systems of few competing species or strains within constant environments. This is somewhat artificial, but there are some systems for which it is relevant. Microfluidic work, in addition to its testing capabilities, could model systems with flow, like industrial food processing or the digestive tract. The *C. elegans* gut microbiome work of Gore and others [161, 178] suggests that the theories in this thesis could be applicable to microbiota more generally, be they in the gut or other areas [43, 51, 60, 103, 122, 174, 186]. My results rely on a well-mixed assumption, so environments like the gut or the ocean surface are good candidates, but situations like plaque growth [189] or some plants [168] are not. Species need not rely on the environment to mix them well; animals that are mobile or trees with far-travelling seeds would also be candidates.

Chapters 2 and 3 briefly touch on the idea of small population sizes. For instance, the second chapter's figure 2.5 suggests that the exponential term is less relevant than the algebraic term when it comes to the fixation time of two competing species as compared to a similarly sized Moran-like system. Indeed, exponential dependence is only dominant when system sizes are large. This large population size is relevant in many (if not most) biological contexts, from *e. coli* and their typical $10^6 - 10^8$ bacteria/mL density [112] to lynx in Canada's arctic which are more spread out but easily number in the tens of thousands [106]. But not all biology is overflowing with individuals. One example is that of plasmids in a cell [67]. Plasmids are small loops of DNA that typically code for a few/handful genes, often one of which confers some antibiotic resistance[120]. Their reproduction can be thought of as asexual, since only one plasmid copy is required as a template to make a new copy. Plasmid copy numbers, the average number of copies of a plasmid per cell, tend to be low, ranging from 10^1 to 10^3. The copy number can be thought of as the carrying capacity of that plasmid in the cell, and is maintained primarily by a negative regulatory circuit, whereby a protein expressed by the plasmid acts to inhibit the replication of new plasmids. There is also a stochastic effect when the cell divides and the plasmids are distributed between the two daughters, as plasmids can be divided unevenly, resulting in sampling that can lead to cells without plasmids. But given the differing time scales of plasmid (DNA) replication and cell division this uneven distribution is unlikely to be the sole mechanism of local extinction; demographic fluctuations

like those described in this thesis may also be relevant. The bacterial chromosome is typically thousands or a million times longer than that of a plasmid, and one expects a similarly disparate timescale for their replication. The bacterium divides when it has copied its whole chromosome, so a thousand or a million plasmid 'generations' may have occurred before division. A low copy number plasmid might have a carrying capacity of $K = 20$, which would suggest a mean extinction time of 20 million replications, which is a long time for a bacterium, despite the differing time scales of DNA replication and cell division, though for a quickly replicating, low copy number plasmid in a slowly dividing bacterium this could be of relevance. What's more, different types of plasmids can have the same or similar maintenance mechanisms, such that they compete, as mediated by their shared inhibitor proteins. Then the relevant comparison would not be chapter 1's extinction of a single species but the competition of chapters 2 and 3. Each plasmid type would have its carrying capacity given by its copy number if it were alone in the bacteria. The niche in this case is defined by the replication inhibitor, and niche overlap relates how much the inhibitor of each plasmid type stymies the replication of the other; if there is a shared inhibitor, the plasmids are in the Moran limit, and we expect fixation to be rapid, much faster than the cell division time scale.

Similar to plasmids, the number of mitochondria in a cell is small and tends to be controlled within a cell. In brewer's yeast there are typically 34 ± 2 mitochondria per cell [**?**]. Of interest to researchers is how the integrity of mitochondrial DNA is maintained [**?**]. Sometimes a mitochondrion will have large deletions in its DNA [**?**]. There are conflicting selection forces in this system: the mutant mitochondria reproduce faster than the wildtype but hinder the viability of the cell, hence its reproduction. But when one mutant arises in a population, what is the chance it will fixate, and will fixation occur before the cell reproduces? The analyses of chapter 3 are relevant to such a problem.

Coalescent theory is a model that predicts the time in the past when two variants of a gene most recently shared a common ancestor [26, 97, 162, 164]. In its simplest form it treats all mutants (at least, all that survived to the present day) as equally viable, interacting with other variants as strongly as they do with themselves [160, 163]. In this way it is like a Moran model, or a symmetric Lotka-Volterra model with complete niche overlap. The time it predicts since the last common ancestor is approximately exponentially distributed, with a mean proportional to the system size. An inclusion of incomplete niche overlap, such as has been investigated in chapter 2, would only act to increase the estimated times. Niche overlap less than one would be most appropriate for very dissimilar variants that now serve different but equally vital purposes in the organism. The longer timescale of incomplete niche overlap of course would not change the historical record. Rather, coalescent theory is used to make inferences about historical population genetic parameters, like mutation rate and population size. For those genes to which incomplete niche overlap applies, the longer timescales of $a < 1$ must be balanced by shortened timescales from a smaller population size or greater mutation rate in order for the observed records to match. Conversely, if we know the historic population size and mutation rate, we could infer the niche overlap between disparate gene variants. Phylogenetic reconstruction is related to coalescent theory, and would be similarly affected by incomplete niche overlap [160].

As discussed in the previous chapter, the Hubbell model also relies on assumptions similar to those of the Moran model, to the point that it is effectively a Moran model with immigration [76], albeit with each immigrant coming from a new species, and accounting for the abundance of species not just a focal one. The Hubbell model is used to predict the number of species that on average can be found in a system, and the distribution of abundances of the species therein. As with coalescent theory, the underlying

assumption of Hubbell's neutral theory is that species occupy the same niche. This is effectively what he means by the term "neutral", a claim which has been controversial [32, 160**?**]. Apologists defend the theory by explaining that, in an abstracted sense, species in the same trophic level are effectively competing with each other as much as they compete with themselves [77, 163]. The alternative to neutral theory is traditionally taken to be niche theory, the idea that each species in a system occupies its own niche, and any newcomers must either die out as a transient species or invade a niche, suppressing and evicting its previous occupant. I have shown, in chapter 3, that there are other alternatives. My research investigated the situation where two species have overlapping, but not necessarily identical, niches, such that they do not exclude each other entirely. Neither is selected for, and I have focused on symmetric interactions where each species affects the other to the same degree, has the same carrying capacity, and turnover rate. Thus I situate myself among those theories which accommodate both niche and neutral theories [58, 91, 110, 141, 154]. With partial niche overlap, the abundance distribution is still influenced by the niche apportionment distribution, as with niche theories. My results predict that invasion is easier with incomplete niche overlap, so compared to neutral theory there will be more species with large abundance. However, those small populations due to transients are lessened because times for both successful and failed invasion attempts are shorter, so I expect there will be fewer species at small abundance.

4.4 Conclusions

This thesis treats extinction of a one dimensional logistic system in chapter 1, extinction of a coupled logistic system in chapter 2, and invasion into a coupled logistic system in chapter 3. The coupled logistic system of chapters 2 and 3, which typically has a deterministic fixed point, acts like a neutral model in the Moran limit, and I have characterized the transition to this limit. Chapter 3 also looks at dynamics and steady state distributions of a single species in the Moran model with immigration. The results, in short, are:

- higher commensurate birth and death rates (*i.e.* higher δ, lower q) leads to faster extinction;
- the WKB approximation is usually fine to recover the dominant scaling of the MTE, as often is the Fokker-Planck equation;
- two species will effectively coexist unless they have exactly the same niche;
- similarly, greater niche overlap leads to longer invasion times, and less likelihood of success of an invasion attempt;
- in a Moran model with repeated immigration a focal species will be most likely to have a moderate population size if $K\nu > \max\big(1/g, 1/(1-g)\big)$, where K is the system size, ν is the immigration rate, and g is the fractional abundance of the focal species in the nearby reservoir population.

More detailed discussions and conclusions specifically related to these topics can be found in their respective chapters; below I shall summarize them and extend them beyond the topics of their chapters and to the broader questions discussed in this thesis.

How long will a single species with only intraspecies interactions persist before going extinct? As was already known in the literature, the simplest model of a deterministically stable species, namely the

logistic model, gives a mean extinction time whose scale is dominated by an exponential dependence on the system size. What was *not* known was the particulars of how the extinction time depends on the other parameters of the model. Along with carrying capacity K and mean reproductive rate r these parameters are the basal death rate δ (as opposed to the difference of basal birth and death rate, r) and a parameter which scales the intraspecies interactions from reducing the birth rate to increasing the death rate. I have demonstrated that, after the carrying capacity, the most impactful parameter on the quasi-steady state distribution and extinction time is the death rate. I find that increasing the death rate while maintaining the reproductive rate (and consequently also increasing the birth rate) tends to broaden the probability distribution and decreases the extinction time. Acting to simultaneously increase the effect of interspecies interactions on both birth and death while holding their difference constant has a similar but lesser effect. More significantly, in chapter 1 I conclude that a researcher should start from the stochastic model relevant to the system being studied and thereafter find the deterministic limit, rather than the common practice of starting with a deterministic equation and adding noise later. Furthermore, I used this exemplar system to investigate which mathematical techniques are effective to model stochastic extinction. If a researcher wants to model noise in their system but is only concerned with near equilibrium dynamics, the Fokker-Planck and WKB approximations appear acceptable. It is only when investigating far-from-equilibrium quantities like the rare fluctuations that lead to extinction in a deterministically stable system do subtleties start to arise. Specifically, while these two approximations do still capture the exponential dependence on system size, they incorrectly calculate the algebraic prefactor. These approximations remain appealing for getting an idea of the qualitative far-from-equilibrium behaviour but if the goal is to be precise there are better alternatives. For instance, the approximation employed throughout most of this thesis, namely introducing a cutoff to the transition matrix and then inverting it to solve the master equation directly, is both accurate and fast.

It has been long known in the literature that extinction from the stochastic logistic model is dominated by an exponential scaling with carrying capacity [15, 85, 140, 142], and so too is the fixation time of two independent logistic systems. More recently, it was noted that when the Lotka-Volterra model has equal intra- and interspecies interactions it obeys fixation dynamics similar to the Moran model [40, 44, 114, 190]. Some of these papers even looked at partial niche overlap, and find the system still exhibits the long coexistence of a logistic model [**?**]. So then how long will a species exist with intraspecies interactions and some lesser but non-zero interspecies interactions? That is, how long will two species coexist given some partial niche overlap? I conducted a systematic study of the MTE's scaling with carrying capacity to find out how the LV model transitions from the independent to the Moran limit. I find that the MTE transitions from slow exponential scaling to the relatively fast extinction of algebraic scaling as found in the Moran limit by having the exponential prefactor decrease continuously to zero. Only when there is complete niche overlap does the exponential dependence disappear. For large carrying capacity, I interpret this to mean that two species will effectively coexist if there is even a slight mismatch in their niches.

Hubbell's model, being neutral, has equal intra- and interspecies interactions. There have been many pages written either decrying the unintuitive supposition that two disparate species might be equivalent [32, 160**?**], and many others defending the theory, arguing there must be a way in which species are effectively neutral [77, 163]. My research shows that there is no room for compromise between neutral and niche theories of two species coexisting. Even though neutral theory appears as a limit of niche theory,

there is no such thing as being 'close' to neutral, as even partial niche mismatch leads to qualitatively different dynamics. Unless the species are truly neutral they will coexist, and their respective carrying capacities should regulate their abundance [116, 172], rather than the random fluctuations of a neutral model. It remains possible that collections of species are neutral with each other but together exist in a different niche from other such collections, such that neutral theory is applicable on a small scale.

I also investigate some consequences of a neutral model, and the more general Lotka-Volterra model, as regarding the entrance of a new species into a system. For an ecosystem with a species already established, I have shown that the probability of failure of an invasion attempt of a new species in the large carrying capacity limit is directly proportional to the niche overlap between the established and invading species. The timescale of a successful invasion attempt is never exponential in the system size, being linear at most, in the Moran limit of complete niche overlap, and following the deterministic trend of logarithmic scaling when the invader has independent resource needs from the established species. I find that unsuccessful invasion attempts are even faster to resolve. The implication is that one could test the Hubbell model by measuring invasion success probability or timescale. If invasion (as defined in chapter 3) is more common than Hubbell predicts then it suggests that the neutral model is not a good model of the system. Similarly, if invasion attempts, whether successful or not, resolve themselves more rapidly than the neutral model then the system is better characterized by a theory of niches.

The Hubbell model assumes that each invader is from a new species [76], but was inspired by the island model of MacArthur and Wilson [117], which supposes that a small island gets repeated invasions from a larger repository of species on the mainland. This was the motivation for considering the Moran model with immigration in chapter 3, which allows for the calculation of the probability distribution of a species in a neutral system, and how this distribution depends on the immigration rate. The research is similar to that of McKane [131], but I offer a more biological analysis of the results. I find that the probability distribution has three characteristic qualitative shapes, with the probability either concentrated at the extremes of extinction and fixation, somewhere near the middle, or mostly near the middle but with sizable density at one of the extremes. The three shapes occur in different regimes of parameter space, bounded by how $K\nu$ compares with $1/g$ and $1/(1-g)$. Each mainland species will have its own abundance g, and the distribution of g's, specifically the number of species with g's greater than $1/(N\nu)$, suggests the number of species we expect to see with population around Kg in the island system. Those with lesser g's will likely have low or zero population in the system.

In the end, I cannot conclude whether neutral or niche theories are more appropriate for explaining the maintenance of biodiversity. Neutral theory is more parsimonious [110]; above I have suggested some bounds or checks to what it should predict, namely that invasions should be rare and slow, and that the island abundance distribution should follow the mainland abundance distribution. Others have suggested different tests that call neutral theory into question [4, 32, 128, 160, 163**?**]. Niche theories are hard to disprove, as they suffer from an overabundance of parameters. Competitive exclusion within a niche and the observation that the ocean surface has very few resources compared to its abundance of species were the initial motivators for my research: the paradox of the plankton. What I can say is that coexisting species need not be in entirely disparate niches; they can effectively coexist with even large, albeit incomplete, niche overlaps.

4.5 Next steps for the research

I will now indulge in some speculation. In this section I present some straightforward extensions of my research. Also included are some more extensive next steps. As with all my research, there is the obvious next step of applying my results to specific real biological systems, finding a way to estimate the phenomenological parameters based on measurable evidence, and then making predictions. See the Experimental Tests section of this chapter for more details, but two promising systems are microfluidic devices [**?**] and small microbiomes like the gut of nematodes [178].

The content of the first chapter has some obvious extensions. The "hidden parameters" were those that did not show up in the deterministic analogue of the system which nevertheless affect the stochastic dynamics. Suppose we write the system as

$$b(n) = r\,n + f(n)$$
$$d(n) = r\,n^2/K + f(n)$$

for arbitrary $f(n)$. It is unclear how f affects the stochastic measurable quantities like the MTE. Writing f as a polynomial, I predict the higher orders will have a lesser and lesser effect, and that there will be some conditions placed on $f^{(k)}(0)/k!$, the kth coefficient. Furthermore, I investigated the deterministic equation $\dot{x} = r\,x(1 - x/K)$. I speculate that any concave down system will behave similarly, as is the case with logistic difference equations [171]. Assaf and Meerson [14] included the Allee effect and found that the MTE still scales exponentially with carrying capacity; I predict there is an effective carrying capacity given by the distance between the stable and unstable fixed points.

In chapter 2 I regarded how the scaling of the extinction time changes as niche overlap increases from independence ($a = 0$) to $a = 1$, at which point the MTE is that of the Moran model. Despite the biological significance of this limit, in phase space it is only one point, measure zero, and seems unlikely to arise randomly. Perhaps there is a way to show convergence toward this point. If a mutant strain arises from a single population, it is likely to have a very similar niche to the wildtype, hence a large niche overlap. And from there, what would the forces of evolution dictate? One could simulate the evolution of the niche overlap (for instance following the work of MacArthur [116]) in an individual based model with a given resource distribution. It is unclear to me whether optimizing fitness would cause the niches to converge to better match the resource distribution, supporting neutral models, or diverge to minimize niche overlap and competition, supporting niche theory. In any case, it would be insightful to see whether fitness considerations act to make the already-unlikely Moran limit entirely untenable, or whether this limit is actually a natural consequence of evolution.

A natural extension of my work would be to include selection, explicit fitness advantages, to the system, for instance by increasing one r to increase the birth rate while simultaneously increasing K to keep the same death rate. I have not done so already because selection has been treated many times in many ways [**?**] and actually tends to act to simplify the system. The higher fitness species rapidly fixates, quickly reducing the dimensionality of the problem. Nevertheless there are some advantages to how I treat stochastic systems that would aid the analysis of systems with selection. In the independent limit any fitness advantage should be irrelevant, so there will at least be a transition between coexistence in the independent limit and rapid fixation otherwise. What is more, most models with selection, including those of Kimura [**?**] and Moran [**?**] [and others???] must make the assumption that the effect of selection is weak, typically much less than $1/K$. Inverting the transition matrix, as I do in chapter 2,

is arbitrarily precise, and so does not suffer from any requirement of such an assumption. It can treat the range of selection, from weak to strong. Not only does this give access to regimes not normally considered, it provides a way to verify the small selection results that rely on approximation. In the literature there is a debate about selective sweeps [84], specifically whether it is more common for a new fit mutant to quickly fixate in a population, or whether it is more often the case that a mutant trait in a population is neutral until the environment changes, after which it is more fit and fixates. The distinction between these hard and soft selective sweeps requires more careful treatment, with fewer assumptions; the method employed in chapter 2 of this thesis would be an ideal tool to use, given its arbitrary accuracy. Selection can also be incorporated into the invasion dynamics of chapter 3.

One extension applicable to all my work, that I did not account for, is the inclusion of environmental noise. This has a fundamentally different action on the system. Whereas demographic stochasticity comes from the discrete nature of population sizes and therefore can be mapped onto a transition matrix or graph (as in figure 2.2), environmental noise is continuous, especially for the phenomenological parameters I use, which cannot be fixed to any one cause, let alone a discrete one. Such an advancement in my research would involve the abandonment of the transition matrix, and likely would require the use of Fokker-Planck, which I am dubious about, based on my findings in chapter 1.

The techniques applied in this thesis, specifically the use of a truncated transition matrix being inverted to solve for the first passage times exactly, can easily be applied to other low species number systems. The calculation for each point in parameter space is not lengthy; the main constraint is RAM, rather than time, and so a larger memory computer could deal with problems with larger carrying capacities or more species. For example, in chapter 2 I considered a two dimensional generalized Lotka-Volterra system to explore competition between two species. The Lotka-Volterra system has been generalized to any dimension, any number of species. A judicious choice of parameters (*e.g.* $a_{12} < 0$, $a_{21} > 0$) will recreate the predator-prey dynamics from which the generalized Lotka-Volterra system gets its name. Gottesman and Meerson [68] analyzed the predator-prey system using a clever rotating reference frame and the WKB approximation. The deterministic system is marginally stable, with trajectories orbiting a zero-eigenvalue fixed point. As such, I expect an algebraic time to extinction, as well as a stronger dependence on initial conditions. However, the period depends on the value of the Lyapunov function associated with the orbit. Thus as it "diffuses" tangentially to the orbit its characteristic time scale will change, which may complicate the analysis. Arbitrarily correct data obtained via the matrix inverse (rather than the approximate results of WKB) allows for a complete analysis of the scaling of the MTE with system size.

From the two dimensional Lotka-Volterra system one arrives at the predator-prey system by choosing the parameters correctly. One can also move to the third dimension, in order to account for a third species in the system. This allows for the investigation of many systems of interest, with much more diversity. The simplest extension in this regard would be to have three species all with overlapping niches [118]. I could observe how a species whose niche is situated between those of two others (such that they each overlap with the first species but not with each other) would go extinct more readily as the overlap of the encroaching species is increased.

One model of three interacting species has species that each are excluded by one other and exclude the other, *e.g.* $a_{12}, a_{23}, a_{31} > 0$ and $a_{21}, a_{32}, a_{13} < 0$. For this reason it is called a rock-paper-scissors system, after the children's game. In any pairwise competition there is a winner, but when all three are combined none has a clear advantage. The model is not just fun, it is also relevant to real-world

systems, for instance of lizards or bacteria [22, 88, 100]. Such systems have stable limit cycles, which is another way of allowing for deterministic coexistence of species (along with fixed points) [9, 169]. This contradicts the intuition that the number of resources constrains the number of species that can exist in a system. Fluctuations cause the system to ultimately end in extinction. Future investigations will probe whether the MTE from a stable limit cycle also scales exponentially with the system size, and how the system size should be characterized given that there is no asymptotic population size. This could serve as a way to distinguish between systems with a fixed point and those with an extended attractor. Extending to three dimensions also allows for the possibility of observing a chaotic system [171]. It is unclear whether chaotic and non-chaotic regimes of a system can be distinguished upon the inclusion of stochastic fluctuations, but the scaling of the MTE may serve such a purpose.

Another three species model that has enjoyed widespread usage is the SIR model of disease outbreak [55, 63, 115]. It counts the number of susceptible (S), infected (I), and recovered (R) individuals with regards to the disease. There are many variations of this model, but the simplest has a stable spiral node deterministic fixed point. Application of the WKB approximation showed a route to extinction that spiraled in the opposite direction [85]. In chapter 1 I showed that WKB does not recover the correct prefactor for the extinction time, and in chapter 2 I showed that the idea of a route to extinction is questionable. Thus the SIR model is ripe for further analysis. Specifically, the next step is to calculate the residence times for the model, and from these times construct a probable route to extinction, to compare to the WKB route.

The final next step I will outline is the coupling of the ecology of this thesis with evolution. If species were to change their parameters in response to their environment and the other species, how would the dynamics change? Perhaps each species would evolve to minimize niche overlap while maximizing r and K. If the niches were tied to underlying resources, the species might be constrained in how their niche overlap could evolve, such that they would reach some equilibrium. Or if the evolution itself were stochastic, it might be that whichever strain happens to find a beneficial mutation first would end up dominating the system. Coupling ecology with evolution is a large field of research [3, 34, 37, 40, 44, 52, 84, 91, 111, 112, 114, 119, 125, 126, 147, 151, 156, 175, 189**? ? ?**], and there is more work to be done with stochasticity, especially demographic stochasticity.

Bibliography

[1] P.A. Abrams. Density-Independent Mortality and Interspecific Competition: A test of Pianka's niche overlap hypothesis. *Am. Nat.*, 111(979):539–552, 1977.

[2] Peter Abrams. Some Comments on Measuring Niche Overlap. *Ecology*, 61(1):44–49, 1980.

[3] Peter Abrams. The Theory of Limiting Similarity. *Annu. Rev. Ecol. Syst.*, 14(1):359–376, 1983.

[4] Peter B. Adler, Stephen P. Ellner, and Jonathan M. Levine. Coexistence of perennial plants: An embarrassment of niches. *Ecol. Lett.*, 13(8):1019–1029, 2010.

[5] Edward J Allen, Linda J S Allen, and Henri Schurz. *A comparison of persistence-time estimation for discrete and continuous stochastic population models that include demographic and environmental variability.*, volume 196. jul 2005.

[6] Linda J S Allen. *An Introduction to Stochastic Processes with Applications to Biology.* Pearson Education, Inc, New Jersey, 2003.

[7] Linda J S Allen and Edward J. Allen. A comparison of three different stochastic population models with regard to persistence time. *Theor. Popul. Biol.*, 64(4):439–449, 2003.

[8] Tibor Antal and Istvan Scheuring. Fixation of strategies for an evolutionary game in finite populations. *Bull. Math. Biol.*, 68(8):1923–1944, 2006.

[9] Robert A Armstrong and Richard McGehee. Coexistence of species competing for shared resources. *Theor. Popul. Biol.*, 9:317–328, 1976.

[10] Robert A. Armstrong and Richard McGehee. Competitive Exclusion. *Am. Nat.*, 115(2):151–170, 1980.

[11] Peter Ashcroft, Franziska Michor, and Tobias Galla. Stochastic tunneling and metastable states during the somatic evolution of cancer. *Genetics*, 199(4):1213–1228, 2015.

[12] Michael Assaf, Alex Kamenev, and Baruch Meerson. Population extinction risk in the aftermath of a catastrophic event. *Phys. Rev. E*, 79(1):011127, jan 2009.

[13] Michael Assaf and Baruch Meerson. Spectral theory of metastability and extinction in birth-death systems. *Phys. Rev. Lett.*, 97(20):1–4, 2006.

[14] Michael Assaf and Baruch Meerson. WKB theory of large deviations in stochastic populations. *J. Phys. A. Math. Gen.*, page 63, 2016.

[15] Michael Assaf, Baruch Meerson, and Pavel V Sasorov. Large fluctuations in stochastic population dynamics: momentum-space calculations. *J. Stat. Mech. Theory Exp.*, 2010(07):P07018, jul 2010.

[16] MattheW A Badali, Jeremy Rotheschild, and Anton Zilman. Intraspecies interactions in birth or in death rates. *(in Prep.*, 2018.

[17] MattheW A Badali, Jeremy Rotheschild, and Anton Zilman. Intraspecies Interactions In Birth Or In Death Rates. *(in Prep.*, 2019.

[18] MattheW A Badali and Anton Zilman. Effects of niche overlap on co-existence, fi xation and invasion in a population of two interacting species. *(in Prep.*, 2019.

[19] Bell and G. Neutral Macroecology. *Ecology*, 293(5539):2413–2418, 2001.

[20] Graham Bell. The Distribution of Abundance in Neutral Communities. *Am. Nat.*, 155(5):606–617, 2000.

[21] A. Belle, A. Tanay, L. Bitincka, R. Shamir, and E. K. O'Shea. Quantification of protein half-lives in the budding yeast proteome. *Proc. Natl. Acad. Sci.*, 103(35):13004–13009, 2006.

[22] Maximilian Berr, Tobias Reichenbach, Martin Schottenloher, and Erwin Frey. Zero-One Survival Behavior of Cyclically Competing Species. *Phys. Rev. Lett.*, 102(4):048102, jan 2009.

[23] W Bez and P Talkner. A new variational method to calculate escape rates in bistable systems. *Phys. Lett. A*, 82(7):313–316, 1981.

[24] David Bickford, David J. Lohman, Navjot S. Sodhi, Peter K L Ng, Rudolf Meier, Kevin Winker, Krista K. Ingram, and Indraneil Das. Cryptic species as a window on diversity and conservation. *Trends Ecol. Evol.*, 22(3):148–155, 2007.

[25] Andrew J. Black and Alan J. McKane. Stochastic formulation of ecological models and their applications. *Trends Ecol. Evol.*, 27(6):337–345, 2012.

[26] Richard A Blythe and Alan J Mckane. Stochastic Models of Evolution in Genetics , Ecology and Linguistics. *J. Stat. Mech. Theory Exp.*, 2007(07):P07018, 2007.

[27] Immanuel M Bomze. Lotka-Volterra Equation and Replicator Dynamics: A Two-Dimensional Classification. *Biol. Cybern.*, 211:201–211, 1983.

[28] Vanni Bucci, Carey D Nadell, and João B Xavier. The evolution of bacteriocin production in bacterial biofilms. *Am. Nat.*, 178(6):E162–73, dec 2011.

[29] Yang Cao, Daniel T Gillespie, and Linda R Petzold. Efficient step size selection for the tau-leaping simulation method. *J. Chem. Phys.*, 124(4):044109, jan 2006.

[30] Youfang Cao, Anna Terebus, and Jie Liang. State Space Truncation with Quantified Errors for Accurate Solutions to Discrete Chemical Master Equation. *Bull. Math. Biol.*, 78(4):617–661, 2016.

[31] José A. Capitán, Sara Cuenda, and David Alonso. Stochastic competitive exclusion leads to a cascade of species extinctions. *J. Theor. Biol.*, 419(1980):137–151, 2017.

[32] Ian T. Carroll and Roger M. Nisbet. Departures from neutrality induced by niche and relative fitness differences. *Theor. Ecol.*, 8(4):449–465, 2015.

[33] Ted J Case and RG Casten. Global stability and multiple domains of attraction in ecological systems. *Am. Nat.*, 113(5):705–714, 1979.

[34] Mario Castro, Grant Lythe, Carmen Molina-París, and Ruy M. Ribeiro. Mathematics in modern immunology. *Interface Focus*, 6(2):14, 2016.

[35] Fabio A.C.C. Chalub and Max O. Souza. Fixation in large populations: a continuous view of a discrete problem. *J. Math. Biol.*, 72(1-2):283–330, 2016.

[36] P. Chesson. MacArthur ' s Resource Model. *Theor. Popul. Biol.*, 37:26–38, 1990.

[37] Peter Chesson. Mechanisms of Maintenance of Species Diversity. *Annu. Rev. Ecol. Syst*, 31(May):343–66, 2000.

[38] Peter Chesson and Jessica J Kuang. The interaction between predation and competition. *Nature*, 456(7219):235–238, 2008.

[39] Peter L. Chesson and Nancy Huntly. The Roles of Harsh and Fluctuating Conditions in the Dynamics of Ecological Communities. *Am. Nat.*, 150(5):519–553, 1997.

[40] Thiparat Chotibut and David R. Nelson. Evolutionary dynamics with fluctuating population sizes and strong mutualism. *Phys. Rev. E - Stat. Nonlinear, Soft Matter Phys.*, 92(2), 2015.

[41] Thiparat Chotibut, David R. Nelson, and Sauro Succi. Striated populations in disordered environments with advection. *Phys. A Stat. Mech. its Appl.*, 465:500–514, 2017.

[42] Jens Claussen and Arne Traulsen. Non-Gaussian fluctuations arising from finite populations: Exact results for the evolutionary Moran process. *Phys. Rev. E*, 71(2):025101, feb 2005.

[43] Bryan Coburn, Pauline W Wang, Julio Diaz Caballero, Shawn T Clark, Vijaya Brahma, Sylva Donaldson, Yu Zhang, Anu Surendra, Yunchen Gong, D Elizabeth Tullis, Yvonne C W Yau, Valerie J Waters, David M Hwang, and David S Guttman. Lung microbiota across age and disease stage in cystic fibrosis. *Sci. Rep.*, 5:10241, 2015.

[44] George W.A. Constable and Alan J. McKane. Models of genetic drift as limiting forms of the Lotka-Volterra competition model. *Phys. Rev. Lett.*, 114(3):1–5, 2015.

[45] Jukka Corander, Christophe Fraser, Michael U. Gutmann, Brian Arnold, William P. Hanage, Stephen D. Bentley, Marc Lipsitch, and Nicholas J. Croucher. Frequency-dependent selection in vaccine-associated pneumococcal population dynamics. *Nat. Ecol. Evol.*, 1(12):1950–1960, 2017.

[46] J Theodore Cox, Mathieu Merle, and Edwin Perkins. Coexistence in a two-dimensional lotka-volterra model. *Electron. J. Probab.*, 15:1190–1266, 2010.

[47] J Cremer, T Reichenbach, and E Frey. Neutral evolution can maintain cooperation in social dilemmas. *Imprint*, 2009.

[48] Jonas Cremer, Tobias Reichenbach, and Erwin Frey. The edge of neutral evolution in social dilemmas. *New J. Phys.*, 11, 2009.

[49] James Crow and Motoo Kimura. Some Genetic Problems in Natural Populations. In *Proc. Third Berkeley Symp. Math. Stat. Probab. Vol. 4 Contrib. to Biol. Probl. Heal.*, number 580, pages 1–22, 1956.

[50] Peter Czuppon and Arne Traulsen. Fixation probabilities in populations under demographic fluctuations. pages 1–33, 2017.

[51] Manoshi S. Datta, Elzbieta Sliwerska, Jeff Gore, Martin F. Polz, and Otto X. Cordero. Microbial interactions lead to rapid micro-scale successions on model marine particles. *Nat. Commun.*, 7(May):1–7, 2016.

[52] Michael M. Desai and Daniel S. Fisher. Beneficial mutation-selection balance and the effect of linkage on positive selection. *Genetics*, 176(3):1759–1798, 2007.

[53] Paula C Dias. Sources and sinks in population biology. *Trends Ecol. Evol.*, 11(8):326–330, 1996.

[54] Alexander Dobrinevski and Erwin Frey. Extinction in neutrally stable stochastic Lotka-Volterra models. *Phys. Rev. E - Stat. Nonlinear, Soft Matter Phys.*, 85(5):1–14, 2012.

[55] Charles R Doering, Khachik V Sargsyan, and Leonard M Sander. Extinction times for birth-death processes: exact results, continuum asymptotics, and the failure of the Fokker-Planck approximation. *Multiscale Model. Simul.*, 3(2):283–299, 2005.

[56] Vlad Elgart and Alex Kamenev. Rare event statistics in reaction-diffusion systems. *Phys. Rev. E - Stat. Nonlinear, Soft Matter Phys.*, 70(4 1):1–12, 2004.

[57] Alison M Etheridge, Robert C Griffiths, and Jesse E Taylor. A coalescent dual process in a Moran model with genic selection, and the lambda coalescent limit. *Theor. Popul. Biol.*, 78(2):77–92, sep 2010.

[58] C. K. Fisher and P. Mehta. The transition between the niche and neutral regimes in ecology. *Proc. Natl. Acad. Sci.*, 111(36):13111–13116, 2014.

[59] Charles K. Fisher and Pankaj Mehta. Identifying keystone species in the human gut microbiome from metagenomic timeseries using sparse linear regression. *PLoS One*, 9(7):1–10, 2014.

[60] Charles K. Fisher, Thierry Mora, and Aleksandra M. Walczak. Habitat Fluctuations Drive Species Covariation in the Human Microbiota. pages 1–18, 2015.

[61] R.A. Fisher. *The Genetical Theory of Natural Selection*. Clare, Oxford, 1930.

[62] Alan Gabel, Baruch Meerson, and S. Redner. Survival of the scarcer. *Phys. Rev. E*, 87(1):010101, 2013.

[63] Saikrishna Gadhamsetty, Joost B. Beltman, and Rob J. de Boer. What do mathematical models tell us about killing rates during HIV-1 infection? *Immunol. Lett.*, 168(1):1–6, 2015.

[64] C.W. Gardiner. *Handbook of Stochastic Methods*. Springer, New York, 3 edition, 2004.

[65] C.W. Gardiner. *Handbook of Stochastic Methods for Physics, Chemistry and the Natural Sciences*. Springer-Verlag, Berlin, third edition, 2004.

[66] Daniel T Gillespie. Exact Stochastic Simulation of couple chemical reactions. *J. Phys. Chem.*, 81(25):2340–2361, 1977.

[67] Robert Gooding-Townsend, Steven Ten Holder, and Brian Ingalls. Displacement of Bacterial Plasmids by Engineered Unilateral Incompatibility. *IEEE Life Sci. Lett*, 1:19–21, 2015.

[68] Omer Gottesman and Baruch Meerson. Multiple extinction routes in stochastic population models. *Phys. Rev. E*, 85(2):021140, feb 2012.

[69] Sidhartha Goyal, Sanggu Kim, Irvin SY Chen, and Tom Chou. Mechanisms of blood homeostasis: lineage tracking and a neutral model of cell populations in rhesus macaques. *BMC Biol.*, 13(1):85, 2015.

[70] J. Grasman and D. Ludwig. The accuracy of the diffusion approximation to the expected time to extinction for some discrete stochastic processes. *J. Appl. Probab.*, 20(2):305–321, 1983.

[71] Jessica L. Green, Alan Hastings, Peter Arzberger, Francisco J. Ayala, Kathryn L. Cottingham, Kim Cuddington, Frank Davis, Jennifer a. Dunne, Marie-Josée Fortin, Leah Gerber, and Michael Neubert. Complexity in Ecology and Conservation: Mathematical, Statistical, and Computational Challenges. *Bioscience*, 55(6):501–510, 2005.

[72] David Greenhalgh. An epidemic model with a density-dependent death rate. *Math. Med. Biol.*, 7(1):1–26, 1990.

[73] Charles M Grinstead and Laurie J Snell. *Introduction to Probability*. American Mathematical Society, Providence, RI, 2nd edition, 2003.

[74] P Hänggi, P Talkner, and M Borovec. Reaction rate theory - 50 years after Kramers. *Rev. Mod. Phys.*, 62(2):251–341, 1990.

[75] Robert D Holt, James P Grover, and David Tilman. Simple Rules for Interspecific Dominance in Systems with Exploitative and Apparent Competition. *Am. Nat.*, 144(5):741–771, 1994.

[76] S.P. Hubbell. *The Unified Theory of Biodiversity and Biogeography*. Princeton University Press, 2001.

[77] Stephen P Hubbell. Neutral Theory and the Evolution of Ecological Equivalence. *Ecology*, 87(6):1387–1398, 2006.

[78] Paul J Hung, Philip J Lee, Poorya Sabounchi, Nima Aghdam, Robert Lin, and Luke P Lee. A novel high aspect ratio microfluidic design to provide a stable and uniform microenvironment for cell growth in a high throughput mammalian cell culture array. *Lab Chip*, 5(1):44–8, 2005.

[79] Stuart H. Hurlbert. The Measurement of Niche Overlap and Some Relatives. 59(1):67–77, 1978.

[80] G.E. Hutchinson. The Paradox of the Plankton. 95(882):137–145, 1961.

[81] Yen T ing Lin, Hyejin Kim, and Charles R. Doering. Demographic stochasticity and evolution of dispersion I. Spatially homogeneous environments. *J. Math. Biol.*, 70(3):647–678, 2015.

[82] Srividya Iyer-Biswas and Anton Zilman. First passage processes in cellular biology. *Adv. Chem. Phys.*, 160(261), 2016.

[83] C O Jacob. Cytokines and anti-cytokines. *Curr. Opin. Immunol.*, 2(2):249–257, 1989.

[84] Jeffrey D Jensen. On the unfounded enthusiasm for soft selective sweeps, 2014.

[85] Alex Kamenev and Baruch Meerson. Extinction of an infectious disease: a large fluctuation in a non-equilibrium system. *Phys. Rev. E*, pages 1–4, 2008.

[86] Alex Kamenev, Baruch Meerson, and Boris Shklovskii. How Colored Environmental Noise Affects Population Extinction. *Phys. Rev. Lett.*, 101(26):268103, dec 2008.

[87] Tadeusz J. Kawecki and Dieter Ebert. Conceptual issues in local adaptation. *Ecol. Lett.*, 7(12):1225–1241, 2004.

[88] Benjamin Kerr, Margaret a Riley, Marcus W Feldman, and Brendan J M Bohannan. Local dispersal promotes biodiversity in a real-life game of rock-paper-scissors. *Nature*, 418(6894):171–4, jul 2002.

[89] David A Kessler, Robert H Austin, and Herbert Levine. Resistance to chemotherapy: Patient variability and cellular heterogeneity. *Cancer Res.*, 74(17):4663–4670, 2014.

[90] David a. Kessler and Nadav M. Shnerb. Extinction Rates for Fluctuation-Induced Metastabilities: A Real-Space WKB Approach. *J. Stat. Phys.*, 127(5):861–886, 2007.

[91] David A. Kessler and Nadav M. Shnerb. Generalized model of island biodiversity. *Phys. Rev. E - Stat. Nonlinear, Soft Matter Phys.*, 91(4), 2015.

[92] Motoo Kimura. Stochastic processes and distribution of gene frequencies under natural selection. *Cold Spring Harb. Symp. Quant. Biol.*, 20:33–53, 1955.

[93] Motoo Kimura. Diffusion Models in Population Genetics. *J. Appl. Probab.*, 1(2):177–232, 1964.

[94] Motoo Kimura. Theoretical Foundation of Population Genetics at the Molecular Level. 208:174–208, 1971.

[95] Motoo Kimura. A simple method for estimating evolutionary rates of base substitutions through comparitive studies of nucleotide sequences. *J. Mol. Evol.*, 16:111–120, 1980.

[96] Motoo Kimura. *The Neutral Theory of Molecular Evolution*. Cambridge University Press, 1983.

[97] J Kingman. The coalescent. *Stoch. Process. their Appl.*, 13(3):235–248, 1982.

[98] James M Kinross, Ara W Darzi, and Jeremy K Nicholson. Gut microbiome-host interactions in health and disease. *Genome Med.*, 3(3):14, 2011.

[99] David Kirchman, Hugh Ducklow, and Ralph Mitchell. Estimates of bacterial growth from changes in uptake rates and biomass . Estimates of Bacterial Growth from Changes in Uptake Rates and Biomass. *Appl. Environ. Microbiol.*, 44(6):1296–1307, 1982.

[100] Benjamin C Kirkup and Margaret a Riley. Antibiotic-mediated antagonism leads to a bacterial game of rock-paper-scissors in vivo. *Nature*, 428(6981):412–4, mar 2004.

[101] Peter H. Klopfer and Robert MacArthur. On the Causes of Tropical Species Diversity : Niche Overlap. *Univ. Chicago Press Am. Soc. Nat.*, 95(883):223–226, 1961.

[102] A Klug. Rosalind Franklin and the Discovery of the Structure of DNA. *Nature*, 219:808, 1968.

[103] Jeremy E Koenig, Aymé Spor, Nicholas Scalfone, Ashwana D Fricker, Jesse Stombaugh, Rob Knight, Largus T Angenent, and Ruth E Ley. Succession of microbial consortia in the developing infant gut microbiome. *Proc. Natl. Acad. Sci. U. S. A.*, 108 Suppl:4578–4585, 2011.

[104] T. Korem, D. Zeevi, J. Suez, A. Weinberger, T. Avnit-Sagi, M. Pompan-Lotan, E. Matot, G. Jona, A. Harmelin, N. Cohen, A. Sirota-Madi, C. A. Thaiss, M. Pevsner-Fischer, R. Sorek, R. Xavier, E. Elinav, and E. Segal. Growth dynamics of gut microbiota in health and disease inferred from single metagenomic samples. *Science (80-.).*, 349(6252):1101–1106, 2015.

[105] K. S. Korolev and David R. Nelson. Competition and cooperation in one-dimensional stepping-stone models. *Phys. Rev. Lett.*, 107(8):1–5, 2011.

[106] Dejian Lai. Comparison study of AR models on the Canadian lynx data: A close look at BDS statistic. *Comput. Stat. Data Anal.*, 22(4):409–423, 1996.

[107] Amaury Lambert. Probability of fixation under weak selection: A branching process unifying approach. *Theor. Popul. Biol.*, 69(4):419–441, 2006.

[108] Russell Lande. Risks of Population Extinction from Demographic and Environmental Stochasticity and Random Catastrophes. *Am. Nat.*, 142(6):911–927, 1993.

[109] S. S. Lee, I. A. Vizcarra, D. H. E. W. Huberts, L. P. Lee, and M. Heinemann. Whole lifespan microscopic observation of budding yeast aging through a microfluidic dissection platform. *Proc. Natl. Acad. Sci.*, 109(13):4916–4920, 2012.

[110] M A Leibold and Mark A McPeek. Coexistance of the Niche and Neutral Perspectives in Community Ecology. *Ecology*, 87(6):1399–1410, 2006.

[111] Matthew A Leibold. The Niche Concept Revisited : Mechanistic Models and Community Context. *Ecology*, 76(5):1371–1382, 1995.

[112] Richard E. Lenski, Michael R. Rose, Suzanne C. Simpson, and Scott C. Tadler. Long-Term Experimental Evolution in Escherichia coli. I. Adaptation and Divergence During 2,000 Generations. *Am. Nat.*, 138(6):1315, 1991.

[113] Simon A. Levin. Community Equilibria and Stability, and an Extension of the Competitive Exclusion Principle. *Am. Nat.*, 104(939):413–423, 1970.

[114] Yen T Lin, Hyejin Kim, and Charles R. Doering. Features of Fast Living: On the Weak Selection for Longevity in Degenerate Birth-Death Processes. *J. Stat. Phys.*, 148(4):646–662, 2012.

[115] Marta Luksza and Michael Lässig. A predictive fitness model for influenza. *Nature*, 507(7490):57–61, 2014.

[116] R. H. MacArthur. On the relative abundance of bird species. *Proc. Natl. Acad. Sci. U. S. A.*, 43(3):293–295, 1957.

[117] R. H. MacArthur and E. O. Wilson. *The theory of island biogeography.* Princeton University Press, Princeton, New Jersey, 1 edition, 1967.

[118] Robert MacArthur. Species Packing and Competitive Equilibrium for Many Species. *Theor. Popul. Biol.*, 11, 1970.

[119] Robert MacArthur and Richard Levins. The Limiting Similarity, Convergence, and Divergence of Coexisting Species. *Am. Nat.*, 101(921):377–385, 1967.

[120] Michael T Madigan and John Martinko. *Brock Biology of Microorganisms*. Prentice Hall, Upper Saddle River, NJ, 11th edition, 2006.

[121] Thomas Malthus. An Essay on the Principle of Population. *St. Paul's church-yard, London*, pages 1–126, 1798.

[122] Chaysavanh Manichanh, Jens Reeder, Prudence Gibert, Encarna Varela, Marta Llopis, Maria Antolin, Roderic Guigo, Rob Knight, and Francisco Guarner. Reshaping the gut microbiome with bacterial transplantation and antibiotic intake. *Genome Res.*, 20(10):1411–1419, 2010.

[123] Rachael A Maplestone, Martin J Stone, and Dudley H Williams. The evolutionary role of secondary metabolites–a review. *Gene*, 115(1-2):151–7, 1992.

[124] BJ Matkowsky, Z Schuss, C Knessl, C Tier, and M Mangel. Asymptotic solution of the Kramers-Moyal equation and first-passage times for Markov jump processes. *Phys. Rev. A*, 29(6):3359, 1984.

[125] R May. Unanswered questions in ecology. *Philos. Trans. R. Soc. Lond. B. Biol. Sci.*, 354(1392):1951–9, 1999.

[126] Margaret M. Mayfield and Jonathan M. Levine. Opposing effects of competitive exclusion on the phylogenetic structure of communities. *Ecol. Lett.*, 13(9):1085–1093, 2010.

[127] Richard McGehee and Robert A. Armstrong. Some mathematical problems concerning the ecological principle of competitive exclusion. *J. Differ. Equ.*, 23(1):30–52, 1977.

[128] Brian McGill and Cathy Collins. A unified theory for macroecology based on spatial patterns of abundance. *Evol. Ecol. Res.*, 5(4):469–492, 2003.

[129] Alan McKane, David Alonso, and Ricard V. Sole. Mean-field stochastic theory for species-rich assembled communities. *Phys. Rev. E - Stat. Physics, Plasmas, Fluids, Relat. Interdiscip. Top.*, 62(6 B):8466–8484, 2000.

[130] Alan McKane, David Alonso, and Ricard V. Sole. Analytic solution of Hubbell's model of local community dynamics. *Evolution (N. Y).*, 65:10, 2004.

[131] Alan J. McKane and Martin B. Tarlie. Optimal paths and the calculation of state selection probabilities. *Phys. Rev. E - Stat. Physics, Plasmas, Fluids, Relat. Interdiscip. Top.*, 69(4):10, 2004.

[132] Baruch Meerson and Pavel V. Sasorov. Noise-driven unlimited population growth. *Phys. Rev. E - Stat. Nonlinear, Soft Matter Phys.*, 78(6):2–5, 2008.

[133] Patrick Moran. *The Statistical Processes of Evolutionary Theory*. Clarendon Press, Oxford, 1962.

[134] Brian Munsky and Mustafa Khammash. The finite state projection algorithm for the solution of the chemical master equation. *J. Chem. Phys.*, 124(4), 2006.

[135] Carey D. Nadell, Joao B. Xavier, Simon A. Levin, and Kevin R. Foster. The evolution of quorum sensing in bacterial biofilms. *PLoS Biol.*, 6(1):0171–0179, 2008.

[136] I Nåsell. Extinction and quasi-stationarity in the Verhulst logistic model. *J. Theor. Biol.*, 211(1):11–27, jul 2001.

[137] Claudia Neuhauser and Stephen W . Pacala. An Explicitly Spatial Version of the Lotka-Volterra Model with Interspecific Competition. *Ann. Appl. Probab.*, 9(4):1226–1259, 1999.

[138] T J Newman, Jean-Baptiste Ferdy, and C Quince. Extinction times and moment closure in the stochastic logistic process. *Theor. Popul. Biol.*, 65(2):115–26, mar 2004.

[139] R.M. Nisbet and W.S.C. Gurney. *Modelling Fluctuating Populations*. John Wiley & Sons, Toronto, 1982.

[140] R H Norden. On the Distribution of the Time to Extinction in the Stochastic Logistic Population-Model. *Adv. Appl. Probab.*, 14(4):687–708, 1982.

[141] I. D. Ofiteru, M. Lunn, T. P. Curtis, G. F. Wells, C. S. Criddle, C. A. Francis, and W. T. Sloan. Combined niche and neutral effects in a microbial wastewater treatment community. *Proc. Natl. Acad. Sci.*, 107(35):15345–15350, 2010.

[142] Otso Ovaskainen and Baruch Meerson. Stochastic models of population extinction. *Trends Ecol. Evol.*, 25(11):643–52, 2010.

[143] Jr Palmer, K. Kazmerzak, M. C. Hansen, and P. E. Kolenbrander. Mutualism versus independence: Strategies of mixed-species oral biofilms in vitro using saliva as the sole nutrient source. *Infect. Immun.*, 69(9):5794–5804, 2001.

[144] Matthew Parker and Alex Kamenev. Extinction in the Lotka-Volterra model. *Phys. Rev. E*, 80(2):021129, 2009.

[145] Todd L. Parsons. Invasion probabilities, hitting times, and some fluctuation theory for the stochastic logistic process. *J. Math. Biol.*, 77(4):1193–1231, 2018.

[146] Todd L. Parsons and Christopher Quince. Fixation in haploid populations exhibiting density dependence II: The quasi-neutral case. *Theor. Popul. Biol.*, 72(4):468–479, 2007.

[147] Todd L. Parsons, Christopher Quince, and Joshua B. Plotkin. Some consequences of demographic stochasticity in population genetics. *Genetics*, 185(4):1345–1354, 2010.

[148] Z Patwa and L M Wahl. The fixation probability of beneficial mutations. *J. R. Soc. Interface*, 5(28):1279–89, nov 2008.

[149] Pleuni S Pennings, Sergey Kryazhimskiy, and John Wakeley. Loss and recovery of genetic diversity in adapting populations of HIV. *PLoS Genet.*, 10(1):e1004000, jan 2014.

[150] Elizabeth Pennisi. What determines species diversity? *Science (80-.).*, 309:90, 2005.

[151] Garry Peterson, Craig R. Allen, and C. S. Holling. Ecological Resilience, Biodiversity, and Scale. *Ecosystems*, 1(1):6–18, 1997.

[152] E. R. Pianka. Niche Overlap and Diffuse Competition. *Proc. Natl. Acad. Sci.*, 71(5):2141–2145, 1974.

[153] E.R. Pianka. The Structure of Lizard Communities. 1973.

[154] S. Pigolotti, R. Benzi, P. Perlekar, M. H. Jensen, F. Toschi, and D. R. Nelson. Growth, competition and cooperation in spatial population genetics. *Theor. Popul. Biol.*, 84(1):72–86, 2013.

[155] S Pimm, H L Jones, and Diamond J. On the risk of extinction. *Am. Nat.*, 132(6):757–785, 1988.

[156] Anna Posfai, Thibaud Taillefumier, and Ned S. Wingreen. Metabolic Trade-Offs Promote Diversity in a Model Ecosystem. *Phys. Rev. Lett.*, 118(2):028103, 2017.

[157] E O Powell. Growth rate and generation time of bacteria, with special reference to continuous culture. *J. Gen. Microbiol.*, 15(3):492–511, 1956.

[158] Daniel J Rankin, Leighton A Turner, Jack A Heinemann, and Sam P Brown. The coevolution of toxin and antitoxin genes drives the dynamics of bacterial addiction complexes and intragenomic conflict. *Proc. Biol. Sci.*, 279(1743):3706–15, 2012.

[159] Sean H. Rice. *Evolutionary theory: mathematical and conceptual foundations*. Sinauer Associates, Sunderland, Mass., 2004.

[160] Robert E Ricklefs. The neutral theory of biodiversity: do the numbers add up. *Ecology*, 87(6):1424–1431, 2006.

[161] Guus Roeselers, Erika K. Mittge, W. Zac Stephens, David M. Parichy, Colleen M. Cavanaugh, Karen Guillemin, and John F. Rawls. Evidence for a core gut microbiota in the zebrafish. *ISME J.*, 5(10):1595–1608, 2011.

[162] Jeffrey Rogers and Richard A Gibbs. Comparative primate genomics: emerging patterns of genome content and dynamics. *Nat. Rev. Genet.*, 15(5):347–59, 2014.

[163] James Rosindell, Stephen P. Hubbell, and Rampal S. Etienne. The Unified Neutral Theory of Biodiversity and Biogeography at Age Ten. *Trends Ecol. Evol.*, 26(7):340–348, 2011.

[164] I. M. Rouzine, A. Rodrigo, and J. M. Coffin. Transition between Stochastic Evolution and Deterministic Evolution in the Presence of Selection: General Theory and Application to Virology. *Microbiol. Mol. Biol. Rev.*, 65(1):151–185, 2001.

[165] Shovonlal Roy and J. Chattopadhyay. Towards a resolution of 'the paradox of the plankton': A brief overview of the proposed mechanisms. *Ecol. Complex.*, 4(1-2):26–33, 2007.

[166] Serguei Saavedra, Rudolf P Rohr, Vasilis Dakos, and Jordi Bascompte. Estimating the tolerance of species to the effects of global environmental change. *Nat. Commun.*, 4:2350, aug 2013.

[167] Thomas W. Schoener. Some comments on Connell's and my reviews of field experiments on interspecific competition. *Am. Nat.*, 125(5):730–740, 1985.

[168] A Shmida and S Ellner. Coexistence of plant-species with similar niches. *Vegetatio*, 58(1):29–55, 1984.

[169] S Smale. On the differential equations of species in competition. *J. Math. Biol.*, 3:5–7, 1976.

[170] Emily R. Stirk, Grant Lythe, Hugo A. van den Berg, and Carmen Molina-Paris. Stochastic competitive exclusion in the maintenance of the naive T cell repertoire. *J. Theor. Biol.*, 265(3):396–410, 2010.

[171] Steven H Strogatz. *Nonlinear Dynamics and Chaos*. Perseus Books, Reading, Massachusetts, 1994.

[172] G. Sugihara, L.-F. Bersier, T. R. E. Southwood, S. L. Pimm, and R. M. May. Predicted correspondence between species abundances and dendrograms of niche similarities. *Proc. Natl. Acad. Sci.*, 100(9):5246–5251, 2003.

[173] Christine Taylor, Drew Fudenberg, Akira Sasaki, and Martin a Nowak. Evolutionary game dynamics in finite populations. *Bull. Math. Biol.*, 66(6):1621–44, nov 2004.

[174] Casey M Theriot, Mark J Koenigsknecht, Paul E Carlson Jr, Gabrielle E Hatton, Adam M Nelson, Bo Li, Gary B Huffnagle, Jun Li, and Vincent B Young. Antibiotic-induced shifts in the mouse gut microbiome and metabolome increase susceptibility to Clostridium difficile infection. 2014.

[175] Arne Traulsen, Jens Christian Claussen, and Christoph Hauert. Coevolutionary dynamics in large, but finite populations. *Phys. Rev. E*, 74(1):011901, jul 2006.

[176] N.G. Van Kampen. *Stochastic Processes in Physics and Chemistry*. North-Holland, Amsterdam, 1992.

[177] Laurence Van Melderen and Manuel Saavedra De Bast. Bacterial toxin-Antitoxin systems: More than selfish entities? *PLoS Genet.*, 5(3), 2009.

[178] Nicole M. Vega and Jeff Gore. Stochastic assembly produces heterogeneous communities in the Caenorhabditis elegans intestine. *PLoS Biol.*, 15(3):1–20, 2017.

[179] Pierre-Fran{\c{c}}ois Verhulst. Notice sur la loi que la population suit dans son accroissement. *Corresp. Math. Phys.*, 10:113–126, 1838.

[180] Vito Volterra. Fluctuations in the Abundance of a Species considered Mathematically. *Nature*, 118(2972):558–560, 1926.

[181] Marin Vulic and Roberto Kolter. Evolutionary Cheating in. *Genetics*, (March), 2001.

[182] Ping Wang, Lydia Robert, James Pelletier, Wei Lien Dang, Francois Taddei, Andrew Wright, and Suckjoon Jun. Robust growth of escherichia coli. *Curr. Biol.*, 20(12):1099–1103, 2010.

[183] J. D. Watson and F. H. C. Crick. Molecular Structure of Nucleic Acids: A Structure for Deoxyribose Nucleic Acids. *Nature*, 171:737–738, 1953.

[184] Aaron R. Wheeler, William R. Throndset, Rebecca J. Whelan, Andrew M. Leach, Richard N. Zare, Yish Hann Liao, Kevin Farrell, Ian D. Manger, and Antoine Daridon. Microfluidic device for single-cell analysis. *Anal. Chem.*, 75(14):3581–3586, 2003.

[185] Michael Wink. Evolution of secondary metabolites from an ecological and molecular phylogenetic perspective. *Phytochemistry*, 64(1):3–19, 2003.

[186] Benjamin E. Wolfe, Julie E. Button, Marcela Santarelli, and Rachel J. Dutton. Cheese rind communities provide tractable systems for in situ and in vitro studies of microbial diversity. *Cell*, 158(2):422–433, 2014.

[187] Sewall Wright. Evolution in Mendelian Populations. *Genetics*, 16(2):97, 1931.

[188] Thomas A. Wynn. Type 2 cytokines: mechanisms and therapeutic strategies. *Nat. Rev. Immunol.*, 15:271–282, 2015.

[189] Joao B Xavier, Kevin R Foster, Joao B Xavier, and Kevin R Foster. Cooperation and conflict in microbial biofilms. 2006(January), 2007.

[190] Glenn Young and Andrew Belmonte. Explicit probability of fixation formula for mutual competitors in a stochastic population model under competitive trade-offs. pages 1–24, 2018.

[191] Xiaoquan Yu and Xiang-Yi Li. Application of WKB and Fokker-Planck methods in analyzing demographic stochasticity. pages 1–19, 2017.

[192] J. X. Zhou, M. D. S. Aliyu, E. Aurell, and S. Huang. Quasi-potential landscape in complex multi-stable systems. *J. R. Soc. Interface*, 9(77):3539–3553, 2012.